

**APPENDIX 2.11.1**  
**TABLE OF CONTENTS**

	<u>Page</u>
2.11.1 FUEL BASKET STRUCTURAL ANALYSIS.....	2.11.1-1
2.11.1.1 Approach.....	2.11.1-1
2.11.1.2 Analysis.....	2.11.1-3
2.11.1.3 Results.....	2.11.1-23
2.11.1.4 Conclusions.....	2.11.1-25
2.11.1.5 References.....	2.11.1-26

**LIST OF FIGURES**

2.11.1-1 Free Body Diagram of Oak Ridge Container Subjected to a Vertical or Near Vertical Lid End Drop.....	2.11.1-27
2.11.1-2 Free Body Diagram of Oak Ridge Container Subjected to a Vertical or Near Vertical Bottom End Drop....	2.11.1-28
2.11.1-3 Free Body Diagram of Oak Ridge Container Fuel Basket Subjected to a Side Drop .....	2.11.1-29
2.11.1-4 Free Body Diagram of Oak Ridge Container Flux Trap Subjected to a Lid End Drop .....	2.11.1-30

## APPENDIX 2.11.1

### FUEL BASKET STRUCTURAL ANALYSIS

#### 2.11.1.1 Approach

The Oak Ridge SNF Container includes the following components:

- Tie Rod and Standoff (spacer)
- Fuel Compartment
- Poison Enclosure
- Support disc
- Container Shell
- Container lid and lid bolt

The purpose of this appendix is to evaluate the structural adequacy of the tie rods, standoffs, fuel compartments, poison enclosures, and support disc bearing stress. Appendix 2.11.2 presents the detailed structural analysis of the container shell due to internal pressure, external pressure and end drop loads. Appendix 2.11.3 presents the finite element analysis of the support discs and container shell subjected to side and end drop accelerations. The container lid bolt analysis is presented in Appendix 2.11.4. The maximum operating temperature is taken to be 250° F. (Section 3.4).

The applied loads analyzed in this appendix are as follows.

- Thermal stresses due to a maximum temperature change of 180° F (250° F – 70° F room temp.).
- The following accelerations due to normal and accident conditions end and side drops (TN-FSV SARP Appendix 2.10.2), including a value of 1.10 for the Dynamic Amplification Factor (Appendix 2.11.6):

#### Summary of Applied Load Caused by Free Drop Event

Impact Load		Normal Conditions (1 foot drop)	Accident Conditions (30 foot drop)
Axial g load (end drop)		14 g × 1.10 ~ 16 g.	54 g × 1.10 ~ 60 g.
70° Corner Drop	Axial g load	-	37 g × 1.10 ~ 41 g.
	Transverse g load	-	13 g × 1.10 ~ 15 g
Transverse g load (side drop)		17 g × 1.10 ~ 20 g.	71 g × 1.10 ~ 80 g.

Properties of the fuel basket poison plate enclosures, support discs, flux traps, fuel compartments and tie rod materials (Type 304 stainless steel) at 250° F are as follows<sup>(1)</sup>.

$$S_m = 20.0 \text{ ksi.}$$

$$S_y = 23.75 \text{ ksi.}$$

$$S_u = 68.5 \text{ ksi.}$$

$$E = 27.3 \times 10^6 \text{ psi.}$$

$$\alpha = 8.90 \times 10^{-6} \text{ in./in. } ^\circ\text{F}^{-1}$$

Properties of fuel basket standoff materials (SA-564, type 630, Condition H1150) at 250° F are as follows<sup>(1)</sup>.

$$S_m = 45.0 \text{ ksi.}$$

$$S_y = 95.05 \text{ ksi.}$$

$$S_u = 135.00 \text{ ksi.}$$

$$E = 28.2 \times 10^6 \text{ psi.}$$

$$\alpha = 5.90 \times 10^{-6} \text{ in./in. } ^\circ\text{F}^{-1}$$

The design criteria are described in Chapter 2. The basis for the fuel basket stress allowable is Section III, Subsection NG<sup>(3)</sup> for normal condition loads and Appendix F<sup>(2)</sup> for accident loads. The allowable stresses are as follows.

### Summary of Allowable Stresses

Stress Category	Normal Conditions (Level A)		Accident Conditions (Level D)	
	Tie rods, Support discs, Flux traps, Fuel compartments, and Poison enclosures	Standoffs	Tie rods, Support discs, Flux traps, Fuel compartments, and Poison enclosures	Standoffs
Primary membrane (general), $P_m$	$S_m$ , 20.00 ksi.	$S_m$ , 45.00 ksi.	Lesser { $2.4 S_m$ , $0.7 S_u$ }, 47.95 ksi.	Lesser { $2.4 S_m$ , $0.7 S_u$ }, = 94.50 ksi.
Primary membrane + bending, $P_m + P_b$	$1.5S_m$ , 30.00 ksi.	$1.5S_m$ , 67.50 ksi.	Lesser { $3.6 S_m$ , $S_u$ }, 68.50 ksi.	Lesser { $3.6 S_m$ , $S_u$ }, 135.00 ksi.
Bearing Stress	$S_y$ , 23.75 ksi.	$S_y$ , 95.05 ksi.	$S_u$ , 68.50 ksi.	$S_u$ , 135.00 ksi.
Pure shear stress	$0.6 S_m$ , 12.00 ksi.	$0.6 S_m$ , 27.00 ksi.	$0.42 S_u$ , 28.77 ksi.	$0.42 S_u$ , 56.70 ksi.

### 2.11.1.2 Analysis

#### A) Tie Rods and Standoffs (Appendix 1.4, Drawing 3044-70-7, Items 19 and 18)

##### Tie Rod Nut Torque Computation

The thread used at both ends of the tie rod is 1/2-13UNC-2A. The number of threads per inch,  $N = 13$ . Therefore, the thread pitch,  $p = 1/13 = 0.0769$  in. The nominal tie rod diameter of the 1/2-13UNC threads,  $D_b = 0.500$  in. From Reference 6, the diameter of the tie rod at the threads used for stress calculations,  $D_{ba}$ , is,

$$D_{ba} = D_b - 0.9743 p = 0.500 - 0.9743(0.0769) = 0.425 \text{ in.}$$

The stress area at the tie rod threads is,

$$\text{Stress Area} = \pi/4 (0.425)^2 = 0.142 \text{ in.}^2$$

A tie rod nut torque range of 6 to 8 ft. lb. has been selected. From Reference 6, using the minimum torque,

$$F_a = Q/KD_b = 6 \times 12 / (0.1 \times 0.500) = 1,440 \text{ lb., and}$$

$$\text{Preload stress} = F_a / \text{Stress Area} = 1,440 / 0.142 = 10,141 \text{ psi.} < 20,000 \text{ psi. ... o.k.}$$

Where  $Q$  is the applied nut torque, and  $K$  is the Nut factor for empirical relation between the applied torque and achieved preload (assume 0.1 with neolube lubricant). Using the maximum torque,

$$F_a = Q/KD_b = 8 \times 12 / (0.1 \times 0.500) = 1,920 \text{ lb., and}$$

$$\text{Preload stress} = F_a / \text{Stress Area} = 1,920 / 0.142 = 13,521 \text{ psi.} < 20,000 \text{ psi. ... o.k.}$$

##### Minimum Engagement Length for Tie Rod, Bottom Spacer Disc, and Nut

The tie rod material is SA-479, Type 304, the bottom spacer disc material is SA-240, Type 304, and the tie rod nut material is SA-194, Grade 8. All of these materials are type 304 stainless steel with very similar material properties. Therefore, the effect of material strength on the tie rod thread engagement length is negligible.

The minimum engagement length,  $L_e$ , for the bolt and flange is (Ref. 7),

$$L_e = \frac{2A_t}{3.1416K_{n \max} \left[ \frac{1}{2} + .57735n(E_{s \min} - K_{n \max}) \right]}$$

For a 1/2 13UNC tie rod,

$$\begin{aligned} A_t &= \text{tensile stress area} = 0.142 \text{ in.}^2, \\ n &= \text{number of threads per inch} = 13, \\ K_{n \max} &= \text{maximum minor diameter of internal threads} = 0.434 \text{ in.}, \text{ (Ref. 7).} \\ E_{s \min} &= \text{minimum pitch diameter of external threads} = 0.4435 \text{ in.}, \text{ (Ref. 7).} \end{aligned}$$

Substituting the values given above,

$$L_e = \frac{2(0.142)}{(3.1416)0.434 \left[ \frac{1}{2} + .57735(13)(0.4435 - 0.434) \right]} = 0.365 \text{ in.}$$

The actual minimum engagement length is the length of tie rod nut, which is 0.438 in. > 0.365 in. Therefore, the thread engagement length is adequate.

#### Compressive Stress in Standoffs due to Tie Rod Nut Preload

The cross sectional area of a single standoff is,

$$A = \pi/4 \times (0.875^2 - 0.5625^2) = 0.3528 \text{ in.}^2$$

Therefore, the maximum compressive stress,  $\sigma_{cp}$ , generated in the standoffs by the maximum tie rod nut preload is,

$$\sigma_{cn} = \frac{F_a}{A} = \frac{1,920}{0.3528} = 5,442 \text{ psi.} < 45,000 \text{ psi.} \dots \text{ o.k.}$$

#### Tensile Stress in Tie Rods due to Tie Rod Nut Preload

The cross sectional area of the tie rod is,

$$A = \pi/4 \times (0.50^2) = 0.1963 \text{ in.}^2$$

Therefore the maximum tensile stress,  $\sigma_{cp}$ , generated in the tie rods by the maximum tie rod nut preload is,

$$\sigma_{cn} = \frac{F_a}{A} = \frac{1,920}{0.1963} = 9,778 \text{ psi.} < 20,000 \text{ psi.} \dots \text{ o.k.}$$

### Stress in Standoffs due to Side Drop

During a side drop event the standoffs and tie rods are subjected to their own inertial load plus the inertial load of the poison enclosures and poison plates (see Figure 2.11.1-3). The tie rods are supported by the transverse reaction force of the spacer discs. This reaction force generates shear stresses in the tie rods at the spacer disc locations, and bending stresses in both the tie rods and standoffs between the spacer discs. Consequently, shear stress generated in the standoffs, during a side drop event, is negligible. Bending stress in both the standoffs and the tie rods is computed in the tie rod analysis Section 2.11.1.2.F.

### Compressive Stress in Standoffs due to Vertical End Drop

During the vertical lid end drop (see Figure 2.11.1-1), the support disc and poison enclosure (including poison plates within the enclosure) nearest to the impact bear directly on the inner surface of the container lid for the lid end drop (or inner surface of the container bottom plate for the bottom end drop – see Figure 2.11.1-2). The standoffs do not carry this inertial load. Therefore, for the end drop analysis, the inertial loads of the support disc and poison enclosure with poison plates nearest to the impact are not included in the axial compressive load applied to the standoffs.

Since the fuel compartments, canisters, and flux traps also bear directly on the inner surface of the container lid during a lid end drop (or inner surface of the compartment spacer, which bears directly on the container bottom plate for the bottom end drop), their loads are also not included in the compressive load applied to the standoffs.

Figure 2.11.1-1 is a free body diagram of the of the Oak Ridge Container subjected to a vertical, or near vertical, lid end drop. As shown in this force equilibrium diagram, the fuel compartments, canisters, and flux traps are directly supported by the container lid. Therefore, the inertial loads of the fuel compartments, canisters, and flux traps,  $F_3$ , is not transmitted to the standoff. Consequently, for the vertical end drop, only the inertia load,  $F_2$ , is used to calculate the standoff compressive stress.

The weight of the TN-FSV container components is conservatively taken to be the maximum dimension weights given in Table 2-5. The applied compressive load per standoff,  $P$ , under normal conditions is,

$$P = 16g \times [\text{weight of 45 standoffs, 112 lb.} + \text{weight of 80 poison plates, } 194 \times (80/90) \text{ lb.} \\ + \text{the weight of 8 poison enclosures, } 285 \times (8/9) \text{ lb.} + \text{the weight of 8 support discs,} \\ \text{including the 1.75 in. thick disc at the bottom, } 217 \times (7.75/8.5) \text{ lb.}] / 5 \text{ standoffs} = \\ 2,354 \text{ lb. ... say 2,500 lb.}$$

The cross sectional area of a single standoff is,

$$A = \pi/4 \times (0.875^2 - 0.5625^2) = 0.3528 \text{ in.}^2$$

The lid end drop is the most severe for a standoff, because of the bottom most 1.75 in. thick support plate. The maximum compressive stress,  $\sigma_{cn}$ , generated in the standoffs during a 16 g normal condition vertical end drop is,

$$\sigma_{cn} = \frac{P}{A} = \frac{2,500}{0.3528} = 7,086 \text{ psi.} < 45,000 \text{ psi. ... o.k.}$$

During accident conditions (60 g end drop), the stress generated in the standoffs,  $\sigma_{ca}$ , is,

$$\sigma_{ca} = 7,086 \times \frac{60}{16} = 26,573 \text{ psi.} < 94,500 \text{ psi. ... o.k.}$$

### Compressive Stress in Standoffs Due to Drop Orientation Other Than Vertical End Drop

In addition to the 90° end drop load case, a corner drop load case generating compressive loads in the standoffs is also considered. During a near vertical corner drop, the lateral inertial loads of the fuel compartments, canisters, and flux traps acting on the support discs will generate an axial friction force on the support discs. This additional axial friction force is ultimately transmitted to the standoff nearest to the impact end.

Figure 2.11.1-1 shows a free body diagram of the Oak Ridge Container subjected to a vertical or near vertical lid end drop. During the near vertical drop, the transverse internal loads of the fuel compartments, canisters, and flux traps,  $F_4$ , are transmitted to the support disc. This transverse load generates a friction force,  $F_5$ , that is ultimately transmitted to the standoff at the impact end, in addition to the inertial loads of the support discs and poison enclosures,  $F_2$ . The inertial load of the container bottom, flange, and shell,  $F_1$ , however, is transferred directly to the container lid and TN-FSV cask lid.

Based on the combinations of axial and transverse g loads tabulated in TN-FSV SAR Table 2.10.2-3 for maximum wood crush stress properties, the 60° corner drop is considered the worst case in terms of combination of axial inertial load and axial friction force generated by lateral acceleration. Therefore, the inertial g loads from the 60° ADOC run are used to bound all other near vertical drop orientations.

The maximum compressive load applied to the standoffs during a 60° accident condition corner drop,  $P$ , is,

$$P = F_2 + F_5 + \text{applied load of bottom 5 standoffs nearest to the impact themselves.}$$

$$F_2 = 41g \times [\text{weight of 40 standoffs, } 112 \times (40/45) \text{ lb.} + \text{weight of 80 poison plates, } 194 \times (80/90) \text{ lb.} + \text{the weight of 8 poison enclosures, } 272 \times (8/9) \text{ lb.} + \text{the weight of 8 support discs, including the 1.75 in. thick disc at the bottom, } 217 \times (7.75/8.5) \text{ lb.}] / 5 \text{ standoffs} = 5,839 \text{ lb.}$$

$$\text{Applied load of 5 standoffs nearest to the impact} = 41g \times 112 \times (5/45) \text{ standoffs} = 99 \text{ lb.}$$

Assuming a friction coefficient,  $\mu = .74$ , for mild steel on mild steel (Ref. 1), the applied friction force from the Oak Ridge Canisters, flux traps, and fuel compartments,  $F_5$ , is,

$$F_5 = 15 g \times 0.74 \times [\text{weight of 5 fuel compartments, 741 lb. + weight of 20 Oak Ridge Canisters, 1,600 lb. + weight of 15 flux traps, 189 lb.}] / 5 \text{ standoffs} = 5,617 \text{ lb.}$$

Therefore, the total applied load acting on a standoff,  $P$ , is,

$$P = 5,839 + 99 + 5,617 = 11,555 \text{ lb. ....say 12,000 lb.}$$

The cross sectional area of a single standoff is,

$$A = \pi/4 \times (0.875^2 - 0.5625^2) = 0.3528 \text{ in.}^2$$

Therefore the maximum compressive stress,  $\sigma_{ca}$ , generated in the standoffs during a  $60^\circ$  hypothetical accident condition corner drop is,

$$\sigma_{ca} = \frac{P}{A} = \frac{12,000}{0.3528} = 34,014 \text{ psi.} < 94,500 \text{ psi. ... o.k.}$$

#### Standoff Buckling due to Compressive Stress

The allowable axial buckling stress,  $F_a$ , for normal conditions (Level A) is calculated in accordance with reference 4, Section NF-3322.1 (c) (2).

The moment of inertia,  $I$ , of a single standoff is,

$$I = \frac{\pi}{64} [D_o^4 - D_i^4] = \frac{\pi}{64} [0.875^4 - 0.5625^4] = 0.02386 \text{ in.}^4$$

The radius of gyration,  $r$ , of the standoff is,

$$r = \left( \frac{I}{A} \right)^{1/2} = \left( \frac{0.02386}{0.3528} \right)^{1/2} = 0.2601 \text{ in.}$$

The effective length factor,  $K$ , is taken to be  $1^{(4)}$ , From reference 4,

$$\frac{Kl}{r} = \frac{(1)(20.21)}{0.2601} = 77.72 < 120 \text{ therefore,}$$

$$F_a = S_y \left( 0.47 - \frac{Kl/r}{444} \right) = 95,050 \left( 0.47 - \frac{77.72}{444} \right) = 28,036 \text{ psi.}$$

As per reference 2, Section F-1334, for accident conditions (Level D), the allowable axial buckling stress,  $F_a$ , can be increased by the following factor.

Since  $S_u > 1.2 S_y$  (135.00 ksi. > 114.06 ksi.),  $F_a$  can be increased by,

$$\text{Lesser of } \{ 2 \text{ or } 1.167 S_u / S_y \} = 1.657.$$

Therefore, for accident conditions,

$$F_a = 28,036 \times 1.657 = 46,456 \text{ psi.}$$

For normal conditions, the maximum compressive stress in the standoffs is generated by the combination of the tie rod nut preload stress and the normal condition 90° end drop stress, which is,

$$\text{Max. Normal Condition Stress} = 7,086 \text{ psi.} + 5,442 \text{ psi.} = 12,528 \text{ psi.} < 28,036 \text{ psi.} \dots \text{ o.k.}$$

For accident conditions, the maximum compressive stress in the standoffs is generated by the combination of the tie rod nut preload stress and the accident condition 60° corner drop stress, which is,

$$\text{Max. Accident Condition Stress} = 34,014 \text{ psi.} + 5,442 \text{ psi.} = 39,456 \text{ psi.} < 46,456 \text{ psi.} \dots \text{ o.k.}$$

## B) Support Disc (Appendix 1.4, Drawing 3044-70-7, Items 17A, 17B, and 17B)

### Bearing Stress

The maximum bearing stress applied to the Oak Ridge support disc by the standoff is equal to the maximum compressive stress generated in the top standoff. Therefore, for normal conditions, the maximum bearing stress,  $\sigma_{bn}$ , is,

$$\sigma_{bn} = 12,528 \text{ psi.} < 23,750 \text{ psi.} \dots \text{ o.k.}$$

The maximum bearing stress,  $\sigma_{ba}$ , during an accident conditions is,

$$\sigma_{ba} = 39,456 \text{ psi.} < 68,500 \text{ psi.} \dots \text{ o.k.}$$

### Buckling and Stress Analysis

The support disc buckling and stress analysis is performed using finite element analysis presented in appendix 2.11.3.

### C) Fuel Compartment (Appendix 1.4, Drawing 3044-70-7, Items 9 and 10)

#### Compressive Stress due to End Drop

The inertial load applied to the container shell, during a 30 ft. end drop, is conservatively calculated using the maximum weight of the fuel compartment including the lower end compartment spacer (Section 2.2). The corresponding applied force under accident conditions,  $F_{axial}$ , is,

$$F_{axial} = [741 / 5 \text{ lb. (single fuel compartment weight, Section 2.2)}] \times 60 \text{ gs} = 8,892 \text{ lb.}$$

The cross sectional area,  $A$ , of the fuel compartment shell is,

$$A = \frac{\pi}{4} [D_o^2 - D_i^2] = \frac{\pi}{4} [5.563^2 - 5.295^2] = 2.285 \text{ in.}^2$$

Therefore, the accident condition compressive stress applied to the fuel compartment during a 30 ft. lid end drop is,

$$\sigma_a = P / A = 8,892 \text{ lb.} / 2.285 \text{ in.}^2 = 3,891 \text{ psi.} < 47,950 \text{ psi.} \dots \text{o.k.}$$

For normal conditions,

$$\sigma_n = 3,891 \text{ psi.} \times 16 \text{ gs} / 60 \text{ gs} = 1,038 \text{ psi.} < 20,000 \text{ psi.} \dots \text{o.k.}$$

#### Fuel Compartment Buckling due to Compressive Stress

The allowable axial buckling stress,  $F_a$ , for normal conditions (Level A) is calculated in accordance with Reference 4, Section NF-3322.1 (c) (2).

The moment of inertia,  $I$ , of the container shell section is,

$$I = \frac{\pi}{64} [D_o^4 - D_i^4] = \frac{\pi}{64} [5.563^4 - 5.295^4] = 8.425 \text{ in.}^4$$

The radius of gyration,  $r$ , of the container shell section is,

$$r = \left( \frac{I}{A} \right)^{1/2} = \left( \frac{8.425}{2.285} \right)^{1/2} = 1.920 \text{ in.}$$

From reference 4,

$$\frac{Kl}{r} = \frac{(1)(189.88)}{1.920} = 98.9 < 120 \text{ therefore,}$$

$$F_a = S_y \left( 0.47 - \frac{Kl/r}{444} \right) = 23,750 \left( 0.47 - \frac{98.9}{444} \right) = 5,872 \text{ psi.} > 1,038 \text{ psi. ... o.k.}$$

As per reference 2, Section F-1334, for accident conditions (Level D), the normal condition allowable axial buckling stress,  $F_a$ , can be increased by the following factor.

Since  $S_u > 1.2 S_y$  (68.5 ksi. > 28.5 ksi.),  $F_a$  can be increased by,

$$\text{Lesser of } \{ 2 \text{ or } 1.167 S_u / S_y \} = 2.$$

Therefore, for accident conditions,

$$F_a = 5,872 \times 2 = 11,744 \text{ psi.} > 3,891 \text{ psi. ... o.k.}$$

### Bending Stress in Fuel Compartment due to Side Drop

The maximum bending stress generated in the fuel compartment shell is calculated by applying 1/9 of the maximum payload weight per fuel compartment as a uniform load on a section of the fuel compartment between two adjacent support discs. The end conditions of the fuel compartment section analyzed are conservatively assumed to be pinned. The weight of the payload (fuel assemblies and flux traps) is conservatively taken to be the maximum dimension weight given in Section 2.2.

Under normal conditions, (20 g side drop), the applied load,  $P$ , is,

$$P = (1/9) \times [(1,600 \times (4/20) \text{ lb. weight of 4 fuel assemblies}) + (189 \times (3/20) \text{ lb. weight of 3 flux traps})] \times 20 \text{ gs} = 733 \text{ lb.}$$

Conservatively take  $P = 1,000 \text{ lb.}$  The corresponding moment,  $M$ , in the fuel compartment is,

$$M = \frac{PL}{8} = \frac{1,000 \times 20.21}{8} = 2,526 \text{ in. lb. (Ref. 5)}$$

Where  $L$  is the length of fuel compartment between spacer discs. The moment of inertia of the fuel compartment section is computed above, and is  $I = 8.425 \text{ in.}^4$ . Therefore, the bending stress,  $\sigma_{bn}$ , generated in the fuel compartment during a 20 g normal condition side drop is,

$$\sigma_{bn} = \frac{Mc}{I} = \frac{2,526 \times (5.563/2)}{8.425} = 834.0 \text{ psi.} < 20,000 \text{ psi. ... o.k.}$$

Where  $c$  is the maximum distance from the fuel compartment axis to its outer radius. Under accident conditions (80 g side drop), the bending stress,  $\sigma_{ba}$ , in the fuel compartment is,

$$\sigma_{ba} = 834.0 \times (80 / 20) = 3,336 \text{ psi.} < 47,950 \text{ psi. ... o.k.}$$

## D) Flux Traps (Appendix 1.4, Drawing 3044-70-3, Item 24)

### Compressive Stress in Flux Trap due to End Drop

Even though the nominal dimensions are used to calculate the flux trap's section properties, the inertial load applied to the flux trap, during a 30 ft. end drop, is conservatively calculated using the maximum dimension weight of the flux trap. The weight of a single flux trap is,

Flux Trap weight =  $189/15 = 12.6$  lb. (Section 2.2).

The maximum axial compressive force taken by a flux trap,  $F_{axial}$ , is,

$$F_{axial} = [2 \times 12.6 \text{ lb. (weight of 2 flux traps)} + 3 \times 80 \text{ (weight of 3 Oak Ridge Canisters)}] \times 60 \text{ gs} \\ = 15,910 \text{ lb.}$$

An axial load of 17,400 is conservatively used.

The minimum cross sectional area,  $A$ , of the flux trap shell is the following.

$$A = \frac{\pi}{4} [D_o^2 - D_i^2] = \frac{\pi}{4} [5.00^2 - 4.76^2] = 1.840 \text{ in.}^2$$

Therefore the accident condition compressive stress applied to the flux trap during a 30 ft. lid end drop is,

$$\sigma_a = P / A = 17,400 \text{ lb.} / 1.840 \text{ in.}^2 = 9,457 \text{ psi.} < 47,950 \text{ psi.} \dots \text{o.k.}$$

For normal conditions,

$$\sigma_n = 9,457 \text{ psi.} \times 16 \text{ gs} / 60 \text{ gs} = 2,522 \text{ psi.} < 20,000 \text{ psi.} \dots \text{o.k.}$$

### Flux Trap Buckling due to Compressive Stress

The allowable axial buckling stress,  $F_a$ , for normal conditions (Level A) is calculated in accordance with reference 4, Section NF-3322.1 (c) (2).

The moment of inertia,  $I$ , of the flux trap section is,

$$I = \frac{\pi}{64} [D_o^4 - D_i^4] = \frac{\pi}{64} [5.00^4 - 4.76^4] = 5.480 \text{ in.}^4$$

The radius of gyration,  $r$ , of the flux trap section is,

$$r = \left( \frac{I}{A} \right)^{1/2} = \left( \frac{5.480}{1.840} \right)^{1/2} = 1.726 \text{ in.}$$

From reference 4,

$$\frac{Kl}{r} = \frac{(1)(16.00)}{1.726} = 9.27 < 120 \text{ therefore,}$$

$$F_a = S_y \left( 0.47 - \frac{Kl/r}{444} \right) = 23,750 \left( 0.47 - \frac{9.27}{444} \right) = 10,667 \text{ psi.} > 2,522 \text{ psi. ...o.k.}$$

As per reference 2, Section F-1334, for accident conditions (Level D), the allowable axial buckling stress,  $F_a$ , can be increased by the following factor.

Since  $S_u > 1.2 S_y$  (68.5 ksi. > 28.5 ksi.),  $F_a$  can be increased by,

$$\text{MIN} \{ 2 \text{ or } 1.167 S_u / S_y \} = 2.$$

Therefore, for accident conditions,

$$F_a = 10,667 \times 2 = 21,334 \text{ psi.} > 9,457 \text{ psi. ... o.k.}$$

Both stress and buckling limit for the flux trap lifting disc are bounded by that of the central shell since the lifting disc section is shorter and thicker than that of the central shell.

### Weld Stress

The partial penetration groove welds at the top and bottom plates of the flux trap are subjected to the same compressive load as the shell. The weld used to join the shell to the top and bottom plates is a continuous 0.06 in. groove weld. The weld area is,

$$A_w = (\pi/4) \times [ 5.0^2 - (5.0 - 2 \times 0.06)^2 ] = 0.931 \text{ in.}^2$$

Therefore, the accident condition compressive stress in the flux trap weld,  $\sigma_{wn}$ , is,

$$\sigma_{wa} = P / A_w = 17,400 \text{ lb.} / 0.931 \text{ in.}^2 = 18,670 \text{ psi.} < 47,950 \text{ psi. ...o.k.}$$

For normal conditions,

$$\sigma_{wn} = 18,670 \text{ psi.} \times 16 \text{ gs} / 60 \text{ gs} = 4,979 \text{ psi.} < 20,000 \text{ psi. ...o.k.}$$

### Bending Stress in Bottom Plate

The flux traps are loaded in the Oak Ridge Container fuel compartments between Oak Ridge Canisters. The geometry of the flux trap lifting disc (top plate) and the Oak Ridge Canister handling head are very similar. The Oak Ridge Canister Head only provides support along the outer edge of the spacer cap (bottom plate) of the flux trap (see Figure 2.11.1-4). Therefore, during an end drop, the only load applied to the flux trap bottom and top plates is that generated by their own inertial load plus the inertial loads of the flux trap poison plates (item 24E, TN drawing no. 3044-70-3) and poison plate caps (item 24G). Since the flux trap bottom plate is thinner (0.45 in.) than the flux trap top plate (0.667 in.), the bending stresses generated in the bottom plate are greater than the bending stresses generated in the top plate. Therefore, only the flux trap bottom plate is analyzed, since it is the bounding case.

Figure 2.11.1-4, is a free body diagram of the flux trap subjected to a bottom end drop. Both the loads applied by the canisters and flux traps above, and the reaction force provided by the Oak Ridge Container below, act only on the outer edge of the flux trap and through the flux trap spacer tube (shell). Figure 2.11.1-4, shows that no inertial loads are applied to the flux trap bottom and top plates except for their own inertial loads.

The weight of the flux trap bottom plate, bottom poison plate, and bottom poison cap,  $P$ , is

$$P = (\pi/4) \times [4.69^2 \times 0.25 \times 0.29 + 4.69^2 \times 0.25 \times 0.1 + 5.00^2 \times 0.45 \times 0.29] = 4.25 \text{ lb. say } 5 \text{ lb.}$$

Conservatively assuming the edges are simply supported, from reference 6, Table X, Case 1, the maximum stress at the center of the plate,  $\sigma$ , is,

$$\sigma = \frac{3W}{8\pi mt^2} (3m + 1)$$

Where,  $W$  is the total applied load,  $m$  is the reciprocal of Poisson's ratio ( $1/3 = 3.33$  for stainless steel), and  $t$  is the plate thickness. Therefore, for normal conditions, the maximum flux trap bottom plate stress,  $\sigma_n$ , is,

$$\sigma_n = \frac{3(5 \times 16)}{8\pi (3.33)(0.45)^2} (3(3.33) + 1) = 157 \text{ psi. } < 30,000 \text{ psi. ... o.k.}$$

For accident conditions, the maximum flux trap bottom plate stress,  $\sigma_a$ , is,

$$\sigma_a = 157 \times 60/16 = 589 \text{ psi. } < 68,500 \text{ psi. ... o.k.}$$

E) Poison Enclosure (Appendix 1.4, Drawing 3044-70-5, Item 25 and 26 weldment)

For the poison plate enclosure analysis, the maximum dimension weight is conservatively used (Section 2.2).

Bending stress in 3.268 in. wide plate (Appendix 1.4, Drawing 3044-70-5, Item 25A)

The maximum stress that could occur in the central pentagon portion of the poison enclosure is the bending stress in the largest plate (3.268 in. wide outer sheet) during a side drop event. The bending stress in this plate is computed by applying the inertial load of the enclosed poison plate and the 3.268 in. wide plate itself. The end conditions of the enclosure plate analyzed are conservatively assumed to be pinned.

Under normal conditions, (20 g side drop), the applied load,  $P$ , is,

$$P = [(84 / 45 \text{ lb. weight of 1 small poison plate, Section 2.2}) + (3.268 \text{ in. width} \times 0.0595 \text{ in. thick} \times 20.15 \text{ in. length} \times 0.29 \text{ lb. in.}^3 \text{ density}) \text{ lb. weight of enclosure plate}] \times 20 \text{ gs} = 60 \text{ lb.}$$

Conservatively take  $P = 65 \text{ lb.}$  The corresponding moment,  $M$ , in the fuel compartment is,

$$M = \frac{PL}{8} = \frac{65 \times 3.268}{8} = 26.55 \text{ in. lb. (Ref. 9)}$$

Where  $L$  is the length of enclosure plate. The moment of inertia of the poison enclosure plate,  $I$ , is,

$$I = \frac{bh^3}{12} = \frac{20.15 \times 0.0595^3}{12} = 3.537 \times 10^{-4} \text{ in.}^4$$

Therefore, the bending stress,  $\sigma_{bn}$ , generated in the fuel compartment during a 20 g normal condition side drop is,

$$\sigma_{bn} = \frac{Mc}{I} = \frac{26.55 \times (0.0595/2)}{3.537 \times 10^{-4}} = 2,233 \text{ psi.} < 20,000 \text{ psi.} \dots \text{o.k.}$$

Under accident conditions (80 g side drop) the bending stress,  $\sigma_{ba}$ , in the fuel compartment is,

$$\sigma_{ba} = 2,233 \times (80 / 20) = 8,932 \text{ psi.} < 47,950 \text{ psi.} \dots \text{o.k.}$$

Compressive Stress in Top and Bottom Support Plates (Appendix 1.4, Drawing 3044-70-5, Item 26A)

The maximum compressive force in the top and bottom plates occurs during a side drop event where the top and bottom plates take the transverse inertial load of the poison enclosure including the poison plates. Conservatively assume that the inertial load of the entire poison plate enclosure, including the poison plates themselves, is reacted by the compressive force in two sets of top and bottom plates (there are a total of five sets of top and bottom plates). The maximum compressive stress in the top and bottom plates occurs in the region of the plates where the cross section is the smallest. The applied compressive force during normal conditions (20 g side drop),  $P$ , is,

$$P = [(194 / 9 \text{ lb. weight of 10 poison plates}) + (285 / 9 \text{ lb. weight of 1 poison enclosure})] \times 20 \text{ gs} = 1,064 \text{ lb.}$$

Conservatively take  $P = 1,100 \text{ lb.}$  The minimum cross sectional area,  $A$ , which takes the compressive load, is,

$$A = [0.25 \text{ in. thick} \times 0.41 \text{ in. width}] \times 2 \text{ bottom plates} \times 2 \text{ top plates} = 0.410 \text{ in.}^2$$

Therefore the compressive stress,  $\sigma_{cn}$ , in the top and bottom plates is,

$$\sigma_{cn} = \frac{P}{A} = \frac{1,100}{0.410} = 2,683 \text{ psi.} < 20,000 \text{ psi.} \dots \text{ o.k.}$$

Under accident conditions (80 g side drop) the compressive stress,  $\sigma_{ca}$ , in the bottom and top plates is,

$$\sigma_{ba} = 2,683 \times (80 / 20) = 10,732 \text{ psi.} < 47,950 \text{ psi.} \dots \text{ o.k.}$$

Top and Bottom Plate Buckling due to Compressive Stress (Appendix 1.4, Drawing 3044-70-5, Item 26A)

The allowable axial buckling stress in the poison enclosure top and bottom plates,  $F_a$ , for normal conditions (Level A) is calculated in accordance with reference 4, Section NF-3322.1 (c) (2).

The minimum moment of inertia,  $I$ , of a single top/bottom plate is,

$$I = \frac{bh^3}{12} = \frac{0.41 \times 0.25^3}{12} = 5.339 \times 10^{-4} \text{ in.}^4$$

The Area for a single top/bottom plate,  $A = 0.25 \times 0.41 = 0.1025 \text{ in.}^2$ . The radius of gyration,  $r$ , of the plate is,

$$r = \left( \frac{I}{A} \right)^{1/2} = \left( \frac{5.339 \times 10^{-4}}{0.1025} \right)^{1/2} = 0.07217 \text{ in.}$$

The length of the compression member,  $l$ , is taken to be the length of the segment of the top/bottom plate with the smallest cross sectional area (1.65 in.), since this section does not have the additional support of the inner and outer braces. From reference 4,

$$\frac{Kl}{r} = \frac{(1)(1.40)}{.07217} = 19.40 < 120 \text{ therefore,}$$

$$F_a = S_y \left( 0.47 - \frac{Kl/r}{444} \right) = 23,750 \left( 0.47 - \frac{19.40}{444} \right) = 10,125 \text{ psi.} > 2,683 \text{ psi. ...o.k.}$$

As per reference 2, Section F-1334, for accident conditions (Level D), the normal condition allowable axial buckling stress,  $F_a$ , can be increased by the following factor.

Since  $S_u > 1.2 S_y$  (68.5 ksi. > 28.5 ksi.),  $F_a$  can be increased by,

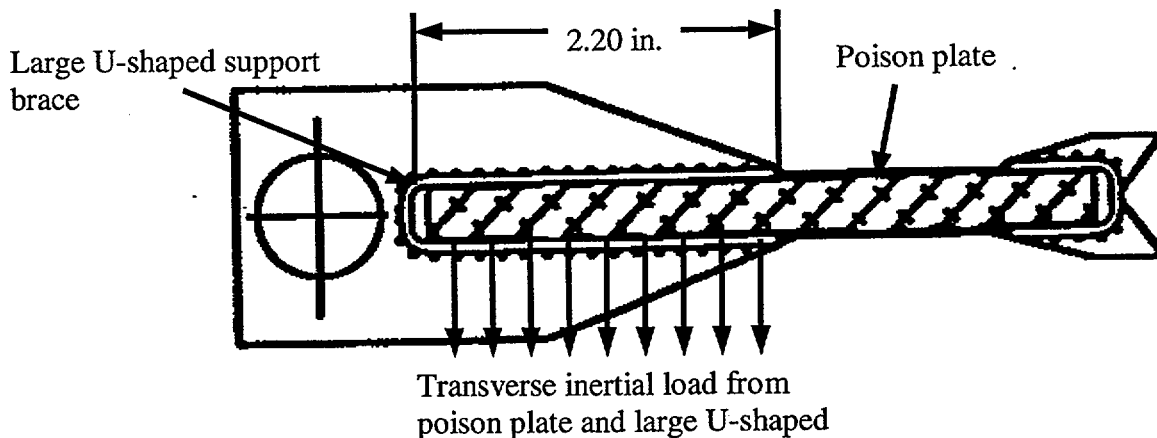
$$\text{MIN} \{ 2 \text{ or } 1.167 S_u / S_y \} = 2.$$

Therefore, for accident conditions,

$$F_a = 10,125 \times 2 = 20,250 \text{ psi.} > 10,732 \text{ psi. ... o.k.}$$

Bending Stress in Large Outer Brace (Appendix 1.4, Drawing 3044-70-5, Item 26B)

The maximum bending stress in the outer brace occurs when the inertial load of approximately 1/2 of the large poison plate and the outer brace itself is applied to the inside face of the outer brace during a side drop event. The assumptions made in the bending stress calculation are that one side plate of the brace carries roughly 1/2 of the load (the other 1/2 load is carried by the inner brace and side panel). The outer brace side plate is fixed on one of the long sides, where the U-shape is, and free on the 3 remaining sides. The load is applied uniformly. The following sketch describes the loading condition analyzed.



The formulae used in this calculation are given in Reference 5, p. 104, Table III, Case 3. The applied load,  $W$ , under normal conditions (20 g side drop) is,

$$W = [(1/2 \times 110 / 45 \text{ lb. weight of half of 1 large poison plate, Section 2.2}) + (2.20 \text{ in.} \times 0.0595 \text{ in.} \times 19.65 \text{ in.} \times 0.29 \text{ lb.in}^{-3} \text{ lb. weight of one side of outer U-shaped brace)}] \times 20 \text{ gs} = 39.36 \text{ lb.}$$

Conservatively take  $W = 45 \text{ lb.}$  The corresponding moment,  $M$ , in the outer brace side plate is,

$$M = \frac{WL}{2} = \frac{45 \times 2.20}{2} = 49.50 \text{ in. lb. (Ref. 5)}$$

Where  $L$  is the short length of outer brace side plate. The moment of inertia of the outer brace side plate,  $I$ , is,

$$I = \frac{bh^3}{12} = \frac{19.65 \times 0.0595^3}{12} = 3.449 \times 10^{-4} \text{ in.}^4$$

Therefore, the bending stress,  $\sigma_{bn}$ , generated in the outer brace during a 20 g normal condition side drop is,

$$\sigma_{bn} = \frac{Mc}{I} = \frac{49.50 \times (0.0595/2)}{3.449 \times 10^{-4}} = 4,270 \text{ psi.} < 20,000 \text{ psi.} \dots \text{ o.k.}$$

Under accident conditions (80 g side drop) the bending stress,  $\sigma_{ba}$ , in the outer brace is,

$$\sigma_{ba} = 4,270 \times (80 / 20) = 17,080 \text{ psi.} < 47,950 \text{ psi.} \dots \text{ o.k.}$$

The bending stress in the side panel and inner brace side plate will be the same as in the outer brace since the side plate and inner brace combined will take the other half of the applied load.

Shear Stress in Weld Between Top/Bottom Plates (Appendix 1.4, Drawing 3044-70-5, Item 26A) and Outer Brace (Appendix 1.4, Drawing 3044-70-5, Item 26B, C, D)

During a side drop event a shear force is reacted by the 0.06" fillet weld between the top/bottom plates and the outer brace. For the purpose of analysis, the shear stress in this weld is taken to be the weight of the entire poison enclosure weldment, divided by the entire weld area on all five legs of the weldment. The total shear force generated in the weld under normal conditions is,

$$V = [(194 / 9 \text{ lb. weight of 10 poison plates}) + (285 / 9 \text{ lb. weight of 1 poison enclosure})] \times 20 \text{ gs} = 1064 \text{ lb.}$$

Conservatively take  $V = 1,100$  lb. The total weld area available to take the shear force,  $A_v$ , is,

$$A_v = [0.06 \text{ in. thick fillet weld} \times \sin(45^\circ) \text{ throat length} \times 9.14 \text{ weld perimeter length}] \times 5 \text{ legs} = 1.939 \text{ in.}^2$$

Therefore the shear stress,  $\tau_n$ , in the top and bottom plates is,

$$\tau_n = \frac{V}{A_v} = \frac{1,100}{1.939} = 567 \text{ psi.} < 12,000 \text{ psi.} \dots \text{o.k.}$$

Under accident conditions (80 g side drop), the shear stress,  $\tau_a$ , in the top and bottom plates is,

$$\tau_a = 567 \times (80 / 20) = 2,268 \text{ psi.} < 28,770 \text{ psi.} \dots \text{o.k.}$$

#### F) Tie Rods (Appendix 1.4, Drawing 3044-70-8, Item 19)

##### Shear Stress

The reaction force of the tie rods supports the inertial load of the poison plates, poison enclosure, standoffs, and the tie rod itself during a side drop event. Conservatively assume that the inertial load of the entire poison plate enclosure, with poison plates, ( $F_3$  – see Figure 2.11.1-3), is reacted by the shear force in two tie rods (there are a total of five tie rods). The inertial load of two standoffs and the two sections of the tie rods themselves also contribute to the applied shear force. The shear stress in the tie rods occurs in the region near the support discs. The applied shear force in the tie rods during normal conditions (20 g side drop),  $V$ , is,

$$V = [(194 / 9 \text{ lb. weight of 10 poison plates}) + (285 / 9 \text{ lb. weight of 1 poison enclosure}) + (112 \times 2/45 \text{ lb. weight of two standoffs}) + (61 \times 20.21/189.63 \times 2/5 \text{ lb. weight of two tie rod sections})] \times 20 \text{ gs} = 1,216 \text{ lb.}$$

Conservatively take  $V = 1,250$  lb. The area available to take the shear force,  $A_v$ , is,

$$A_v = [(\pi/4) \times 0.50^2 \text{ in.}^2 \text{ tie rod cross sectional area}] \times 2 \text{ tie rods} \times 2 \text{ two ends} = 0.785 \text{ in.}^2$$

Therefore, the shear stress,  $\tau_n$ , in the tie rods is,

$$\tau_n = \frac{V}{A_v} = \frac{1,250}{0.785} = 1,592 \text{ psi.} < 12,000 \text{ psi.} \dots \text{o.k.}$$

Under accident conditions (80 g side drop) the shear stress,  $\tau_a$ , in the tie rods is,

$$\tau_a = 1,592 \times (80 / 20) = 6,369 \text{ psi.} < 28,770 \text{ psi.} \dots \text{o.k.}$$

### Bending Stress

The maximum bending stress generated in the tie rod and standoff is calculated by applying the maximum weight of a 20.21 in. length of a tie rod plus one standoff as a uniform load on the tie rod section and standoff supported between two adjacent support discs. The inertial load of the poison enclosure and poison plates is reacted at the ends of the tie rod section (near the spacer discs). Consequently, the inertial load of the poison enclosures and poison plates do not generate a significant bending moment or bending stress in the tie rod. The end conditions of the tie rod section are conservatively assumed to be pinned. The weights of the tie rod section and standoff are conservatively taken to be the maximum dimension weight given in Section 2.2.

Under normal conditions, (20 g side drop), the applied load,  $P$ , is,

$$P = [(61 \times (1/5) \times (20.21/189.63) \text{ lb. weight of 20.21 in length of tie rod}) + (112 \times (1/45) \text{ lb. weight of 1 standoff})] \times 20 \text{ gs} = 75.8 \text{ lb.}$$

Conservatively take  $P = 80 \text{ lb.}$  The corresponding moment,  $M$ , in the tie rod section is,

$$M = \frac{PL}{8} = \frac{80 \times 20.21}{8} = 202.1 \text{ in. lb.}$$

Where,  $L$  is the length of the tie rod section. The moment of inertia of the tie rod section and standoff,  $I$ , is,

$$I = \frac{\pi}{64} (0.50^4 + 0.875^4 - 0.5625^4) = 0.02693 \text{ in.}^4$$

Therefore, the bending stress,  $\sigma_{bnt}$ , generated in the tie rod section during a 20 g normal condition side drop is,

$$\sigma_{bnt} = \frac{Mc}{I} = \frac{202.1 \times 0.25}{.02693} = 1,876 \text{ psi.} < 30,000 \text{ psi.} \dots \text{ o.k.}$$

Where  $c$  is the maximum distance from the tie rod axis to its outer radius. Under accident conditions (80 g side drop) the bending stress,  $\sigma_{bat}$ , in the fuel compartment is,

$$\sigma_{bat} = 1,876 \times (80 / 20) = 7,505 \text{ psi.} < 68,500 \text{ psi.} \dots \text{ o.k.}$$

The maximum bending stress,  $\sigma_{bns}$ , generated in the standoff during a 20 g normal condition side drop is,

$$\sigma_{bns} = \frac{Mc}{I} = \frac{202.1 \times 0.4375}{.02693} = 3,283 \text{ psi.} < 67,500 \text{ psi.} \dots \text{ o.k.}$$

Where  $c$  is the maximum distance from the standoff axis to its outer radius. Under accident conditions (80 g side drop) the bending stress,  $\sigma_{bas}$ , in the standoff is,

$$\sigma_{bas} = 3,283 \times (80 / 20) = 13,133 \text{ psi.} < 135,000 \text{ psi.} \dots \text{ o.k.}$$

Stress Intensity

For normal conditions, the maximum stress intensity generated in the tie rods due to the combination of shear, bending, and preload stresses,  $S.I._n$ , is

$$\begin{aligned} S.I._n &= \sqrt{\sigma^2 + 4\tau^2} = \sqrt{(1,876 + 13,521)^2 + 4(1,592^2)} \\ &= 15,723 \text{ psi.} < 30,000 \text{ psi.} \dots \text{ o.k.} \end{aligned}$$

For accident conditions, the maximum stress intensity generated in the tie rods due to the combination of shear, bending, and preload stresses,  $S.I._a$ , is

$$\begin{aligned} S.I._a &= \sqrt{\sigma^2 + 4\tau^2} = \sqrt{(7,505 + 13,521)^2 + 4(6,369^2)} \\ &= 24,583 \text{ psi.} < 68,500 \text{ psi.} \dots \text{ o.k.} \end{aligned}$$

G. Thermal Stresses

Since the structural components of the TN-FSV Basket are all constructed from either SA-240 type 304 stainless steel or SA-693, type 630, condition H1150 stainless steel, having very similar coefficients of thermal expansion, the container thermal stresses are negligible. The following average accident condition component temperatures (Chapter 3) and coefficients of thermal expansion (Ref. 1) are used to compute the maximum component thermal expansions.

Component	Average accident condition temperature (F)	Coefficient of thermal expansion (in. in. <sup>-1</sup> °F <sup>-1</sup> )
Oak Ridge Container wall (Type 304 SST)	252	8.90×10 <sup>-6</sup>
Support Discs, Tie Rods, Poison Enclosures, and Fuel Compartments (Type 304 SST)	261	8.92×10 <sup>-6</sup>
Standoffs (SA-693, Type 630)	261	5.90×10 <sup>-6</sup>
Poison Plates (Borated Aluminum)	261	13.10×10 <sup>-6</sup>
Oak Ridge Containers (Type 304 SST)	261	8.92×10 <sup>-6</sup>
Peach Bottom Canisters (Alloy 6061 Aluminum)	261	13.10×10 <sup>-6</sup>

### Fuel Basket

The difference in axial thermal expansion between the poison plate enclosure (SA-240, type 304) and the standoffs (SA-693, type 630) due to a maximum accident condition temperature change of 191° F (261° F - 70° F) is,

$$\text{Thermal expansion of standoffs} = 20.21 \text{ in.} \times 191^\circ \text{ F} \times 5.90 \times 10^{-6} \text{ in./in. } ^\circ\text{F}^{-1} = 0.0228 \text{ in.}$$

$$\text{Thermal expansion of poison enclosure} = 20.15 \text{ in.} \times 191^\circ \text{ F} \times 8.92 \times 10^{-6} \text{ in./in. } ^\circ\text{F}^{-1} = 0.0343 \text{ in.}$$

$$\text{Difference in thermal expansion} = 0.0343 \text{ in.} - 0.0228 \text{ in.} = 0.0115 \text{ in.}$$

A maximum thermal expansion difference of 0.0115 in. between the poison plate enclosure and the standoffs will not generate a compressive load in the poison enclosure because of the small axial gap (0.020 in., including worst case tolerances) between the poison enclosure and the support discs.

The difference in axial thermal expansion between the poison plates (borated aluminum) and the poison plate enclosures (SA-240, Type 304) due to a maximum accident condition temperature change of 191° F is,

$$\text{Thermal expansion of poison plates} = 20.12 \text{ in.} \times 191^\circ \text{ F} \times 13.10 \times 10^{-6} \text{ in./in. } ^\circ\text{F}^{-1} = 0.0503 \text{ in.}$$

$$\text{Thermal expansion of poison enclosure} = 20.15 \text{ in.} \times 191^\circ \text{ F} \times 8.92 \times 10^{-6} \text{ in./in. } ^\circ\text{F}^{-1} = 0.0343 \text{ in.}$$

$$\text{Difference in thermal expansion} = 0.0503 \text{ in.} - 0.0343 \text{ in.} = 0.0160 \text{ in.}$$

A maximum thermal expansion difference of 0.0160 in. between the poison plates and the poison enclosure will not generate a compressive load in the poison plates, because of the small axial gap (0.028 in., including worst case tolerances) between the poison enclosure and the support discs.

### Payload

The difference in axial thermal expansion between the Oak Ridge Container cavity length and the container's contents (Fuel Basket and Fuel Assemblies) is bounded by the difference in the thermal expansion between the container cavity and the fuel assembly configuration that includes one Peach Bottom Canister and one Oak Ridge Canister. This is because the Peach Bottom Canister is constructed from aluminum alloy 6061.

The axial thermal expansion of the fuel assembly configuration that includes one Peach Bottom Canister and one Oak Ridge Canister due to a maximum accident condition temperature change of 191° F (161° F - 70° F) is,

$$\begin{aligned} \text{Thermal expansion of Peach Bottom Canister} &= 153 \text{ in.} \times 191^\circ \text{ F} \times 13.10 \times 10^{-6} \text{ in./in. } ^\circ \text{F}^{-1} \\ &= 0.3828 \text{ in.} \end{aligned}$$

$$\begin{aligned} \text{Thermal expansion of Oak Ridge Canister} &= 34.75 \text{ in.} \times 191^\circ \text{ F} \times 8.92 \times 10^{-6} \text{ in./in. } ^\circ \text{F}^{-1} = \\ &= 0.0592 \text{ in.} \end{aligned}$$

$$\text{Total fuel assembly configuration thermal expansion} = 0.3828 \text{ in.} + 0.0592 \text{ in.} = 0.4420 \text{ in.}$$

The axial thermal expansion of the Oak Ridge Container cavity (Type 304 SST) due to a maximum accident condition temperature change of 182° F (252° F - 70° F) is,

$$\begin{aligned} \text{Thermal expansion of container cavity} &= 188.00 \text{ in.} \times 182^\circ \text{ F} \times 8.90 \times 10^{-6} \text{ in./in. } ^\circ \text{F}^{-1} = \\ &= 0.3045 \text{ in.} \end{aligned}$$

$$\text{Difference in thermal expansion} = 0.4420 \text{ in.} - 0.3045 \text{ in.} = 0.1375 \text{ in.}$$

A maximum thermal expansion difference of 0.1375 in. between the poison plates and the poison enclosure will not generate a compressive load in the poison plates, because of the axial gap (0.18 in., including worst case tolerances) between the poison enclosure and the support discs.

2.11.1.3 Results

The following tables summarize the maximum calculated and allowable stresses generated in the Oak Ridge SNF Container Fuel Basket during all normal and accident condition events.

<b>Summary of Calculated and Allowable Stress in TN-FSV Container Standoffs, Support Disc, and Fuel Compartments</b>				
<b>Component</b>	<b>Applied Load</b>	<b>Stress Category</b>	<b>Maximum Stress (ksi.)</b>	<b>Allowable Stress (ksi.)</b>
<b>Standoffs</b>	16 g Vertical End drop + Maximum Preload (Normal conditions)	Compression	12.53	45.00
		Buckling	12.53	28.04
	60 g 60° Corner drop + Maximum Preload (Accident conditions)	Compression	39.46	94.50
		Buckling	39.46	46.46
<b>Support discs</b>	16 g End drop (Normal conditions)	Bearing	11.53	23.75
	60 g End drop (Accident conditions)	Bearing	38.46	68.50
<b>Fuel compartment</b>	16 g End drop (Normal conditions)	Compression	1.04	20.00
		Buckling	1.04	5.87
	60 g End drop (Accident conditions)	Compression	3.89	47.95
		Buckling	3.89	11.74
	20 g Side drop (Normal conditions)	Bending	0.83	20.00
	80 g Side drop (Accident conditions)	Bending	3.34	47.95

<b>Summary of Calculated and Allowable Stress in TN-FSV Container Flux Traps, Flux traps, Tie Rods</b>				
<b>Component</b>	<b>Applied Load</b>	<b>Stress Category</b>	<b>Maximum Stress (ksi.)</b>	<b>Allowable Stress (ksi.)</b>
Flux Traps	16 g End drop (Normal conditions)	Compression	2.52	20.00
		Buckling	2.52	10.67
	60 g End drop (Accident conditions)	Compression	9.46	47.95
		Buckling	9.46	21.33
Flux Trap Welds	16 g End drop (Normal conditions)	Compression	4.98	20.00
	60 g End drop (Accident conditions)	Compression	18.67	47.95
Flux Trap Bottom Plate	16 g End drop (Normal conditions)	Bending	0.16	30.00
	60 g End drop (Accident conditions)	Bending	0.59	68.50
Tie Rods	20 g Side drop (Normal conditions) + Maximum Preload	Stress Intensity	15.72	30.00
	80 g Side drop (Accident conditions) + Maximum Preload	Stress Intensity	24.58	68.50

<b>Summary of Calculated and Allowable Stress in TN-FSV Container Poison Enclosure</b>				
<b>Component</b>	<b>Applied Load</b>	<b>Stress Category</b>	<b>Maximum Stress (ksi.)</b>	<b>Allowable Stress (ksi.)</b>
3.268 in. wide plate	20 g Side drop (Normal conditions)	Bending	2.23	20.00
	80 g Side drop (Accident conditions)	Bending	8.93	47.95
Top and bottom support plates	20 g Side drop (Normal conditions)	Compression	2.68	20.00
		Buckling	2.68	10.13
	80 g Side drop (Accident conditions)	Compression	10.73	47.95
		Buckling	10.73	20.25
Top / bottom support plate welds	20 g Side drop (Normal conditions)	Shear	0.57	12.00
	80 g Side drop (Accident conditions)	Shear	2.27	28.77
Inner and outer braces	20 g Side drop (Normal conditions)	Bending	4.27	20.00
	80 g Side drop (Accident conditions)	Bending	17.08	47.95
Outer Brace Weld	20 g Side drop (Normal conditions)	Shear	0.57	12.00
	80 g Side drop (Accident conditions)	Shear	2.27	28.77

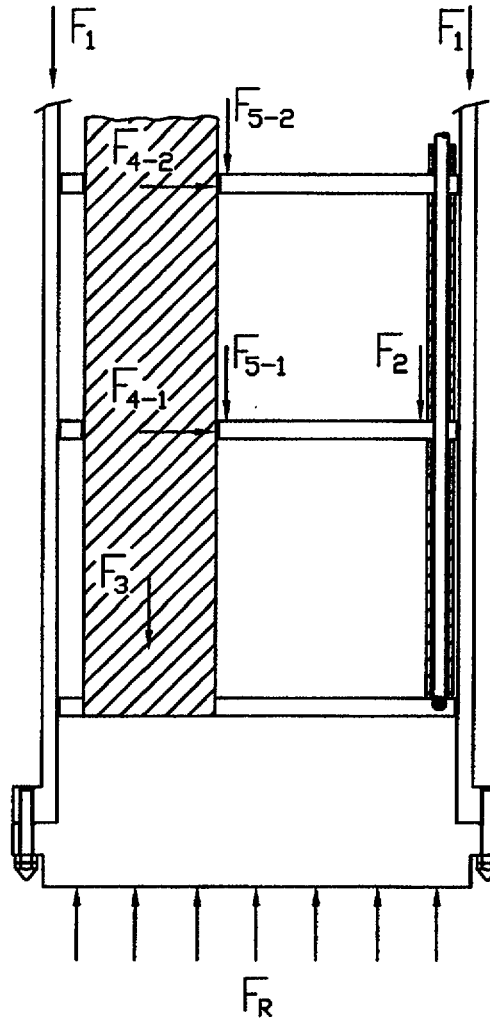
**2.11.1.4 Conclusions**

From the above tables, it can be seen that all of the stresses generated in the Oak Ridge SNF Container Fuel Basket are less than their corresponding allowable stresses.

### 2.11.1.5 References

1. American Society of Mechanical Engineers, ASME Boiler and Pressure Vessel Code, Section II, Part D, 1998.
2. ASME B&PV Code, Section III, Appendix F, 1998.
3. ASME B&PV Code, Section III, Division 1, Subsection NG, 1998.
4. ASME B&PV Code, Section III, Division 1, Subsection NF, 1998.
5. Roark, Raymond J., *Formulas for Stress and Strain*, Fourth Edition, McGraw-Hill Book Company.
6. *Stress Analysis of Closure Bolts for Shipping Casks*, NUREG/CR-6007.
7. Machinery Handbook, 21<sup>st</sup> Edition, Industrial Press, 1979.

**Figure 2.11.1-1**  
**Free Body Diagram of Oak Ridge Container**  
**Subjected to a Vertical or Near Vertical Lid End Drop**



FREE BODY DIAGRAM OF LID END DROP

$F_1$  = INERTIA LOADS OF CONTAINER SHELL + FLANGE + BOTTOM

$F_2$  = INERTIA LOADS OF 8 DISCS + 1.75" THK. CANISTER BOTTOM DISC  
 + 8 POISON ENCLOSURES INCLUDING POISON PLATES

$F_3$  = INERTIA LOADS OF CANISTERS + FLUX TRAPS + FUEL COMPARTMENTS

FOR VERTICAL END DROP

$F_4 = F_5 = 0$

$F_R$  = TOTAL REACTION FORCE =  $F_1 + F_2 + F_3$

FOR DROP ANGLE OTHER THAN VERTICAL END DROP

$F_4 = F_{4-1} + F_{4-2} + F_{4-3} + F_{4-4} + F_{4-5} + F_{4-6} + F_{4-7} + F_{4-8} + F_{4-9}$

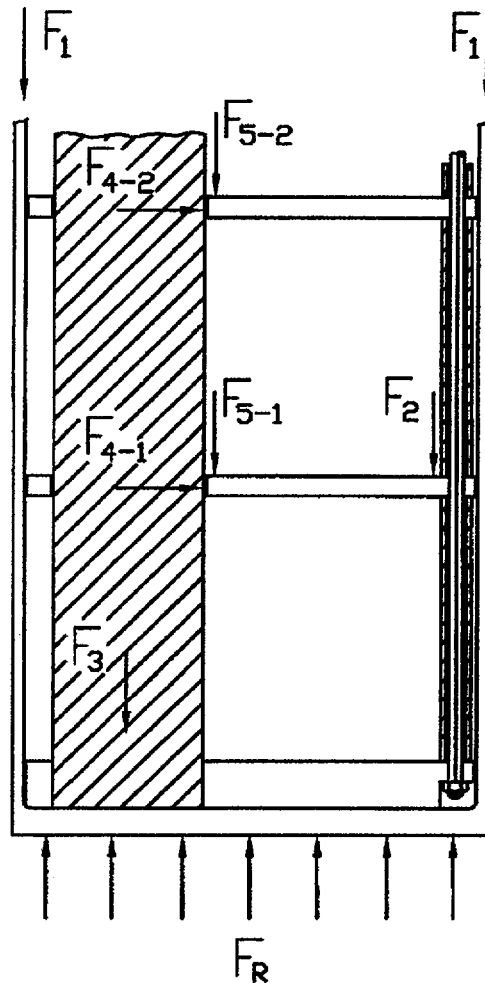
$F_5$  = TOTAL AXIAL FRICTION FORCE

=  $F_{5-1} + F_{5-2} + F_{5-3} + F_{5-4} + F_{5-5} + F_{5-6} + F_{5-7} + F_{5-8} + F_{5-9}$

=  $(F_{4-1} + F_{4-2} + F_{4-3} + F_{4-4} + F_{4-5} + F_{4-6} + F_{4-7} + F_{4-8} + F_{4-9}) \times \mu$

$F_R$  = TOTAL REACTION FORCE =  $F_1 + F_2 + F_3 + F_5$

**Figure 2.11.1-2  
 Free Body Diagram of Oak Ridge Container  
 Subjected to a Vertical or Near Vertical Bottom End Drop**



FREE BODY DIAGRAM OF BOTTOM END DROP

$F_1$  = INERTIA LOADS OF CONTAINER SHELL + FLANGE + LID

$F_2$  = INERTIA LOADS OF 9 DISCS + 8 POISON ENCLOSURES INCLUDING POISON PLATES

$F_3$  = INERTIA LOADS OF CANISTERS + FLUX TRAPS + FUEL COMPARTMENTS

FOR VERTICAL END DROP

$F_4 = F_5 = 0$

$F_R$  = TOTAL REACTION FORCE =  $F_1 + F_2 + F_3$

FOR DROP ANGLE OTHER THAN VERTICAL END DROP

$F_4 = F_{4-1} + F_{4-2} + F_{4-3} + F_{4-4} + F_{4-5} + F_{4-6} + F_{4-7} + F_{4-8} + F_{4-9}$

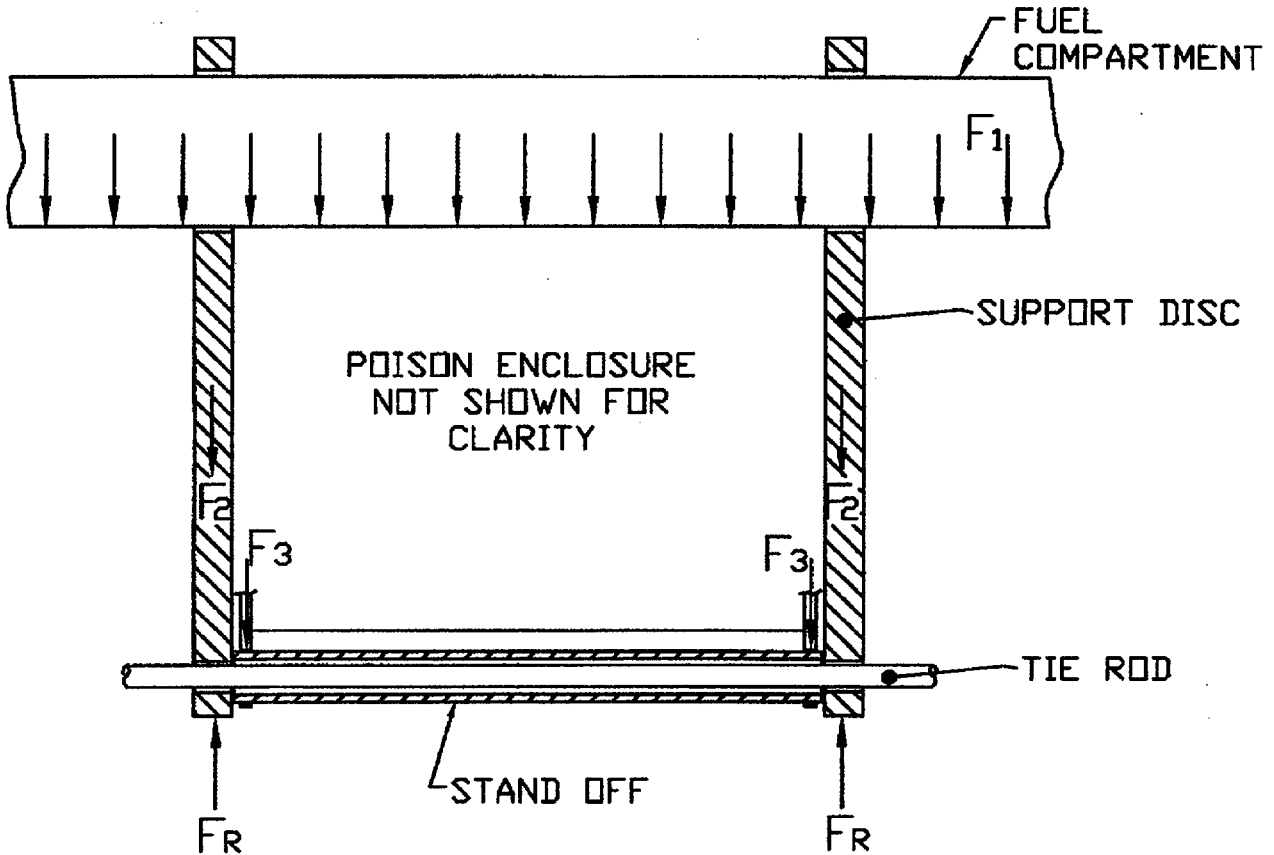
$F_5$  = TOTAL AXIAL FRICTION FORCE

=  $F_{5-1} + F_{5-2} + F_{5-3} + F_{5-4} + F_{5-5} + F_{5-6} + F_{5-7} + F_{5-8} + F_{5-9}$

=  $(F_{4-1} + F_{4-2} + F_{4-3} + F_{4-4} + F_{4-5} + F_{4-6} + F_{4-7} + F_{4-8} + F_{4-9}) \times \mu$

$F_R$  = TOTAL REACTION FORCE =  $F_1 + F_2 + F_3 + F_5$

Figure 2.11.1-3  
Free Body Diagram of Oak Ridge Container Fuel Basket  
Subjected to a Side Drop



FREE BODY DIAGRAM OF SIDE DROP

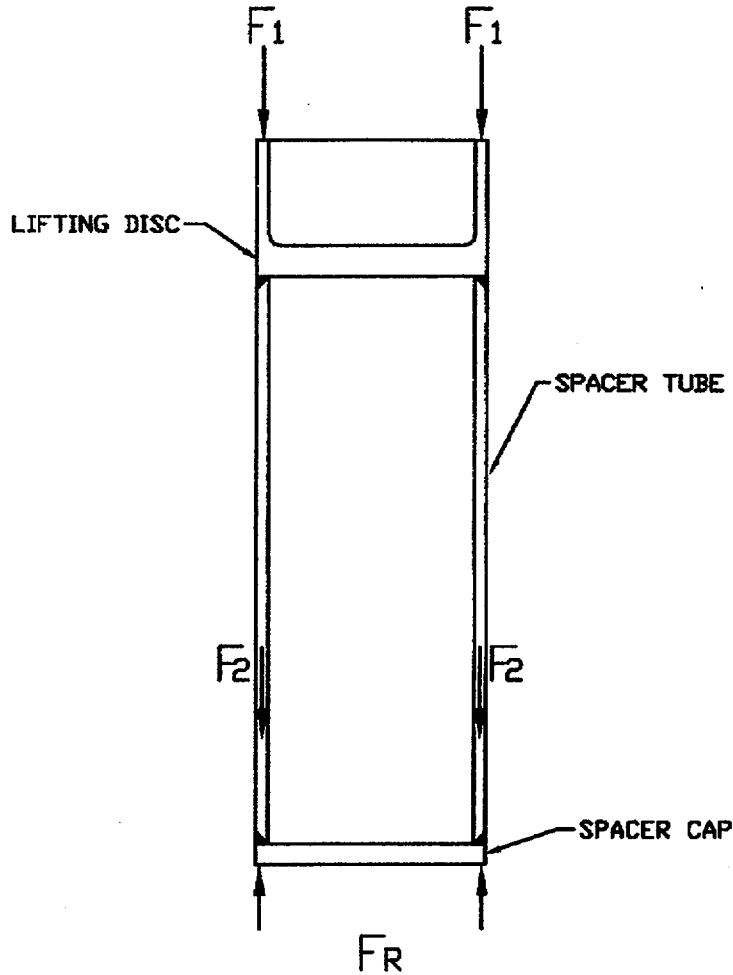
$F_1$  = INERTIA LOADS OF CANISTERS + FUEL COMPARTMENT + FLUX TRAPS

$F_2$  = INERTIA LOADS OF SUPPORT DISC + TIE ROD + STAND OFF

$F_3$  = INERTIA LOADS OF POISON ENCLOSURE + POISON PLATES

$F_R$  = TOTAL REACTION FORCE =  $F_1 + F_2 + F_3$

**Figure 2.11.1-4**  
**Free Body Diagram of Oak Ridge Container**  
**Flux Trap Subjected to a Lid End Drop**



FREE BODY DIAGRAM OF BOTTOM FLUX TRAP DURING BOTTOM END DROP

$F_1$  = TOTAL INERTIA LOAD OF CANISTERS + FLUX TRAPS ABOVE

$F_2$  = INERTIA LOAD OF BOTTOM FLUX TRAP

$F_R$  = TOTAL REACTION FORCE =  $F_1 + F_2$

**APPENDIX 2.11.2**  
**TABLE OF CONTENTS**

	<u>Page</u>
2.11.2 OAK RIDGE CONTAINER SHELL STRUCTURAL ANALYSIS .....	2.11.2-1
2.11.2.1 Approach.....	2.11.2-1
2.11.2.2 Analysis.....	2.11.2-3
2.11.2.3 Results.....	2.11.2-10
2.11.2.4 Conclusions .....	2.11.2-10
2.11.2.5 References.....	2.11.2-11

**APPENDIX 2.11.2**

**OAK RIDGE CONTAINER SHELL STRUCTURAL ANALYSIS**

**2.11.2.1 Approach**

The purpose of this appendix is to evaluate the structural adequacy of the Oak Ridge Container shell when subjected to internal pressure, external pressure, thermal stress, and end drop loads. Finite element models are used for the container shell normal and accident condition side drop stress analyses, and are described in Appendix 2.11.3. The container shell is conservatively assumed to be unstiffened, despite the 10 support discs that are located inside the container. The maximum operating temperature is taken to be 250° F (Section 2.6.1.1).

The applied loads analyzed in this calculation are as follows. All loads are assumed to be at 250° F unless otherwise noted.

- The following normal and accident conditions internal and external pressures. For internal pressure, conservatively assume the TN-FSV cask cavity is at 0 psig, and for external pressure, conservatively assume the Oak Ridge Container cavity is at 0 psig.

Loading Conditions		Calculated Pressures (psig) (Section 4.2.2)	Conservatively Increased Pressure Used for Analysis (psig)
Normal Conditions (Level A)	Internal Pressure	3.1 (Section 4.2.2)	5.0
	External Pressure	2.8 (Section 4.2.2)	5.0
Accident Conditions (Level D)	Internal Pressure	5.3 (Section 4.3.1)	10.0
	External Pressure	5.0 (Section 4.3.1)	10.0

- Thermal stress due to maximum temperature change of 180° F (250° F – 70° F room temperature, Section 2.6.1.1).
- The following accelerations due to normal and accident condition end and side drops (TN-FSV SAR Appendix 2.10.2), including 1.10 Dynamic Amplification Factor (Appendix 2.11.6).

### Summary of Applied Load Caused by Free Drop Event

Impact Load	Normal Conditions (1 foot drop)	Accident Conditions (30 foot drop)
Axial g load (end drop)	$14 \text{ gs} \times 1.10 \approx 16 \text{ gs.}$	$54 \text{ gs} \times 1.10 \approx 60 \text{ gs.}$
Transverse g load (side drop)	$17 \text{ gs} \times 1.10 \approx 20 \text{ gs.}$	$71 \text{ gs} \times 1.10 \approx 80 \text{ gs.}$

Properties of Oak Ridge Container shell material (SA-240 Type 304 stainless steel) at room temperature and 250° F are taken from reference 2 and are as follows.

### Oak Ridge Container Shell Material Properties

	Room Temperature (-20.0° F to 100° F)	250° F.
$S_m$ (ksi)	20.0	20.0
$S_y$ (ksi)	30.0	23.75
$S_u$ (ksi)	75.0	68.5
$E$ (psi)	$28.3 \times 10^6$	$27.3 \times 10^6$

The design criteria are described in Chapter 2. The basis for the Oak Ridge Container shell stress allowable is Section III, Division 3, Subsection WB<sup>(4)</sup> for normal condition loads and Appendix F<sup>(3)</sup> for accident loads. The allowable stresses are as follows:

### Summary of Allowable Stresses

Stress Category	Normal Conditions (Level A)	Accident Conditions (Level D)
Primary membrane (general), $P_m$	$S_m$ , (20.0 ksi.)	Lesser { $2.4 S_m$ , $0.7 S_u$ } (47.95 ksi.)
Primary membrane + bending, $P_m + P_b$	$1.5 S_m$ , (30.0 ksi.)	Lesser { $3.6 S_m$ , $S_u$ } (68.5 ksi.)
Bearing Stress	$S_y$ , (23.75 ksi.)	$S_y$ , (23.75 ksi.)
Pure shear stress	$0.6 S_m$ , (12 ksi.)	$0.42 S_u$ , (28.77 ksi.)

### 2.11.2.2 Analysis

#### A) Oak Ridge Container Shell (Appendix 1.4, Drawing 3044-70-2, Item 2, 3, 4, and 5 weldment)

##### 1. Shell Compressive Stress due to End Drop

The inertial load applied to the container shell, during a 30 ft. end drop, is conservatively calculated using the maximum weight of the container and lid (Section 2.2). The corresponding applied force under accident conditions,  $F_{axial}$ , is,

$$F_{axial} = [540 \text{ lb. (container shell weight)} + 488 \text{ lb. (lid weight)}] \times 60 \text{ gs} = 61,680 \text{ lb.}$$

The cross sectional area,  $A$ , of the container shell is the following.

$$A = \frac{\pi}{4} [D_o^2 - D_i^2] = \frac{\pi}{4} [16.85^2 - 16.58^2] = 7.089 \text{ in.}^2$$

Therefore, the accident condition compressive stress applied to the container shell during a 30 ft. end drop is,

$$\sigma_a = P / A = 61,680 \text{ lb.} / 7.089 \text{ in.}^2 = 8,701 \text{ psi.} < 47,950 \text{ psi.} \dots \text{o.k.}$$

For normal conditions,

$$\sigma_n = 8,701 \text{ psi.} \times 16 \text{ gs} / 60 \text{ gs} = 2,320 \text{ psi.} < 20,000 \text{ psi.} \dots \text{o.k.}$$

##### 2. Shell Buckling due to Compressive Stress

The allowable axial buckling stress,  $F_a$ , for normal conditions (Level A) is calculated in accordance with reference 5, Section NF-3322.1 (c) (2).

The moment of inertia,  $I$ , of the container shell section is,

$$I = \frac{\pi}{64} [D_o^4 - D_i^4] = \frac{\pi}{64} [16.85^4 - 16.58^4] = 247.595 \text{ in.}^4$$

The radius of gyration,  $r$ , of the container shell section is,

$$r = \left( \frac{I}{A} \right)^{1/2} = \left( \frac{247.595}{7.089} \right)^{1/2} = 5.910 \text{ in.}$$

From reference 5,

$$\frac{Kl}{r} = \frac{(1)(198.00)}{5.910} = 33.503 < 120 \text{ therefore,}$$

$$F_a = S_y \left( 0.47 - \frac{Kl/r}{444} \right) = 23,750 \left( 0.47 - \frac{33.503}{444} \right) = 9,370 \text{ psi.} > 2,320 \text{ psi. ... o.k.}$$

As per reference 3, Section F-1334, for accident conditions (Level D), the allowable axial buckling stress,  $F_a$ , can be increased by the following factor.

Since  $S_u > 1.2 S_y$  (68.5 ksi. > 28.5 ksi.),  $F_a$  can be increased by,

$$\text{Lesser of } \{ 2 \text{ or } 1.167 S_u / S_y \} = 2.$$

Therefore, for accident conditions,

$$F_a = 9,370 \times 2 = 18,740 \text{ psi.} > 8,701 \text{ psi. ... o.k.}$$

### 3. Shell Stress due to Side Drop

The stress generated by an 80 g side drop in the container shell is computed using finite element analysis provided in Appendix 2.11.3.

### 4. Shell Stress due to Internal and External Pressure

The hoop stress,  $\sigma_{hoop}$ , generated by internal or external pressure is governed by the following formula.

$$\sigma_{hoop} = \frac{PR}{t}$$

Where  $P$  is the internal or external pressure applied,  $R$ , is the mean radius of the shell, and  $t$  is the shell thickness. For an assumed internal/external pressure of 5 psi. (normal conditions), the corresponding hoop stress,  $\sigma_{np}$ , is,

$$\sigma_{np} = \frac{(5)(8.358)}{0.135} = 310 \text{ psi.} < 20,000 \text{ psi. ... o.k.}$$

For an assumed internal/external pressure of 10 psi. (accident conditions), the corresponding hoop stress,  $\sigma_{ap}$ , is,

$$\sigma_{ap} = \frac{(10)(8.358)}{0.135} = 619 \text{ psi.} < 47,950 \text{ psi.} \dots \text{o.k.}$$

### 5. Shell Buckling due to External Pressure

The analytical method provided in ASME Code Case N-284-1 is used to determine the adequacy of the container shell with respect to buckling due to external pressure.

Since the vessel is assumed to be unstiffened, only the theoretical buckling calculation for unstiffened shells or local buckling between stiffeners of stiffened shells applies (Ref. 1, Section 1712.1).

#### Notation:

The following notation is taken from reference 1, Section -1200.

- Subscripts  $\phi$  and  $\theta$  = axial (meridional) and circumferential directions respectively.
- $l_{\phi}$  = distances between lines of support in the axial direction, use 193.00 in.
- $R$  = shell radius, mean radius = [16.58 inner diameter + 16.85 outer diameter] / 4 = 8.358 in.
- $t$  = shell thickness, 0.135 in.
- $M_{\phi} = \frac{l_{\phi}}{\sqrt{(R)(t)}}$
- $C_{\theta n}$  = elastic buckling coefficient.
- $\sigma_{heL}$  = local theoretical elastic instability stress in the hoop direction for cylinders under external pressure, psi.
- $E$  = modulus of elasticity of the material at design temperature,  $27.3 \times 10^6$  psi. @ 250° F,  $28.3 \times 10^6$  psi. @ room temperature (Ref. 3).
- $\alpha_{\theta L}$  = capacity reduction factor to account for the difference between classical theory and predicted instability stresses for fabricated shells.
- $\sigma_y$  = tabulated yield stress of material at design temperature, 23,750 psi. @ 250° F (Ref. 3).
- $\sigma_{ha}$ ,  $\sigma_{rc}$ , allowable stresses for elastic and inelastic buckling respectively, psi.
- $FS$  = factor of safety, 2 for normal conditions, 1.34 for accident conditions (Ref. 1, Section -1400 (a)).

Theoretical Buckling Value:

Local Buckling (Ref. 1, Section -1712.1.1 (b) (2)):

$$(\sigma_\phi = 0.5 \sigma_\theta)$$

$$M_\phi = \frac{l_\phi}{\sqrt{(R)(t)}} = \frac{193.00}{\sqrt{(8.358)(0.135)}} = 181.69 \text{ in.}$$

$$\frac{R}{t} = \frac{8.358}{0.135} = 61.91, \quad 1.65 \frac{R}{t} = 102.15$$

$$\Rightarrow M_\phi \geq 1.65 \frac{R}{t}$$

Therefore,

$$C_{\theta h} = 0.275 \frac{t}{R} + \frac{2.1}{M_\phi^4} \left( \frac{R}{t} \right)^3 = 0.275 \frac{0.135}{8.358} + \frac{2.1}{181.69^4} \left( \frac{8.358^3}{0.135} \right) = 0.005$$

At 250° F,

$$\Rightarrow \sigma_{heL} = C_{\theta h} \frac{(E)(t)}{R} = 0.005 \frac{(27.3 \times 10^6)(0.135)}{8.358} = 2,204 \text{ psi.}$$

Capacity Reduction Factor ( $\alpha_{\theta L}$ ):

From reference 1, Section -1511 (b), for local buckling of cylindrical shells, stiffened or unstiffened under hoop compression,

$$\alpha_{\theta L} = 0.8.$$

Plasticity Reduction Factor ( $\eta_\phi$ ):

The plasticity reduction factor is computed based on the formulae provided in reference 1, Section -1611 (b) as follows.

At 250° F,

$$\Delta = \frac{\alpha_{\theta L} \sigma_{heL}}{\sigma_y} = \frac{(0.8)(2,204)}{23,750} = 0.0742$$

Since  $\Delta \leq 0.55$ ,

$$\eta_{\phi} = 1.0.$$

Allowable Buckling Stress:

Elastic buckling interaction equations (Ref. 1, Section -1713.1.1):

At 250° F,

$$\sigma_{ha} = \frac{(\alpha_{\theta L})(\sigma_{heL})}{FS} = \frac{(0.8)(2,204)}{2} = 882 \text{ psi.}$$

Inelastic buckling interaction equations for external pressure only (Ref. 1, Section -1713.2.1):

In the following equation,  $\sigma_{ha}$  (allowable elastic buckling stress under hydrostatic pressure) is used in place of  $\sigma_{ra}$  (allowable elastic buckling stress under radial pressure) since reference 1, Section -1713.2.1 equations account for radial external pressure only.

At 250° F,

$$\sigma_{rc} = \eta_{\theta} \sigma_{ra} = (1.0)(882) = 882 \text{ psi.}$$

For accident conditions, at 250° F,

$$\sigma_{rc} = 882 \text{ psi.} \times (2.0 \text{ normal condition F.S.} / 1.34 \text{ accident condition F.S.}) = 1,316 \text{ psi.}$$

Allowable Applied External Pressure:

Based on classical mechanics, an applied external pressure,  $P$ , generates the following hoop stress,  $\sigma_{hoop}$ , in a cylindrical shell.

$$\sigma_{hoop} = \frac{PR}{t}.$$

Based on the allowable inelastic buckling stress,  $\sigma_{rc}$ , calculated above, the allowable applied external pressure,  $P_{allowable}$ , is the following.

At 250° F, for normal conditions,

$$P_{allowable} = \frac{(\sigma_{rc})(t)}{R} = \frac{(882)(0.135)}{8.358} = 14.3 \text{ psi.} > 5 \text{ psi.} \dots \text{ o.k.}$$

At 250° F, for accident conditions,

$$P_{allowable} = 14.3 \times (2.0 \text{ normal F.S.} / 1.34 \text{ accident F.S.}) = 21.3 \text{ psi.} > 10 \text{ psi.} \dots \text{o.k.}$$

## B) Container Shell Bottom Plate

### 1. Stress due to External Pressure

The maximum stress in the bottom plate of the container shell is taken to be the compressive stress,  $P_m$ , at the intersection of the bottom plate and the container shell combined with the bending stress,  $P_b$ , at the outer edge of the bottom plate. The applied load is taken to be 5 psi. internal/external pressure under normal conditions, and 10 psi. internal/external pressure under accident conditions.

#### Bending Stress:

The maximum bending stress at the outer edge of the container bottom plate, subjected to internal/external pressure, is calculated using the following formula given in reference 6, page 217, Table X, Case 6.

$$P_b = \frac{3W}{4\pi t^2}.$$

Where  $W$  is the total force on the bottom plate generated by the pressure, and  $t$  is the thickness of the bottom plate, 1.00 in., Therefore,

For normal conditions,

$$W = (\pi/4 \times 16.85^2) \text{ in.}^2 \times 5 \text{ psi.} = 1,115 \text{ lb.,}$$

$$P_b = \frac{3 \times 1,115}{4\pi \times 1.00^2} = 266.2 \text{ psi.}$$

For accident conditions,

$$P_b = 266.2 \text{ psi.} \times (10 \text{ psi.} / 5 \text{ psi.}) = 532.4 \text{ psi.}$$

### Compressive Stress:

The compressive stress at the intersection of the bottom plate and the container shell is taken to be the total force acting on the bottom plate,  $W$ , divided by the cross sectional area of the container shell,  $A = 7.089 \text{ in.}^2$ . Therefore,

For normal conditions,

$$P_m = \frac{W}{A} = \frac{1,115}{7.089} = 157.3 \text{ psi.} < 20,000 \text{ psi.} \dots \text{ o.k.}$$

The combined membrane and bending stress is,

$$P_m + P_b = 157.3 \text{ psi.} + 266.2 \text{ psi.} = 423.5 \text{ psi.} < 30,000 \text{ psi.} \dots \text{ o.k.}$$

For accident conditions,

$$P_m = 157.3 \text{ psi.} \times (10 \text{ psi.} / 5 \text{ psi.}) = 314.6 \text{ psi.} < 47,950 \text{ psi.} \dots \text{ o.k.}$$

$$P_m + P_b = 314.6 \text{ psi.} + 532.4 \text{ psi.} = 847.0 \text{ psi.} < 68,500 \text{ psi.} \dots \text{ o.k.}$$

### C) Thermal Stress Analysis

Since the container shell, flange, bottom and lid are all constructed from SA-240 type 304 stainless steel, there will be very little stresses generated by thermal expansion. Stresses generated in the closure lid bolts by thermal expansion are analyzed in Appendix 2.11.4.

The TN-FSV cask is also fabricated from Type 304 stainless steel. Consequently, the Oak Ridge Container and the TN-FSV cask body expand at the same rate. No Interference between the Oak Ridge Container and the TN-FSV cask body occurs.

**2.11.2.3 Results**

The following table summarizes the applied and allowable stresses generated in the Oak Ridge Container during all conceivable normal and accident condition events.

<b>Summary of Calculated and Allowable Stress in the Oak Ridge Container Shell</b>				
<b>Component</b>	<b>Applied Load</b>	<b>Stress Category</b>	<b>Maximum Stress (ksi.)</b>	<b>Allowable Stress (ksi.)</b>
Container shell	16 g End drop (Normal conditions)	Compression	2.32	20.00
		Buckling	2.32	9.37
	60 g End drop (Accident conditions)	Compression	8.70	47.95
		Buckling	8.70	18.74
	5 psi. internal & external pressure (Normal conditions)	Hoop	0.31	20.00
		Buckling	0.31	0.88
	10 psi. internal & external pressure (Accident conditions)	Hoop	0.62	47.95
		Buckling	0.62	1.32
Container bottom plate	5 psi. internal & external pressure (Normal conditions)	Compression	0.16	20.00
		Bending + Compression	0.42	30.00
	10 psi. internal & external pressure (Accident conditions)	Compression	0.31	47.95
		Bending + Compression	0.85	68.50

**2.11.2.4 Conclusions**

From the above table, it can be seen that all of the stresses generated in the Oak Ridge Container shell are less than their corresponding allowable stresses.

### 2.11.2.5 References

1. Cases of ASME Boiler and Pressure Vessel Code, Case N-284-1, Metal Containment Shell Buckling Design Methods, Section III, Division 1, Class MC, 1995.
2. American Society of Mechanical Engineers, ASME Boiler and Pressure Vessel Code, Section II, Part D, 1998.
3. ASME B&PV Code, Section III, Division 3, Subsection WB, 1998.
4. ASME B&PV Code, Section III, Appendix F, 1998.
5. ASME B&PV Code, Section III, Division 1, Subsection NF, 1998
6. Roark, Raymond J., Formulas for Stress and Strain, Fourth Edition, McGraw-Hill Book Company.
7. Machinery Handbook, 21<sup>st</sup> Edition, Industrial Press, 1979.

**APPENDIX 2.11.3**  
**TABLE OF CONTENTS**

	<u>Page</u>
2.11.3 SUPPORT DISC AND CONTAINER SHELL FINITE ELEMENT MODEL ANALYSIS.....	2.11.3-1
2.11.3.1 Introduction .....	2.11.3-1
2.11.3.2 Finite Element Model Description .....	2.11.3-4
2.11.3.3 Side Drop Analysis.....	2.11.3-4
2.11.3.4 Thermal Stress Analysis .....	2.11.3-8
2.11.3.5 Conclusions .....	2.11.3-8
2.11.3.6 References.....	2.11.3-9

**LIST OF TABLES**

2.11.3-1 Summary of Normal Condition Stress Analysis.....	2.11.3-10
2.11.3-2 Summary of Accident Condition Stress Analysis .....	2.11.3-11

**LIST OF FIGURES**

2.11.3-1 Finite Element Model of Support Disc and Container .....	2.11.3-12
2.11.3-2 Gap Sizes between Support Disc and Container Shell .....	2.11.3-13
2.11.3-3 Gap Sizes between Container Shell and TN-FSV Cask Wall .....	2.11.3-14
2.11.3-4 Finite Element Model For 0° Side Drop Analysis with Boundary Conditions.....	2.11.3-15
2.11.3-5 Finite Element Model for 36° Side Drop Analysis with Boundary Conditions.....	2.11.3-16
2.11.3-6 Finite Element Model for End Drop Analysis with Boundary Conditions.....	2.11.3-17
2.11.3-7 Stress Intensity for 1g End Drop .....	2.11.3-18
2.11.3-8 Support Disc Stress Intensity for 20g, 0° Side Drop.....	2.11.3-19
2.11.3-9 Container Shell Stress Intensity for 20g, 0° Side Drop.....	2.11.3-20
2.11.3-10 Support Disc Stress Intensity for 20g, 36° Side Drop.....	2.11.3-21
2.11.3-11 Container Shell Stress Intensity for 20g, 36° Side Drop.....	2.11.3-22
2.11.3-12 Support Disc Stress Intensity for 80g, 0° Side Drop.....	2.11.3-23
2.11.3-13 Container Shell Stress Intensity for 80g, 0° Side Drop.....	2.11.3-24
2.11.3-14 Support Disc Stress Intensity for 80g, 36° Side Drop.....	2.11.3-25
2.11.3-15 Container Shell Stress Intensity for 80g, 36° Side Drop.....	2.11.3-26
2.11.3-16 Support Disc Thermal Stress Intensity .....	2.11.3-27

## APPENDIX 2.11.3

### SUPPORT DISC AND CONTAINER SHELL FINITE ELEMENT MODEL ANALYSIS

#### 2.11.3.1 Introduction

The purpose of this appendix is to determine the stresses and buckling load capacity of Oak Ridge Container support disc and container shell due to end and side drop impact loads under normal and accident conditions.

The Oak Ridge Container is designed to transport a payload consisting of Oak Ridge canisters and Peach Bottom fuel assemblies. The basket consists of five fuel compartments, nine poison enclosure weldments, and ten support discs.

The stainless steel support discs laterally support the fuel compartments, canisters, and Peach Bottom assemblies. The discs are laterally supported by the container shell inner surface. The nine support discs are 16.4 inches in diameter, 0.75 in. thick and have five holes to accommodate the 5 inch diameter fuel compartments. The bottom support disc has the same geometry but is 1.75 in thick. The support discs are spaced 20.59 in. center-to-center and are kept in place axially by five tie rod and standoff assemblies. The tie rods and standoffs are positioned near the periphery of each disc.

The basket fuel compartment wall thickness is established to meet heat transfer, nuclear criticality, and structural requirements. The basket structure must provide sufficient rigidity to maintain a subcritical configuration under the applied loads.

#### A) Material Properties

Both the support discs and container shell are fabricated from SA-240, Type 304 or SA-182 F304 stainless steel. The material properties of the 304 stainless plate are taken from the ASME Code, Section II, Part D<sup>(1)</sup>. The applicable material properties of the SA-240 Type 304 and SA-182 F304 stainless steel at 250° F are as follows.

#### Summary of Material Properties

$S_m$ (ksi)	20.0
$S_y$ (ksi)	23.75
$S_u$ (ksi)	68.5
$E$ (psi)	$27.3 \times 10^6$

## B) Design Criteria

### Normal Conditions

The basis for the support disc allowable stress is ASME Code, Section III, Subsection NG<sup>(2)</sup>, and ASME Code, Section III, Subsection WB<sup>(3)</sup> for the container shell. Therefore the primary membrane and primary membrane plus bending stress intensities for both the basket and container shell are limited to  $S_m$  ( $S_m$  is the code allowable stress intensity) and  $1.5 S_m$ , respectively. The ASME Code provides a  $3 S_m$  limit on primary plus secondary stress intensity for Level A conditions. This stress intensity is derived from the highest value at any point across the thickness of a section of the general or local primary membrane stresses, plus primary bending stresses plus secondary stresses, produced by the specified service pressure and other specified mechanical loads and by general thermal effects associated with normal Service Conditions. The following table summarizes the stress limits for both the container support discs and container shell for normal conditions (Level A).

### **Basket Structural Design Criteria for Normal Conditions**

<b>Numerical Values of Primary Stress Intensity Limits</b>			
<b>Stress Category</b>	<b>Stress Limit</b>	<b>Type 304 SS at 250°F (ksi)</b>	<b>ASME Reference</b>
Membrane Stress Intensity, $P_m$	$S_m$	20.0	NG-3221.1 <sup>(2)</sup> NB-3221.1 <sup>(3)</sup>
Membrane + Bending Stress Intensity, $P_m + P_b$	$1.5 S_m$	30.0	NG-3221.2 <sup>(2)</sup> NB-3221.3 <sup>(3)</sup>
Primary + Secondary Stress, $P_m + P_b + Q$	$3 S_m$	60.0	NG-3222.2 <sup>(2)</sup> NB-3222.2 <sup>(3)</sup>

### Accident Conditions

The hypothetical impact accidents are evaluated as short duration Level D conditions. The basis for the accident condition allowable stresses for both the support discs and container shell is ASME, Section III, Appendix F<sup>(4)</sup>. When evaluating the results of the non-linear elastic/plastic analysis for accident conditions, the general primary membrane stress intensity,  $P_m$ , shall not exceed  $0.7 S_u$  and the maximum primary stress intensity (membrane plus bending) is limited to  $0.90 S_u$ . The average primary shear stress is limited to  $0.42 S_u$ .

### Basket Structural Design Criteria for Accident Conditions

Numerical Values of Primary Stress Intensity Limits			
Stress Category	Stress Limit	Type 304 SS at 250°F (ksi)	ASME Reference
Membrane Stress Intensity, $P_m$	$0.7S_u$	47.95	Appendix F F-1341.2 (a) <sup>(4)</sup>
Membrane + Bending Stress Intensity, $P_m + P_b$	$0.9 S_u$	61.65	Appendix F F-1341.2 (b) <sup>(4)</sup>
<u>2.11.1.1</u> <u>Averag</u> <u>e</u> <u>Shear</u> <u>Stress</u>	$0.42 S_u$	24.0	Appendix F F-1341.2 (c) <sup>(4)</sup>

#### C) Applied Loads

The applied loads analyzed in this appendix are the following accelerations due to normal and accident condition end and side drops (TN-FSV SAR Appendix 2.10.2), including 1.10 Dynamic Amplification Factor (Appendix 2.11.6). All loads are assumed to be at 250° F.

#### Summary of Applied Load Caused by Free Drop Event

Impact Load	Normal Conditions (1 foot drop)	Accident Conditions (30 foot drop)
Axial g load (end drop)	$14 \text{ gs} \times 1.10 \approx 16 \text{ gs.}$	$54 \text{ gs} \times 1.10 \approx 60 \text{ gs.}$
Transverse g load (side drop)	$17 \text{ gs} \times 1.10 \approx 20 \text{ gs.}$	$71 \text{ gs} \times 1.10 \approx 80 \text{ gs.}$

### 2.11.3.2 Finite Element Model Description

A two-dimensional finite element model of the support disc and adjoining container shell is constructed using Plane 42, 2-D structural solid (with thickness option) elements. The finite element model of the structure is shown in Figure 2.11.3-1. The fuel canister and fuel compartments are not included in the model. However, their weight is accounted for by applying radial pressure at the inside edge of the support disc holes. All weights are taken from Section 2.2.

The support disc dimensions, within tolerances, that result in maximum stresses in a disc web are chosen. Gap elements (Contact 52) are used to simulate the interface between the support disc and inside surface of container shell as well as between outside surface of container shell and inside surface of TN-FSV cask. The gap nodes specified at the inside surface of the TN-FSV cask are restrained in both  $x$  and  $y$  directions. The gap size at each gap element is determined by the difference between the support disc outside diameter and the inside diameter of the container shell and by the difference between the outer side diameter of container shell and the inside diameter of the TN-FSV cask. The gap sizes are shown in Figures 2.11.3-2 and 2.11.3-3. The gap element spring constant,  $K_n$ , is calculated in the following way.

$$K_n = f E h^{(5)}$$

Where,  $f$  is the thickness used in 2-D plane stress model (0.75 in.),  $E$  is the Modulus of elasticity ( $27.3 \times 10^6$  psi), and  $h$  is a constant usually between 0.01 to 100. So,

$$\underline{2.11.1.2 \quad K_n = 0.205 \times 10^6 \text{ to } 2,050 \times 10^6 \text{ lb/in}}$$

The spring constant used for the gap elements is  $1.0 \times 10^6$  lb/in. This value is chosen to result in good convergence.

The support disc temperature is taken to be 250° F (Section 3.4). The support disc is assumed to have  $10^0$  initial contact with the container shell during side drop analyses.

### 2.11.3.3 Side Drop Analysis

Two side drop orientations, 0° and 36°, are used to characterize the most extreme cases possible so that all possible side drop orientations are bounded. During 0° side drop, the disc is symmetric about the drop axis. Thus, only one-half finite element is used. The finite element model including loading and boundary conditions for the 0° side drop is shown in Figure 2.11.3-4. For 36° side drop, a full finite element model is employed (see Figure 2.11.3-5).

The lateral impact load applied to the support disc and container shell during a side drop accident includes the inertial weights of the fuel canisters, the fuel compartment, and the support disc itself. The inertial loading due to the weight of the fuel canisters and fuel compartments are applied as equivalent pressure on the inside surfaces of the support disc holes.

The inertial loading of the container shell and the support disc is accounted for by applying a body acceleration. The loadings for a 1 g side drop are computed below.

Total load on all 10 discs = 741 lb.(fuel compartments) + 189 lb.(flux traps) + 1,600 lb.  
(fuel assemblies) = 2,530 lbs. ...conservatively use 3,000 lb.

Assuming the support discs at each end only carry ½ load of the intermediate discs,

Load on each intermediate disc =  $3,000/9 = 333.3$  lb.

Load per disc hole =  $333.3/5 = 66.7$  lb.

Pressure on support disc hole (dispersed over 60°) =  $66.7 / [t 2R\sin(30)]$   
=  $66.7 / [0.75 \times 2 \times 2.8435 \sin(30)]$   
= 31.28 psi.

## A) Normal Condition Stress Analysis

A non-linear elastic analysis was conducted with the gap elements for both 0° and 36° normal condition side drops. A pressure and acceleration corresponding to 20 gs was applied to the model. The nodal stress intensities and deformed geometry of the support disc and container shell for 0° and 36° load cases are plotted in Figures 2.11.3-8 through 2.11.3-11. The maximum nodal stresses were linearized in order to extract the primary membrane and bending stress intensities. The results of the normal condition side drop stress analysis are presented in Table 2.11.3-1. The calculated stresses shown in Table 2.11.3-1 are linearized in order to obtain both bending and membrane stresses.

## B) Accident Condition Stress and Buckling Analysis

### 1. Buckling Analysis

A nonlinear elastic/plastic stress analysis of the support disc is conducted in order to compute the buckling loads and stresses for both 0° and 36° side drop orientations. The following types of nonlinearities are considered in the analysis:

### 2. Geometric Nonlinearities

Since the structure experiences large deformations before buckling, the large displacement option in ANSYS is used. The deflections during each load step are used to continuously redefine the geometry of the structure, thus producing a revised stiffness matrix, so the buckling can be analyzed. If the rate of change in deflection, per iteration, is observed, an estimation of the stability of the structure can be made. In particular, if the rate of change of displacement at any node is increasing, the loading is above critical and the structure will eventually buckle.

### 3. Material Nonlinearities

The disc is constructed from SA-240, Type 304 or SA-182 F304 stainless steel. A bilinear stress strain relationship is used to simulate the correct nonlinear material behavior. The following elastic and inelastic material properties are used in the analysis:

#### **Material Properties Used in the Finite Element Structural Analysis**

<b>SA-240, Type304 Stainless Steel, @ 250°F. <sup>(1)</sup></b>	
Modulus of Elasticity (psi)	$27.3 \times 10^6$
Yield Strength (psi)	23,800
Ultimate Strength (psi)	68,500
Tangent Modulus (psi)	112,000

### 4. Gap Element Nonlinearities:

Gap elements (Contact 52) are used to model the actual surface clearances between the support disc and container shell, as well as between container shell and cask inside surface. The gap elements introduce nonlinearities since they only apply a force to the model if they are closed.

A maximum load of 160g was applied in each analysis. The automatic time stepping program option "Autots" was activated. This option lets the program decide the actual size of the load-substep for a converged solution. The program stops at the load substep that fails to result in a converged solution. The last load step, with a converged solution, can be used to calculate the collapse load (Reference 4, Section III, Appendix F, Section F-1341.3). However, for both 0 and 36 degree load runs, the disc did not buckle for the maximum applied g (160) load. Therefore, there is no possibility of disc buckling at the 80-g accident condition load.

### **C) Stress Analysis**

The results of the elastic/plastic analysis were used to evaluate the stresses in the support disc and container shell for both 0° and 36° accident condition side drops. The inelastic runs were made up to 160g load, but the results at the 80g load step were extracted so that the stresses due to an accident condition side drop could be evaluated. The maximum nodal stresses were linearized in order to extract the primary membrane and bending stress intensities. The results of the accident condition side drop stress analysis are presented in Table 2.11.3-2. The calculated stresses shown in Table 2.11.3-2 are linearized in order to obtain both bending and membrane stresses. Figures 2.11.3-12 through 2.11.3-15 show stress intensity plots from the 0° and 36° accident condition side drop analysis.

The disc and container shell finite element model was modified by using three-dimensional elastic SHELL63 elements, since a third degree-of-freedom was needed to apply axial loads in z-direction. The container shell and gap elements have no effect on the end drop results and were consequently deleted from the model (the container shell due to end drop load is analyzed separately in Appendix 2.11.2). The finite element model was supported at the five tie rod locations. At each tie-rod location, model was constrained at 9 nodes. The finite element model used for the end drop analysis is shown in Figure 2.11.3-6.

Under vertical loads, the fuel assemblies and fuel compartments are forced against the bottom or top of the cask. Therefore, for any vertical or near vertical loading the fuel assemblies react directly against the bottom or top of the cask cavity and not through the basket structure as they do in a side drop event.

An additional weight of 100 lb. was applied to a center support disc to account for a weight of a poison enclosure weldment. This load was applied by modifying the density of the support disc in the following way.

Disc model weight = 18.8 lb. (computed by ANSYS)

Stainless steel density =  $0.29 \text{ lb.in}^{-3}$ .

Additional weight acting on disc = 100 lbs.

Modified density =  $0.29 (18.8 + 100) / 18.8 = 1.8326 \text{ lb.in}^{-3}$ .

Since the end drop analysis is completely linear, a 1 g acceleration was applied in the z-direction, so that the results can be linearly extrapolated to obtain the stress distributions for both normal and accident conditions. The stress intensity at the top surface of the support disc due to a 1 g acceleration is given in Figure 2.11.3-7. The stress in the central plane of the support disc is less than 1 psi. Therefore the maximum stress intensity of 322.03 psi. is comprised entirely of bending stress. The 1-g elastic analysis results are ratioed to obtain both normal and accident condition stresses in the following way.

Normal Condition Stresses at 16 g =  $16.0 \times 322.03 = 5,153 \text{ psi}$

Accident Condition Stresses at 60 g =  $60.0 \times 322.03 = 19,322 \text{ psi}$

A summary of the end drop stress analysis for both normal and accident conditions are provided in Tables 2.11.3-1 and 2.11.3-2 respectively.

### 2.11.3.4 Thermal Stress Analysis

The support disc thermal finite element model described in Chapter 3, is used to determine the stresses generated in the support discs due to the maximum temperature gradient. This model is first used to determine the temperature distribution under both normal and accident conditions. The elements of the model are then changed to structural elements, and the computed temperature distribution is applied in order to determine the thermal stresses in the support disc.

The following temperature dependent material properties, taken from Reference 1, are used in the thermal stress analysis.

#### **Material Properties Used in the Thermal Stress Analysis**

<b>Temperature (°F)</b>	<b>Modulus of Elasticity, <i>E</i> (psi.)</b>	<b>Coefficient of thermal Expansion, <i>α</i> (in./in.°F.)</b>
70	$28.3 \times 10^6$	$8.55 \times 10^{-6}$
200	$27.6 \times 10^6$	$8.79 \times 10^{-6}$
300	$27.0 \times 10^6$	$9.00 \times 10^{-6}$

The computed thermal stress distribution is shown in Figure 2.11.3-16. The maximum thermal stress generated in the support disc is 644 psi. The thermal stress at the outer radius of the disc is tension, whereas the interior thermal stress is compression. With the application of the primary loads, the area in contact with the shell is in compression, thus reducing the combined stress. Therefore, this small thermal stress is negligible and has no significant affect on the overall load combinations.

### 2.11.3.5 Conclusions

Based on the results of the above analyses and analyses included in Appendices 2.11.1 and 2.11.2, the support disc and container shell are structurally adequate for both normal and accident condition loads. The support disc will properly support and position the Oak Ridge canisters and Peach Bottom assemblies under both normal and accident loading conditions.

### 2.11.3.6 References

1. American Society of Mechanical Engineers, ASME Boiler and Pressure Vessel Code, Section II, Part D, 1998.
2. American Society of Mechanical Engineers, ASME Boiler and Pressure Vessel Code, Section III, Subsection NG, 1998.
3. American Society of Mechanical Engineers, ASME Boiler and Pressure Vessel Code, Section III, Division 3, Subsection WB, 1998.
4. American Society of Mechanical Engineers, ASME Boiler and Pressure Vessel Code, Section III, Appendix F, 1998.
5. ANSYS Users Manuals, Rev. 5.5.

**TABLE 2.11.3-1**

**SUMMARY OF NORMAL CONDITION STRESS ANALYSIS**

<b>Drop Orientation</b>	<b>Component</b>	<b>Stress Category</b>	<b>Maximum Linearized Stress (ksi)</b>	<b>Allowable Linearized Stress (ksi)</b>
End Drop (16 g)	Support Disc	$P_m$	0.0	20.0
		$P_m + P_b$	5.15	30.0
0° Side Drop (20 g)	Support Disc	$P_m$	11.47	20.0
		$P_m + P_b$	11.97	30.0
	Container Shell	$P_m$	10.04	20.0
		$P_m + P_b$	11.21	30.0
36° Side Drop (20 g)	Support Disc	$P_m$	13.76	20.0
		$P_m + P_b$	29.45	30.0
	Container Shell	$P_m$	5.70	20.0
		$P_m + P_b$	11.69	30.0

**TABLE 2.11.3-2**

**SUMMARY OF ACCIDENT CONDITION STRESS ANALYSIS**

<b>Drop Orientation</b>	<b>Component</b>	<b>Stress Category</b>	<b>Maximum Linearized Stress (ksi)</b>	<b>Allowable Linearized Stress (ksi)</b>
End Drop (60 g)	Support Disc	$P_m$	0.0	47.95
		$P_m + P_b$	19.32	68.4
0° Side Drop (80 g)	Support Disc	$P_m$	29.50	47.95
		$P_m + P_b$	29.78	61.65
	Container Shell	$P_m$	6.38	47.95
		$P_m + P_b$	27.40	61.65
36° Side Drop (80 g)	Support Disc	$P_m$	10.74	47.95
		$P_m + P_b$	33.31	61.65
	Container Shell	$P_m$	24.03	47.95
		$P_m + P_b$	29.48	61.65

FIGURE 2.11.3-1

FINITE ELEMENT MODEL OF SUPPORT DISC AND CONTAINER SHELL

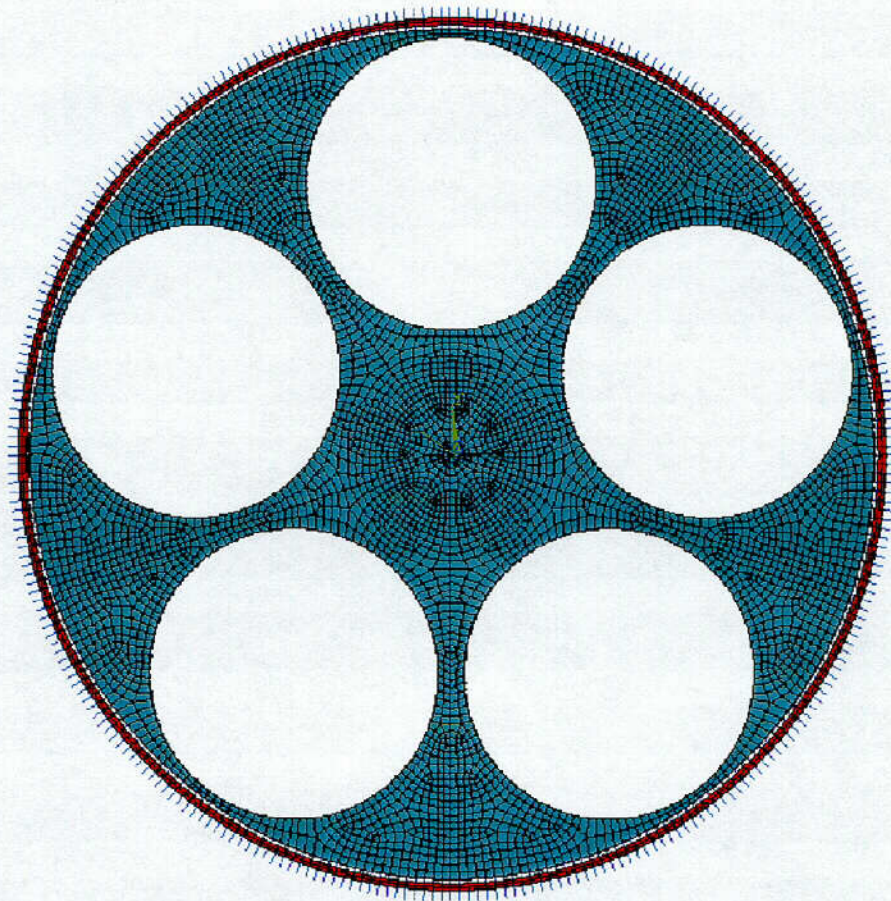


FIGURE 2.11.3-2

GAP SIZES BETWEEN SUPPORT DISC AND CONTAINER SHELL

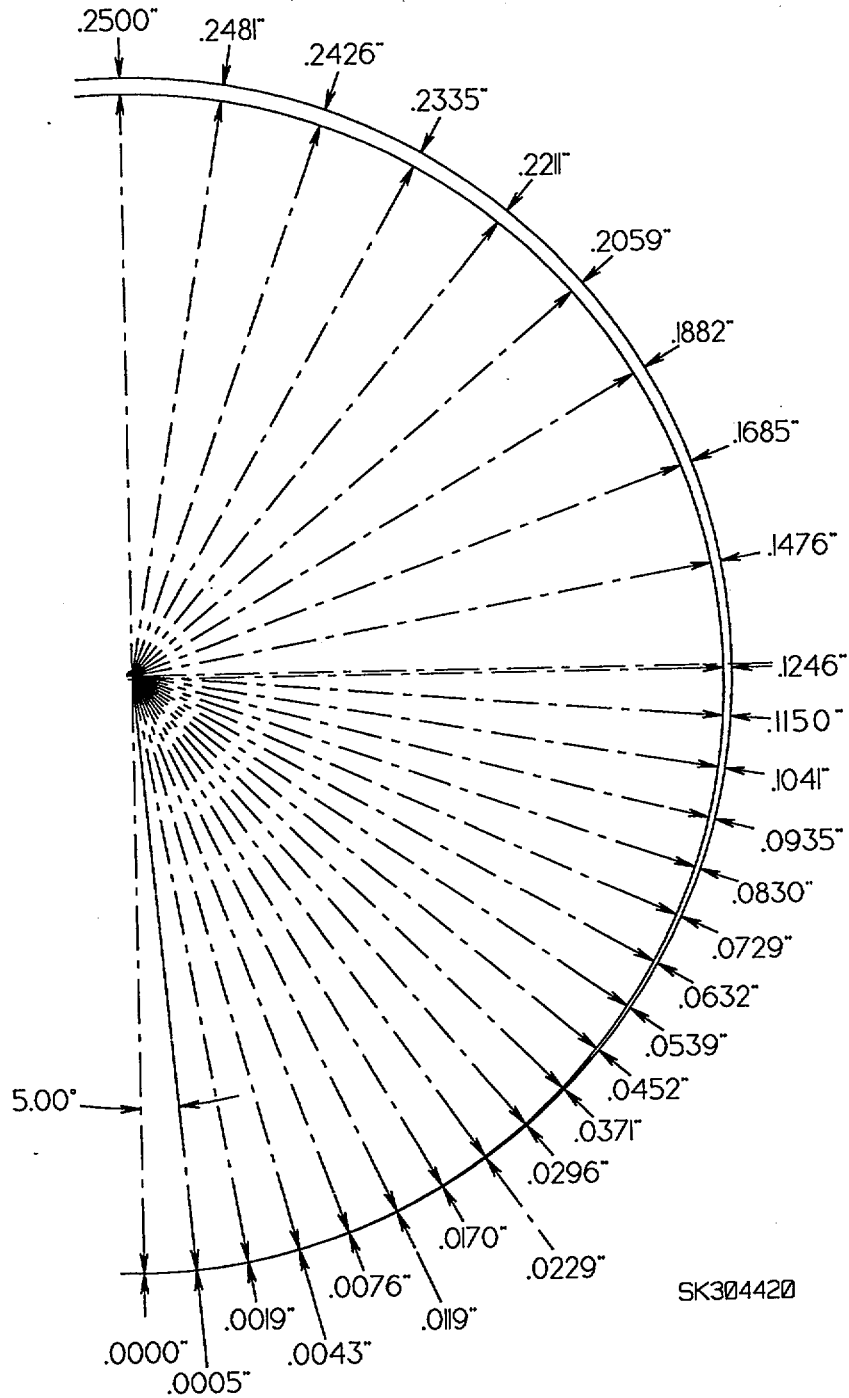


FIGURE 2.11.3-3

GAP SIZES BETWEEN CONTAINER SHELL AND TN-FSV CASK WALL

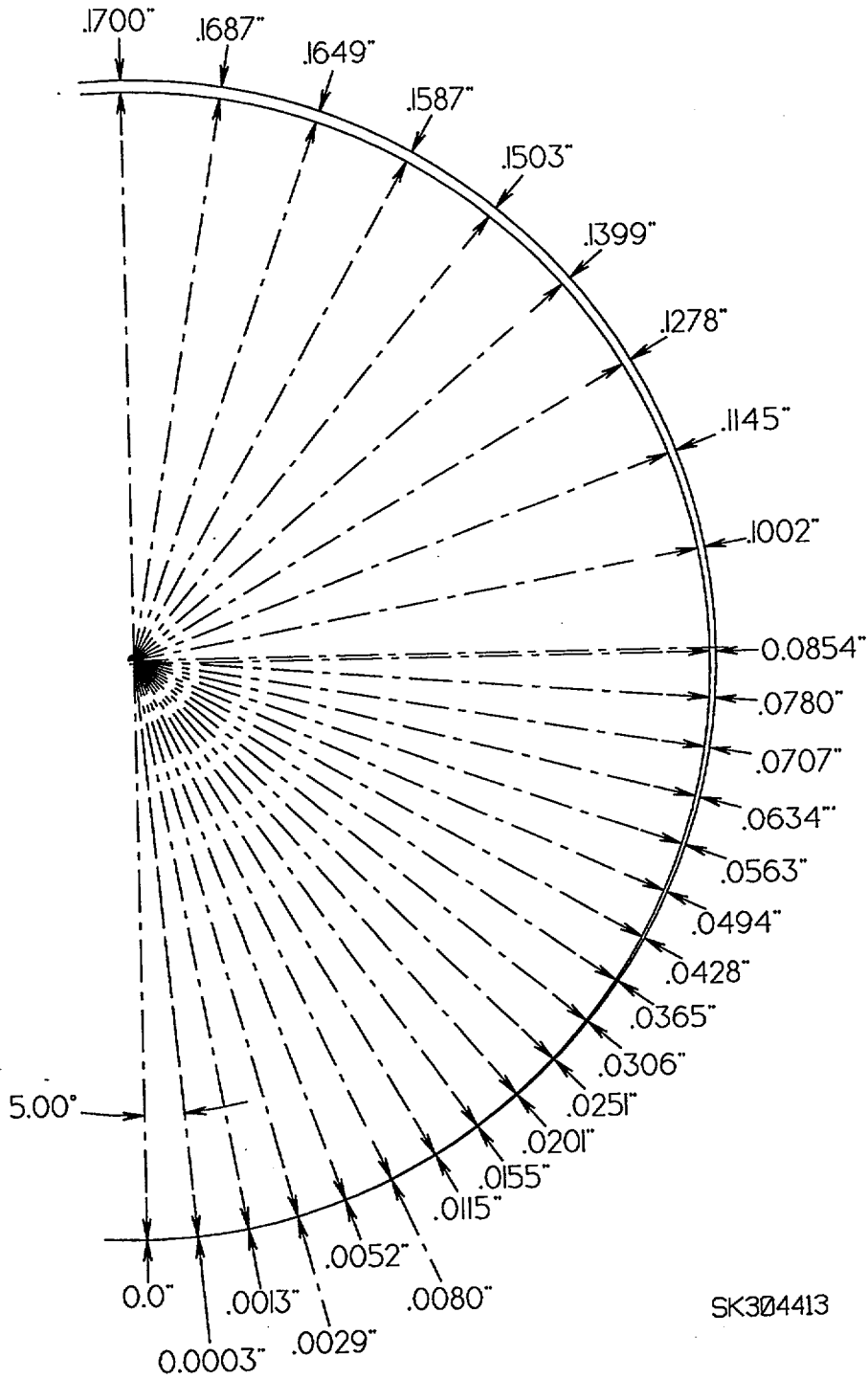


FIGURE 2.11.3-4

FINITE ELEMENT MODEL FOR 0° SIDE DROP ANALYSIS  
WITH BOUNDARY CONDITIONS

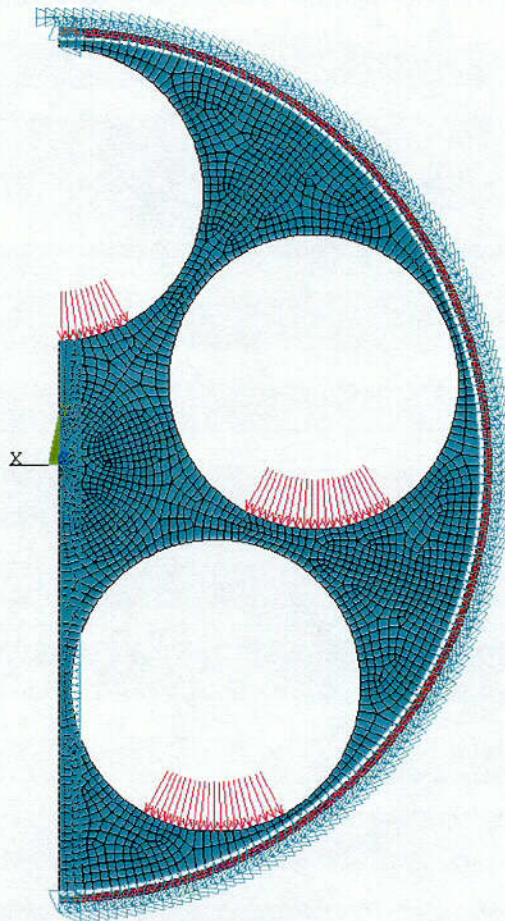
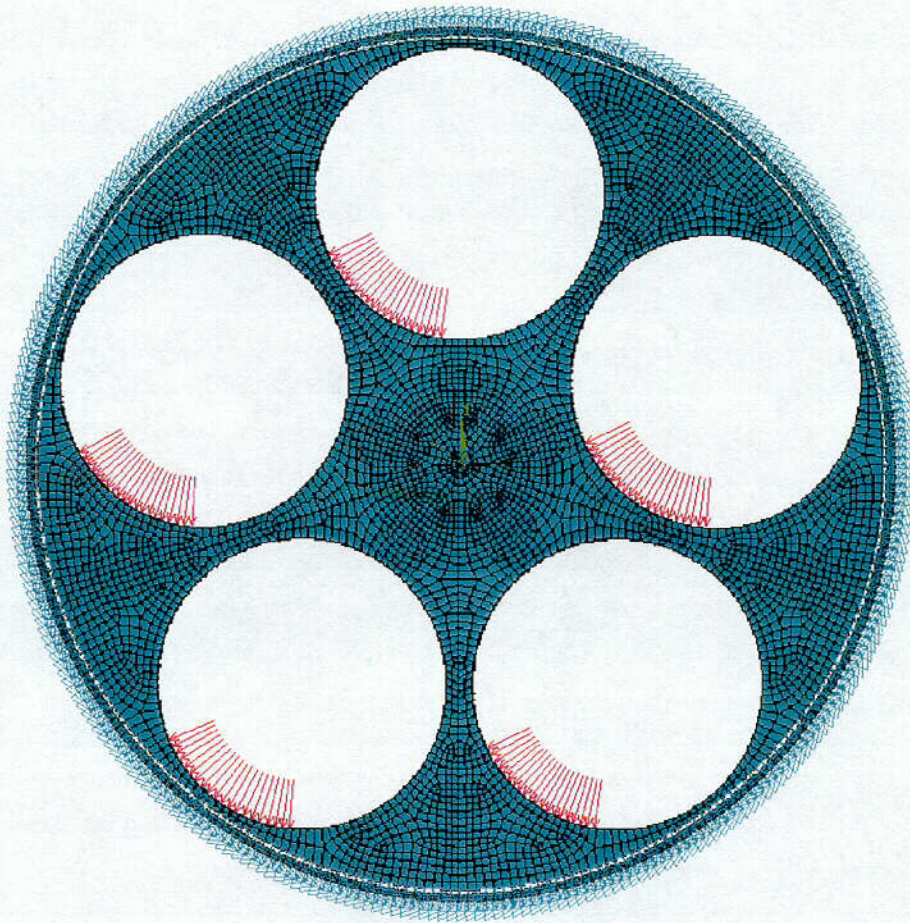


FIGURE 2.11.3-5

**FINITE ELEMENT MODEL FOR 36° SIDE DROP ANALYSIS  
WITH BOUNDARY CONDITIONS**



**FIGURE 2.11.3-6**

**FINITE ELEMENT MODEL FOR END DROP ANALYSIS  
WITH BOUNDARY CONDITIONS**

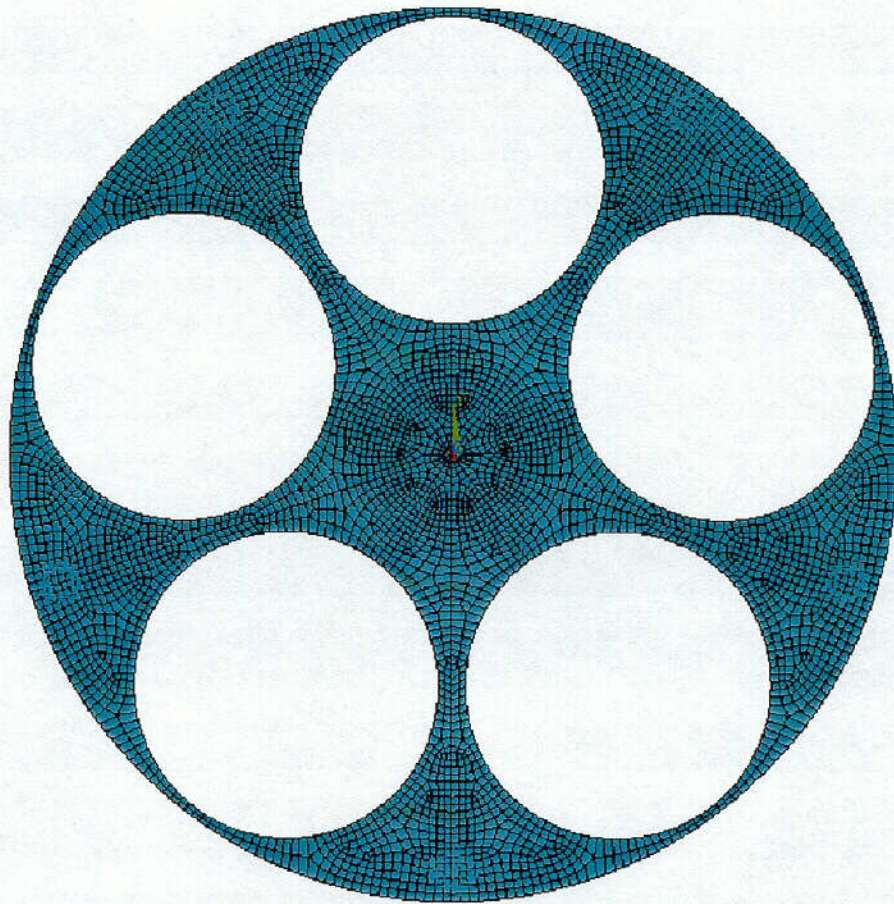


FIGURE 2.11.3-7

STRESS INTENSITY FOR 1g END DROP

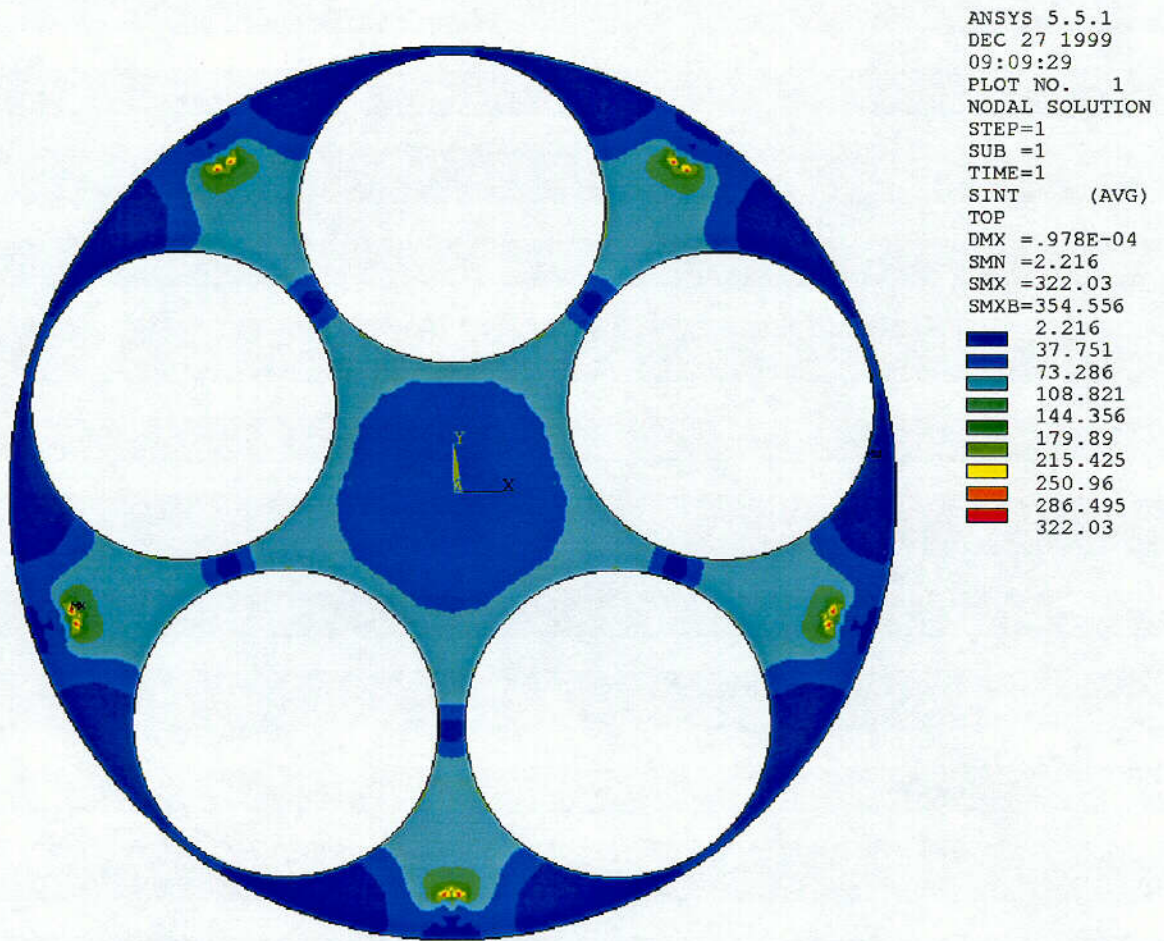
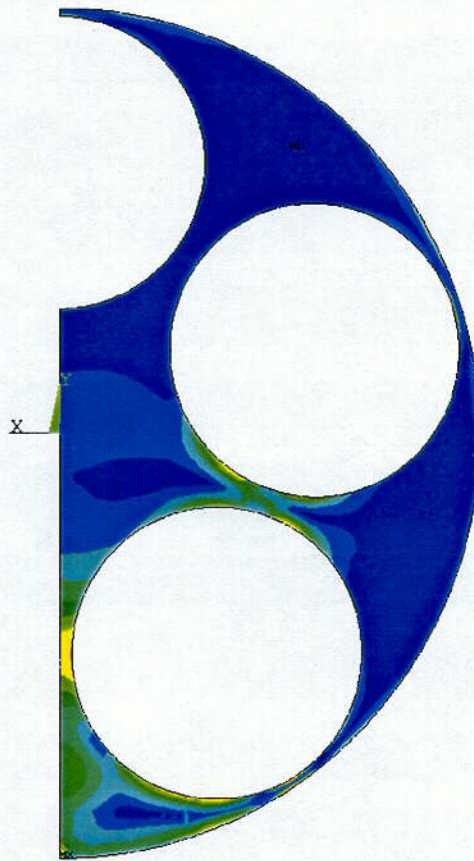


FIGURE 2.11.3-8

SUPPORT DISC STRESS INTENSITY FOR 20g, 0° SIDE DROP

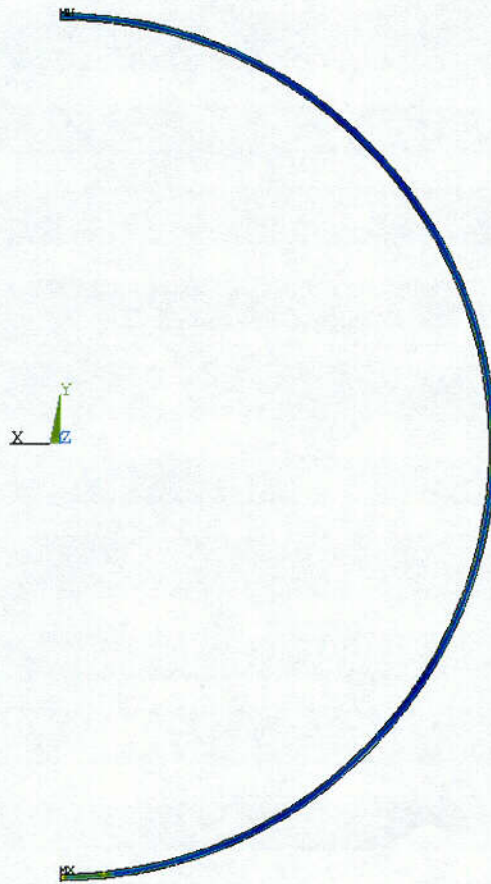


ANSYS 5.5.1  
DEC 22 1999  
14:45:07  
PLOT NO. 1  
NODAL SOLUTION  
STEP=1  
SUB =5  
TIME=1  
SINT (AVG)  
DMX =.121752  
SMN =30.865  
SMX =15465  
SMXB=18612

ZV =-1  
DIST=9.488  
XF =-4.312  
Z-BUFFER  
30.865  
1746  
3461  
5176  
6891  
8605  
10320  
12035  
13750  
15465

FIGURE 2.11.3-9

CONTAINER SHELL STRESS INTENSITY FOR 20g, 0° SIDE DROP

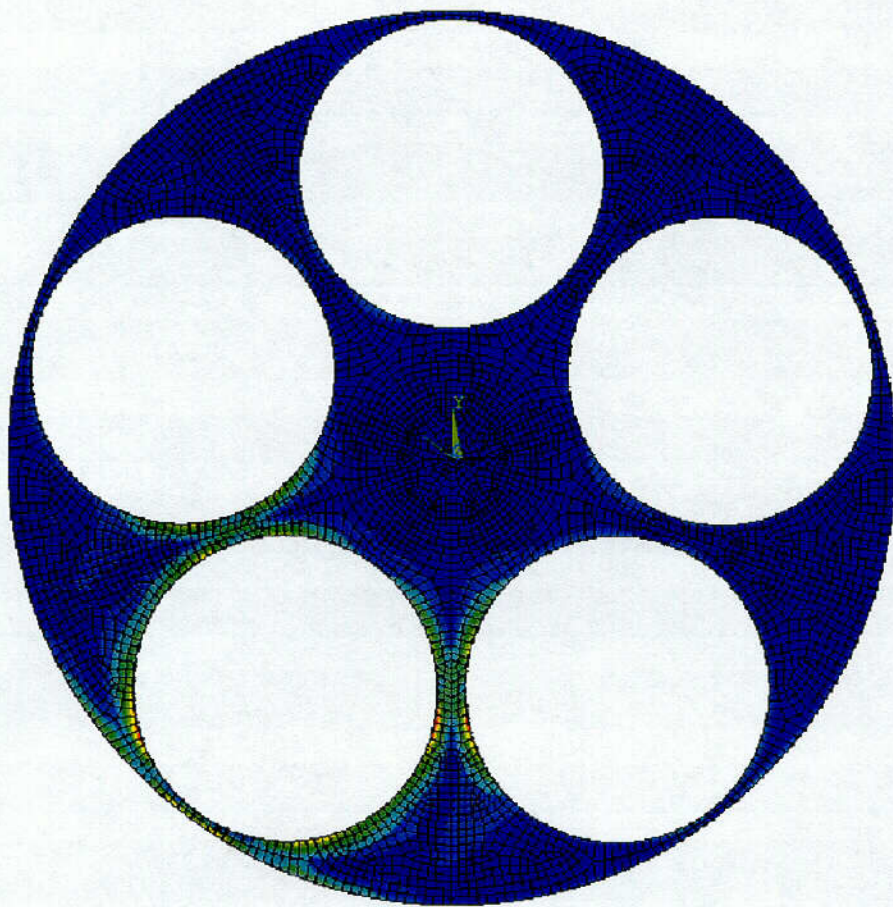


ANSYS 5.5.1  
DEC 22 1999  
14:49:33  
PLOT NO. 1  
NODAL SOLUTION  
STEP=1  
SUB =5  
TIME=1  
SINT (AVG)  
DMX =.121752  
SMN =35.445  
SMX =10953  
SMXB=11448

ZV =-1  
DIST=9.488  
XF =-4.312  
Z-BUFFER  
35.445  
1248  
2462  
3675  
4888  
6101  
7314  
8527  
9740  
10953

FIGURE 2.11.3-10

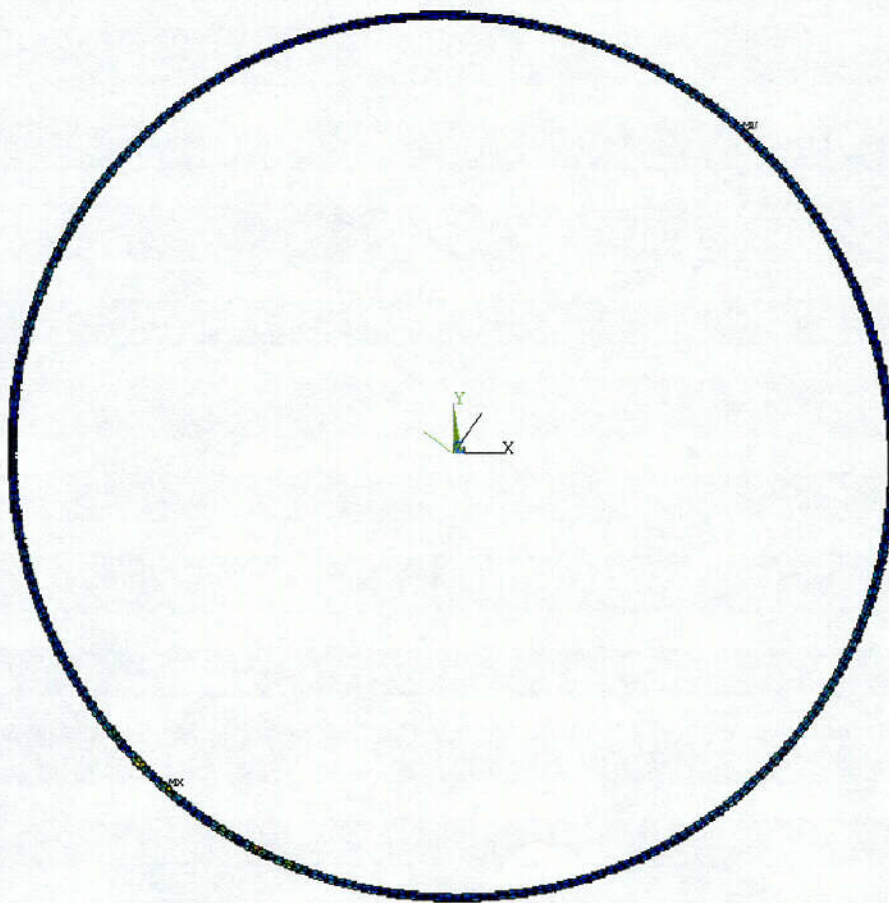
SUPPORT DISC STRESS INTENSITY FOR 20g, 36° SIDE DROP



```
ANSYS 5.5.1  
DEC 27 1999  
13:15:54  
PLOT NO. 1  
NODAL SOLUTION  
STEP=1  
SUB =4  
TIME=1  
SINT (AVG)  
PowerGraphics  
EFACET=1  
AVRES=Mat  
DMX =.019672  
SMN =3.461  
SMX =30613  
3.461  
3405  
6806  
10207  
13608  
17009  
20410  
23811  
27212  
30613
```

FIGURE 2.11.3-11

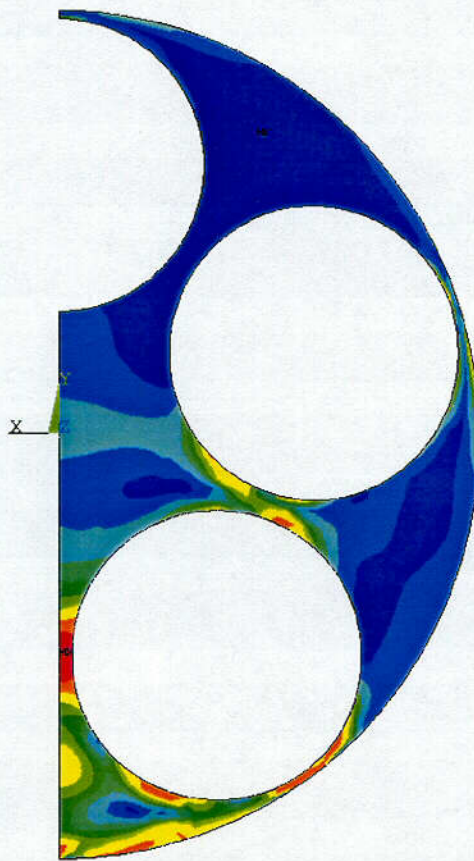
CONTAINER SHELL STRESS INTENSITY FOR 20g, 36° SIDE DROP



ANSYS 5.5.1  
DEC 27 1999  
13:16:34  
PLOT NO. 1  
NODAL SOLUTION  
STEP=1  
SUB =4  
TIME=1  
SINT (AVG)  
PowerGraphics  
EFACET=1  
AVRES=Mat  
DMX =.127111  
SMN =33.95  
SMX =12256  
33.95  
1392  
2750  
4108  
5466  
6824  
8182  
9540  
10898  
12256

FIGURE 2.11.3-12

SUPPORT DISC STRESS INTENSITY FOR 80g, 0° SIDE DROP



ANSYS 5.5.1  
DEC 22 1999  
15:01:58  
PLOT NO. 1  
NODAL SOLUTION  
STEP=1  
SUB =13  
TIME= .5  
SINT (AVG)  
DMX = .200456  
SMN =72.713  
SMX =30872

ZV =-1  
DIST=9.488  
XF =-4.312  
Z-BUFFER  
72.713  
3495  
6917  
10339  
13761  
17184  
20606  
24028  
27450  
30872

FIGURE 2.11.3-13

CONTAINER SHELL STRESS INTENSITY FOR 80g, 0° SIDE DROP

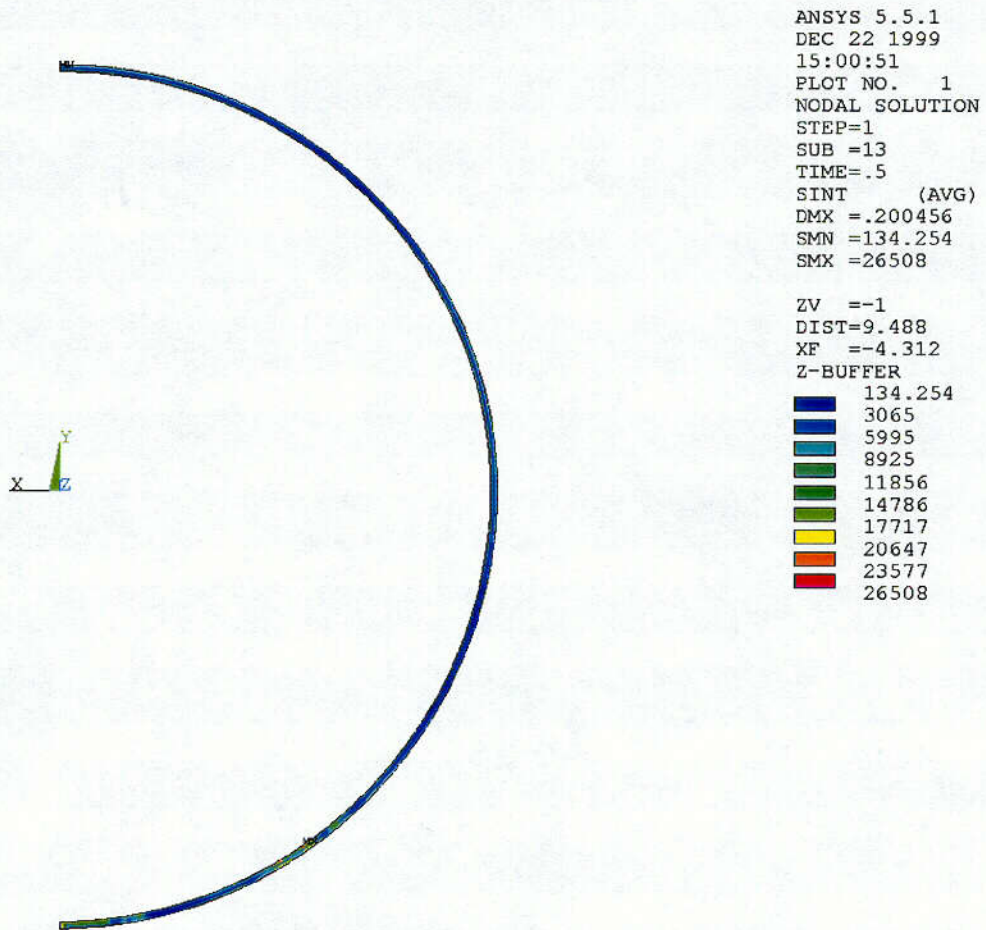
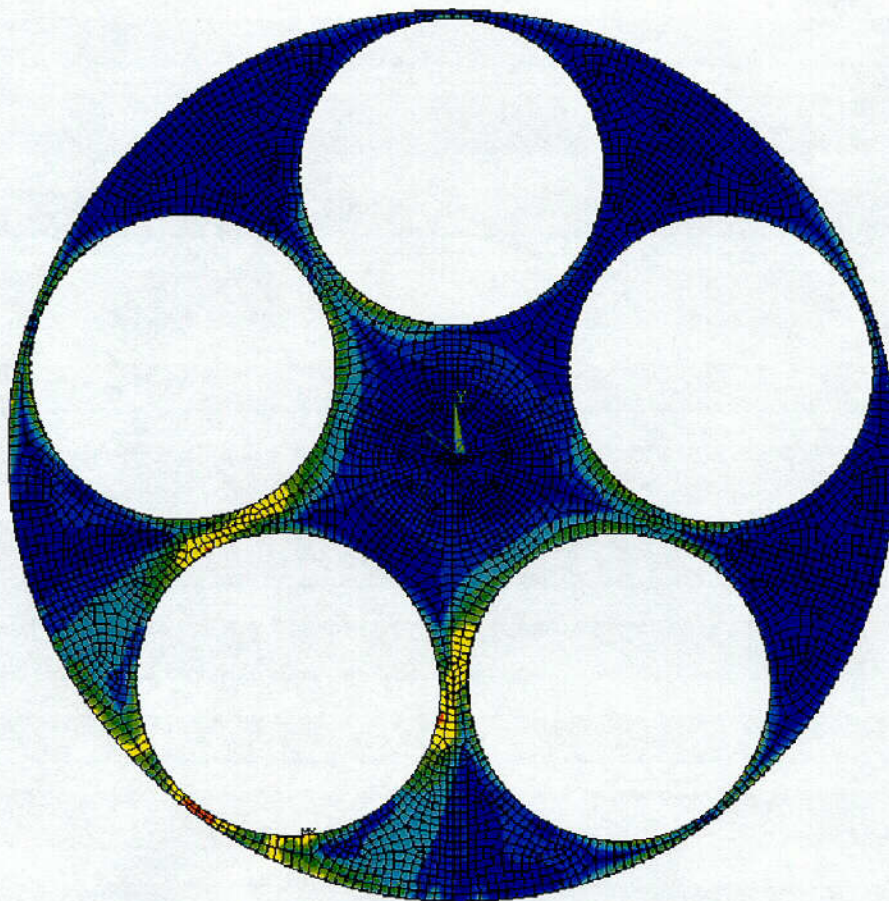


FIGURE 2.11.3-14

SUPPORT DISC STRESS INTENSITY FOR 80g, 36° SIDE DROP



```
ANSYS 5.5.1  
DEC 27 1999  
13:13:02  
PLOT NO. 1  
NODAL SOLUTION  
STEP=1  
SUB =43  
TIME=.500625  
SINT (AVG)  
PowerGraphics  
EFACET=1  
AVRES=Mat  
DMX =.097729  
SMN =59.703  
SMX =35066  
59.703  
3949  
7839  
11729  
15618  
19508  
23398  
27287  
31177  
35066
```

FIGURE 2.11.3-15

CONTAINER SHELL STRESS INTENSITY FOR 80g, 36° SIDE DROP

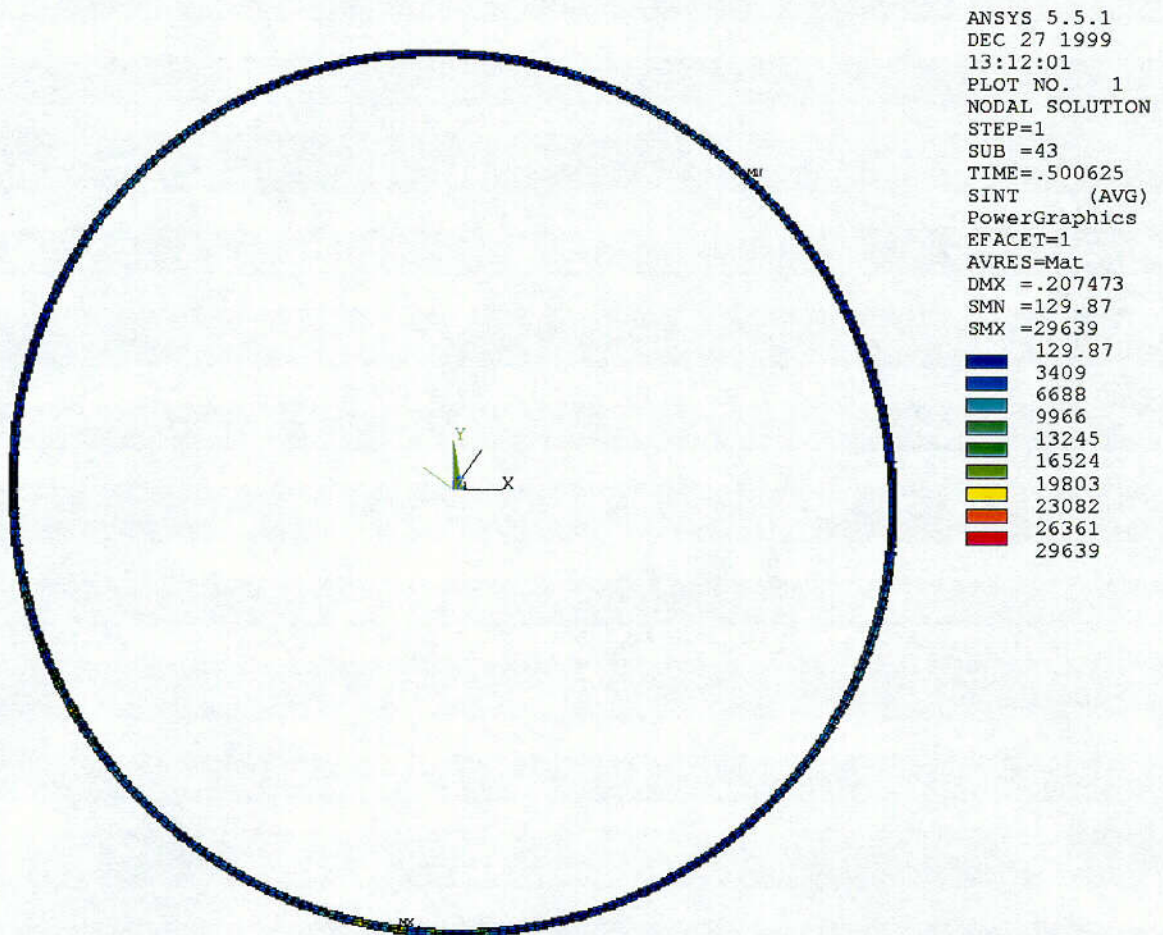
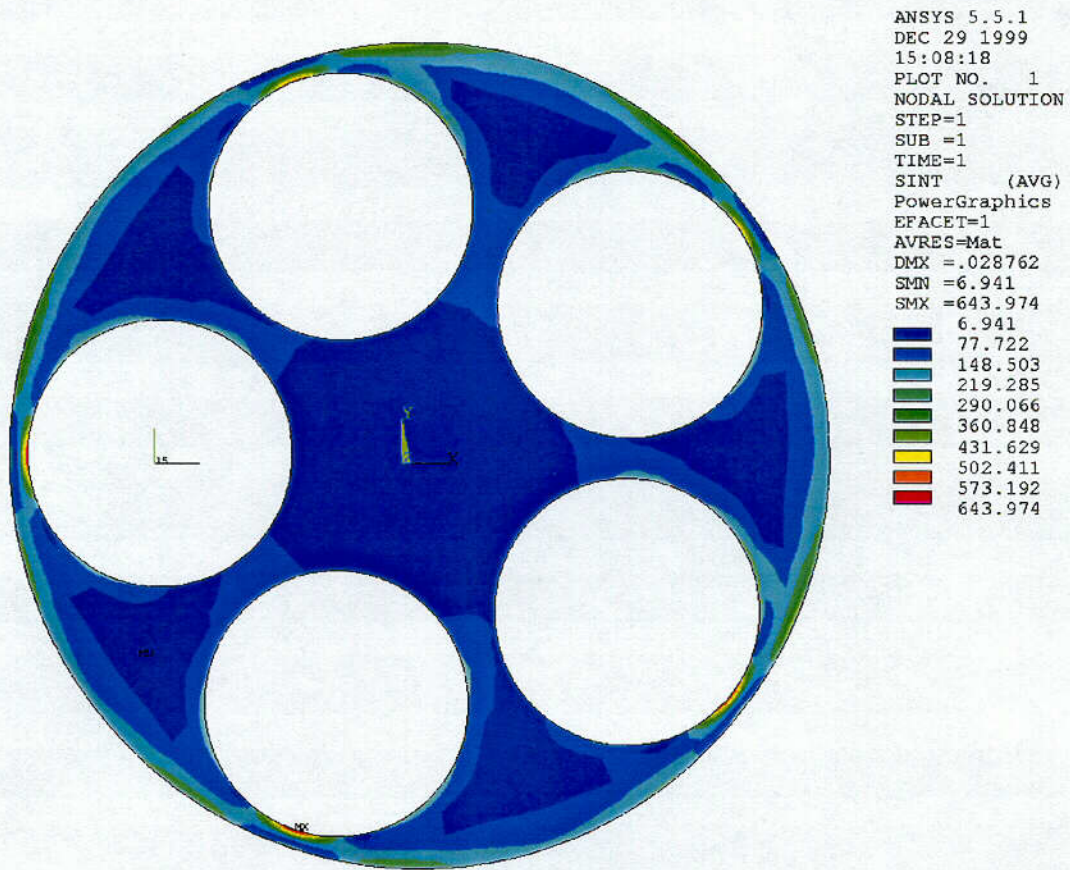


FIGURE 2.11.3-16

SUPPORT DISC THERMAL STRESS INTENSITY



## APPENDIX 2.11.4

### TABLE OF CONTENTS

	<u>Page</u>
2.11.4 OAK RIDGE SNF CONTAINER LID BOLT ANALYSIS.....	2.11.4-1
2.11.4.1 Introduction .....	2.11.4-1
2.11.4.2 Bolt Load Calculations .....	2.11.4-2
2.11.4.3 Load Combinations .....	2.11.4-6
2.11.4.4 Bolt Stress Calculations .....	2.11.4-9
2.11.4.5 Analysis Results.....	2.11.4-12
2.11.4.6 Fatigue Analysis.....	2.11.4-13
2.11.4.7 Minimum Engagement Length for Bolt and Flange .....	2.11.4-16
2.11.4.8 Vent Port Cover Bolt Analysis .....	2.11.4-18
2.11.4.9 Conclusions.....	2.11.4-19
2.11.4.10 References.....	2.11.4-20

#### LIST OF TABLES

2.11.4-1 Design Parameters for Lid Bolt Analysis.....	2.11.4-21
2.11.4-2 Bolt Data .....	2.11.4-23
2.11.4-3 Allowable Stresses in Closure Bolts for Normal Conditions ..	2.11.4-24
2.11.4-4 Allowable Stresses in Closure Bolts for Accident Conditions	2.11.4-25

#### LIST OF FIGURES

2.11.4-1 Oak Ridge SNF Container Lid Closure Arrangement.....	2.11.4-26
2.11.4-2 Oak Ridge SNF Container Lid Bolt.....	2.11.4-27
2.11.4-3 Free Body Diagram of Oak Ridge Container Lid Closure System Subjected to a Lid End Drop .....	2.11.4-28

## APPENDIX 2.11.4

### OAK RIDGE SNF CONTAINER LID BOLT ANALYSIS

#### 2.11.4.1 Introduction

This appendix analyzes the ability of the Oak Ridge SNF Container closure to maintain a leak tight seal under normal and accident conditions. Also evaluated in this section, are the bolt thread and internal thread stresses, and container lid bolt fatigue. The stress analysis is performed in accordance with NUREG/CR-6007<sup>(1)</sup>.

The Oak Ridge SNF Container lid closure arrangement is shown in Figure 2.11.4-1 (page 2.11.4-25). The 7.00 inch thick lid is bolted directly to the end of the container shell flange by 12, 1/2 inch diameter high strength steel bolts. Close fitting alignment pins ensure that the lid is centered in the container.

The lid bolt is shown in Figure 2.11.4-2 (page 2.11.4-26). The bolt material is SA-453, Type 651, class A, which has a minimum yield strength of 70 ksi at room temperature<sup>(2)</sup>.

The following ways to minimize bolt forces and bolt failures for shipping casks are taken directly from with NUREG/CR-6007<sup>(1)</sup>, page xiii. All of the following design methods are employed in the Oak Ridge SNF Container closure system.

- Protect closure lid from direct impact to minimize bolt forces generated by free drops. (use impact limiters)
- Use materials with similar thermal properties for the closure bolts, the lid, and the cask wall to minimize the bolt forces generated by fire accident
- Apply sufficiently large bolt preload to minimize fatigue and loosening of the bolts by vibration.
- Lubricate bolt threads to reduce required preload torque and to increase the predictability of the achieved preload.
- Use closure lid design which minimizes the prying actions of applied loads.
- When choosing a bolt preload, pay special attention to the interactions between the preload and thermal load and between the preload and the prying action.

The following evaluations are presented in this section:

- Lid bolt torque
- Bolt preload
- Gasket seating load
- Pressure load
- Temperature load
- Impact load
- Puncture load
- Thread engagement length evaluation
- Bearing stress
- Load combinations for normal and accident conditions
- Calculated and allowable bolt stresses.
- Lid bolt fatigue

The design parameters of the lid closure are summarized in Table 2.11.4-1 (page 2.11.4-20). The lid bolt data and material allowable stresses are presented in Tables 2.11.4-2 through 2.11.4-4 (pages 2.11.4-22 through 2.11.4-24). A maximum temperature of 250°F is used in the lid bolt region during normal and accident conditions. The following load cases are considered in the analysis.

1. Preload + Temperature Load (normal condition)
2. Pressure Load + 1 Foot Drop (normal condition)
3. Pressure + 30 Foot Corner Drop (accident condition)
4. Pressure + Puncture Load (accident condition)

#### 2.11.4.2 Bolt Load Calculations

Symbols and terminology used in this analysis are taken from NUREG/CR-6007<sup>(1)</sup> and are reproduced in Table 2.11.4-1 (page 2.11.4-20).

##### A) Lid Bolt Torque and Bolt Preload

A bolt torque range of 10 to 15 ft. lb. has been selected. Using the minimum torque,

$$F_a = Q/KD_b = 10 \times 12 / (0.1 \times 0.500) = 2,400 \text{ lb.}, \text{ and}$$

$$\text{Preload stress} = F_a / \text{Stress Area (Table 2.11.4-2, page 2.11.4-22)} = 2,400 / 0.142 = 16,900 \text{ psi.}$$

Using the maximum torque,

$$F_a = Q/KD_b = 15 \times 12 / (0.1 \times 0.500) = 3,600 \text{ lb.}, \text{ and}$$

$$\text{Preload stress} = F_a / \text{Stress Area} = 3,600 / 0.142 = 25,350 \text{ psi.}$$

Residual torsional moment for maximum torque of 15 ft. lb. is,

$$M_{ir} = 0.5Q = .5(15 \times 12) = 90 \text{ in. lb.}$$

Residual torsional moment for minimum torque of 10 ft. lb. is,

$$M_{ir} = 0.5Q = .5(10 \times 12) = 60 \text{ in. lb.}$$

Residual tensile bolt force for maximum torque,

$$F_{ar} = F_a = 3,600 \text{ lb.}$$

### B) Gasket Seating Load

The seals used are two 3/16 inch section diameter o-rings (Ref. 8). Since o-rings are used, the gasket seating load is negligible.

### C) Pressure Loads (Ref. 1, Table 4.3)

Axial force per bolt due to internal pressure is

$$F_a = \frac{\pi D_{lg}^2 (P_{li} - P_{lo})}{4N_b}$$

The worst case pressure load applied to the Oak Ridge SNF Container is conservatively assumed to be  $\pm 10$  psi.  $D_{lg}$  (conservatively used outer seal) = 17.967 in. Then,

$$F_a = \frac{\pi(17.967^2)(\pm 10)}{4(12)} = \pm 211 \text{ lb./bolt.}$$

The fixed edge closure lid force is,

$$F_f = \frac{D_{lb}(P_{li} - P_{lo})}{4} = \frac{19.07(\pm 10)}{4} = \pm 48 \text{ lb. in.}^{-1}$$

The fixed edge closure lid moment is,

$$M_f = \frac{(P_{li} - P_{lo})D_{lb}^2}{32} = \frac{(\pm 10)(19.07^2)}{32} = \pm 114 \text{ in. lb. in.}^{-1}$$

Since the lid shoulder takes the shear force, the shear bolt force per bolt is,  $F_s = 0$ .

#### D) Temperature Loads

The lid bolt material is SA-453, Type 651, class A, 19Cr 9Ni Mo W. Both lid and flange are made of SA-240 Type 304, or SA-182 F304, both of which are 18Cr 8Ni. Therefore, the bolts have coefficient of thermal expansion of  $9.46 \times 10^{-6}$  in./in.  $^{\circ}\text{F}^{-1}$  at 250 $^{\circ}$  F, and the lid and flange have a coefficient of thermal expansion of  $8.90 \times 10^{-6}$  in./in.  $^{\circ}\text{F}^{-1}$  at 250 $^{\circ}$  F (Ref. 2).  $F_a$  is,

$$F_a = 0.25 \pi D_b^2 E_b (a_l T_l - a_b T_b)$$

$$F_a = 0.25(\pi)(0.500^2)(27.3 \times 10^6)[(8.90 \times 10^{-6})(180) - (9.46 \times 10^{-6})(180)] = -540 \text{ lb.}$$

Since the lid and flange will always remain the same temperature, and the lid shoulder takes shear force,

$$F_s = 0.$$

The temperature difference between the inside and outside of the lid will always be less than one degree. Consequently, the resulting bending moment is negligible.

$$M_f = 0.$$

#### E) Impact Loads (1, Table 4.5)

The inertial load of Oak Ridge Container fuel basket, including the SNF, is directly supported by the container lid during a lid end drop. The flat outer surface of the container lid is directly support by the flat inner surface of the TN-FSV lid. Therefore all inertial loads applied to the container lid are directly transferred to the TN-FSV Cask lid.

Figure 2.11.4-3 is a free body diagram of the container lid closure system during a lid end drop. The inertial loads of the container flange, body, and bottom,  $F_3$ , the internals,  $F_2$ , and the container lid,  $F_1$ , are reacted by the support provided by the TN-FSV Cask lid inner surface,  $F_R$ . Figure 2.11.4-3 shows that the inertial load of the container shell, flange, and bottom, and the inertial load of the container internals is transmitted directly to the container lid, and reacted by the TN-FSV Cask. Consequently, the container lid bolts do not experience any tensile loads during a lid end drop.

#### F) Puncture Loads (Ref. 1, Table 4.7)

Since the container is encased in the TN-FSV cask and protected by impact limiters, the container is completely protected from all puncture events.

### Lid Bolt Individual Load Summary

Load Case	Applied Load		Non-Prying Tensile Force, $F_a$ (lb. / bolt)	Torsional Moment, $M_t$ (in. lb./ bolt)	Prying Force, $F_f$ (lb.in. <sup>-1</sup> )	Prying Moment, $M_f$ (in. lb. in. <sup>-1</sup> )
Preload	Residual	Maximum Torque	3,600	90	0	0
		Minimum Torque	2,400	60	0	0
Gasket	Seating Load		0	0	0	0
Pressure	±10 psig Internal		± 211	0	± 48	± 114
Thermal	250°F		- 540	0	0	0
Impact	Normal / accident condition free drops		0	0	0	0
Puncture	Drop on six inch diameter rod		0	0	0	0

2.11.4.3 Load Combinations (Ref. 1, Table 4.9)

A summary of normal and accident condition load combinations is presented in the following table.

**Lid Bolt Normal and Accident Load Combinations**

Load Case	Combination Description		Non-Prying Tensile Force, $F_a$ (lb. / bolt)	Torsional Moment, $M_t$ (in. lb./ bolt)	Prying Force, $F_f$ (lb.in. <sup>-1</sup> )	Prying Moment, $M_f$ (in. lb. in. <sup>-1</sup> )
1.	Preload + Temperature (Normal Condition)	A. Maximum Torque	3,060	90	0	0
		B. Minimum Torque	1,860	60	0	0
2.	Pressure + Normal Impact (Normal Condition)		± 211	0	± 48	± 114
3.	Pressure + Accident Impact (Accident Condition)		± 211	0	± 48	± 114
4.	Pressure + Puncture (Accident Condition)		± 211	0	± 48	± 114

It is observed that the tensile bolt force caused by the minimum bolt preload (with or without additional temperature loads) exceeds the maximum combined tensile stresses (normal and accident conditions). Therefore, the container lid will maintain the containment seal under all loading conditions.

Additional Prying Bolt Force

Forces that are inward acting, normal to the cask lid, generate an additional tensile bolt force,  $F_{ap}$  (Ref. 1, Table 2.1). No additional force is generated for the outward loadings however (load cases 1, 2, 3, and 4 above), because of the gap between the lid and flange at the outer edge. The maximum inward acting load applied to the container is the load generated by a conservatively assumed 10 psi external pressure and 0 psi internal pressure.  $F_{ap}$  due to this pressure load is calculated in the following way.

$$F_{ap} = -\left(\frac{\pi D_{lb}}{N_b}\right) \left[ \frac{\frac{2M_f}{(D_{lo} - D_{lb})} - C_1(B - F_f) - C_2(B - P)}{C_1 + C_2} \right],$$

where,

$$M_f = \frac{(P_{li} - P_{lo})D_{lb}^2}{32} = \frac{(0 - 10)(19.07^2)}{32} = -114 \text{ in. lb. in.}^{-1}.$$

$$C_1 = 1, C_2 = \left(\frac{8}{3(D_{lo} - D_{lb})^2}\right) \left[ \frac{E_l t_l^3}{1 - \nu_{ul}} + \frac{(D_{lo} - D_{li})E_{lf} t_{lf}^3}{D_{lb}} \right] \left(\frac{L_b}{N_b D_b^2 E_b}\right)$$

$$= \left(\frac{8}{3(20.19 - 19.07)^2}\right) \left[ \frac{27.3 \times 10^6 (7.00^3)}{1 - 0.305} + \frac{(20.19 - 16.58)(27.3 \times 10^6)(1.50)^3}{19.07} \right] \left(\frac{1.255}{(12)(0.500^2)(27.3 \times 10^6)}\right)$$

$$= 439.5$$

$B$  is the non-prying tensile bolt force, and  $P$  is the bolt preload. Since  $F_f = 0$  (the container lid/flange interface takes inward acting fixed edge force),  $F_f < P$ , and therefore  $B = P$ . Parameters  $B$ ,  $P$ ,  $F_f$ , and  $M_f$  are quantities per unit length of bolt circle. For the applied inward force,

$$P = B = \frac{F_a N_b}{\pi D_{lb}} = \frac{(3,600)(12)}{\pi(19.07)} = 721 \text{ lb. in.}^{-1},$$

Therefore,

$$F_{ap} = -\left(\frac{\pi(19.07)}{12}\right) \left[ \frac{\frac{2(-114)}{(20.19 - 19.07)} - 1(721 - 0) - 439.5(721 - 721)}{1 + 439.5} \right]$$

$$= 11 \text{ lb./bolt.}$$

It is observed that the additional tensile bolt force due to prying for the external pressure is negligible. The external pressure is therefore not critical for bolt stress evaluation.

**Bolt Bending Moment:** (Ref. 1, Table 2.2)

The maximum bending bolt moment,  $M_{bb}$ , generated by the applied normal condition load is evaluated as follows:

$$M_{bb} = \left( \frac{\pi D_{lb}}{N_b} \right) \left[ \frac{K_b}{K_b + K_l} \right] M_f$$

The  $K_b$  and  $K_l$  are based on geometry and material properties and are defined in reference 1, Table 2.2. The closure lid thickness,  $t_l$ , is conservatively taken to be the lid thickness at the bolt circle (1.315 in) instead of the thickness at the lid's center (7.00 in). By substituting the values given in Table 2.11.4-1 (page 2.11.4-20),

$$K_b = \left( \frac{N_b}{L_b} \right) \left( \frac{E_b}{D_{lb}} \right) \left( \frac{D_b^4}{64} \right) = \left( \frac{12}{1.255} \right) \left( \frac{27.3 \times 10^6}{19.07} \right) \left( \frac{0.500^4}{64} \right) = 13,367, \text{ and}$$

$$K_l = \frac{E_l t_l^3}{3 \left[ (1 - N_{ul}^2) + (1 - N_{ul})^2 \left( \frac{D_{lb}}{D_{lo}} \right)^2 \right] D_{lb}} = \frac{27.3 \times 10^6 (7.00^3)}{3 \left[ (1 - 0.305^2) + (1 - 0.305)^2 \left( \frac{19.07}{20.19} \right)^2 \right] 19.07}$$

$$= 1.223 \times 10^8$$

Therefore,

$$M_{bb} = \left( \frac{\pi 19.07}{12} \right) \left[ \frac{13,367}{13,367 + 1.223 \times 10^8} \right] M_f = 0.000545 M_f$$

For load case 2, 3, and 4,  $M_f = 114$  in. lb. Substituting this value into the equation above gives,

$$M_{bb} = 0.062 \text{ in. lb. / bolt.}$$

#### 2.11.4.4 Bolt Stress Calculations (Ref. 1, Table 5.1)

##### A) Average Tensile Stress

The minimum bolt preload is calculated to withstand the worst case load combination and to maintain a clamping (compressive) force on the closure joint, during both normal and accident conditions. Based upon the load combination results (see Table in Section 2.11.4.3, Lid Bolt Normal And Accident Load Combinations), it is shown that a positive (compressive) load is maintained on the clamped joint for all load combinations. However, for both normal and accident condition load cases, the maximum non-prying tensile force of 3,600 lb., from maximum torque preload without temperature load, is used for bolt stress calculations since the temperature load decreases the applied bolt force.

##### Average Tensile Stress:

Normal Condition:

$$S_{ba} = \frac{F_a}{A_{stress}} = \frac{3,600}{0.142} = 25,350 \text{ psi.} = 25.4 \text{ ksi.}$$

Accident Condition:

$$S_{ba} = \frac{F_a}{A_{stress}} = \frac{3,600}{0.142} = 25,350 \text{ psi.} = 25.4 \text{ ksi.}$$

##### B) Bending Stress

Normal Condition:

$$S_{bb} = 10.186 \frac{M_{bb}}{D_{ba}^3} = 10.186 \frac{0.062}{0.425^3} = 3.5 \text{ psi.}$$

##### C) Shear Stress

For both normal and accident conditions, the average shear stress caused by shear bolt force  $F_s$  is,

$$S_{bs} = 0.$$

For normal and accident conditions the maximum shear stress caused by the torsional moment  $M_t$  is,

$$S_{bt} = 5.093 \frac{M_t}{D_{ba}^3} = 5.093 \frac{90}{0.425^3} = 5,964 \text{ psi.} = 6.0 \text{ ksi.}$$

#### D) Maximum Combined Stress Intensity

The maximum combined stress intensity is calculated in the following way for normal condition combined tension, shear, bending, and residual torsion (Ref. 1, Table 5.1).

$$S_{bi} = [(S_{ba} + S_{bb})^2 + 4(S_{bs} + S_{bt})^2]^{0.5}$$
$$S_{bi} = [(25,350 + 0)^2 + 4(0 + 5,964)^2]^{0.5} = 28,020 \text{ psi.} = 28.0 \text{ ksi.}$$

#### E) Stress Ratios

In order to meet the stress ratio requirement, the following relationship must hold for both normal and accident conditions,

$$R_t^2 + R_s^2 < 1$$

Where  $R_t$  is the ratio of average tensile stress to allowable average tensile stress, and  $R_s$  is the ratio of average shear stress to allowable average shear stress.

For normal conditions:

$$R_t = 25,350/41,200 = 0.615,$$

$$R_s = 5,964/24,800 = 0.240,$$

$$R_t^2 + R_s^2 = (0.615)^2 + (0.240)^2 = 0.435 < 1.$$

For accident conditions:

$$R_t = 25,350/61,800 = 0.410,$$

$$R_s = 5,964/37,100 = 0.161,$$

$$R_t^2 + R_s^2 = (0.410)^2 + (0.161)^2 = 0.194 < 1.$$

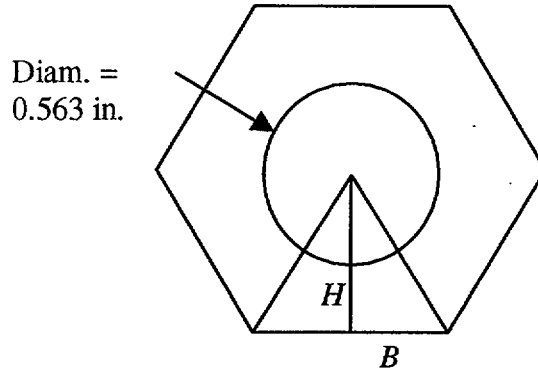
F) Bearing Stress (Under Bolt Head)

The maximum axial force is 3,600 lb. A bolt head corresponding to 1/2" diameter bolt is used, and the clearance hole in the lid is 0.563 inches in diameter.

From reference 3 (page 1134):  $H = 0.375$  in.  
 $B = 0.375 \tan(30^\circ) = 0.217$  in.

Total Area of one triangle  
 $= (0.375)(.217) = 0.081 \text{ in}^2$ .

Total area under Bolt head  
 $= 6(0.081) - (\pi/4)(0.563^2) = 0.237 \text{ in}^2$ .



So the bearing stress is,

$$\text{Bearing Stress} = 3,600 / .273 = 13,187 \text{ psi.} = 13.2 \text{ ksi.}$$

The allowable bearing stress on the lid is taken to be the yield stress of the lid material at 250° F. The lid may be manufactured out of SA-240 Type 304 or SA-182 F304. The yield stress of both materials is 23.75 ksi (Ref. 2).

2.11.4.5 Analysis Results

A summary of the bolt stresses calculated above is presented in the following table:

**Summary of Calculated and Allowable Stresses**

Stress Type	Normal Condition		Accident Condition	
	Stress	Allowable	Stress	Allowable
Average Tensile (ksi.)	25.4	41.2	25.4	61.8
Shear (ksi)	6.0	24.8	6.0	37.1
Combined (ksi)	28.0	56.6	Not Required (Reference 1)	
Interaction E.Q. $R_t^2 + R_s^2 < 1$	0.435	1	0.194	1
Bearing Stress (ksi)	13.2	23.75	Not Required (Reference 1)	

The calculated bolt stresses are all less than the specified allowable stresses.

#### 2.11.4.6 Fatigue Analysis

The purpose of the fatigue analysis is to show quantitatively that the fatigue damage to the bolts during normal transport conditions is acceptable. This is done by determining the fatigue usage factor for each normal transport event. For this analysis it is assumed that the container lid bolts are replaced after 500 round trip shipments. The total cumulative damage or fatigue usage for all events is conservatively determined by adding the usage factors for the individual events. The sum of the individual usage factors is checked to make certain that for the 500 round trip shipments of the Oak Ridge SNF Container, the total usage factor is less than one. The following sequence of events is assumed for the fatigue evaluation.

1. Operating Preload
2. Pressure and Temperature Fluctuations
3. Road vibration
4. Shock
5. 1 foot normal condition drop

Since the bolt preload stress applied to the Oak Ridge SNF Container lid bolts is higher than all of the other normal and accident condition loads, the stresses in the bolts will never exceed the bolt preload stress. Consequently, the application and removal of preload is the only real cyclic loading that occurs in the lid bolts. The following analysis is therefore very conservative since it assumes that the usage factor is the sum of all of the individual event usage factors, and not simply the usage factor for bolt preload.

##### A) Operating Preload

Assuming that the bolts are replaced after 500 round trips, the number of preload cycles is two times the number trips or 1,000 cycles.

The maximum tensile stress due to bolt preload is 25,350 psi., and the maximum shear stress due to residual bolt torsion is 5,964 psi. The corresponding stress intensity is then,

$$S.I. = \sqrt{25,350^2 + 4(5,971^2)} = 28,020 \text{ psi.}$$

##### B) Pressure and Temperature Fluctuations

The following bolt loads result from the maximum temperature change of 180° F (Section 2.11.4.2.4).

$$\begin{aligned} F_a &= -540 \text{ lb./ bolt.} \\ F_s &= 0 \text{ lb. / bolt.} \\ M_f &= 0 \text{ in.lb.in.}^{-1} \end{aligned}$$

The maximum pressure difference between in the inside and the outside of the lid is 10 psi (Section 2.11.4.2.3). The bolt loads due to this pressure difference are,

$$\begin{aligned}
 F_a &= 211 \text{ lb./ bolt.} \\
 F_s &= 0 \text{ lb./ bolt.} \\
 F_f &= 48 \text{ lb.in.}^{-1} \\
 M_f &= 114 \text{ in.lb.in.}^{-1} \\
 M_{bb} &= 0.000545 M_f \text{ in.lb. / bolt.}
 \end{aligned}$$

The minimum lid bolt diameter is 0.425 in. Therefore, if the bolt loads from temperature and pressure changes are conservatively summed, we get the following,

$$S_{ba} = 1.2732 \frac{F_a}{D_{ba}^2} = 1.2732 \frac{540 + 211}{0.425^2} = 5,294 \text{ psi.},$$

$$S_{bb} = 10.186 \frac{M_{bb}}{D_{ba}^3} = 10.186 \frac{0.000545(114)}{0.425^3} = 8.24 \text{ psi.},$$

Since internal pressure and temperature loads cause no bolt torsion, and all shear loads are taken by the lid shoulder,

$$S_{bs} = 0, \text{ and } S_{bt} = 0.$$

The stress intensity due the combined temperature and pressure fluctuations is as follows.

$$S.I. = S_{bi} = [(S_{ba} + S_{bb})^2 + 4(S_{bs} + S_{bt})^2]^{0.5} = [(5,294 + 8.24)^2 + 4(0)^2]^{0.5} = 5,302 \text{ psi.}$$

Conservatively assuming this cycle occurs once each one way shipment, the total number of pressure and temperature fluctuation cycles is 1,000.

### C) Vibration / Shock

#### Shock

Since the number of cycles associated with shock and vibration is very high, all axial inertial loading applied to the cask lid are conservatively assumed to be taken by the container lid bolts, even though any such loading would be transferred directly to the TN-FSV Cask body.

Shock input was obtained from ANSI N14.23<sup>(4)</sup>. This standard specifies shock loads that correspond to normal transport over rough roads or minor accidents such as backing into a loading dock. Since the Oak Ridge SNF Container will be transported on interstate highways or major good roads, the shock loads will not be applied continuously to the normal transport mode for the package. The fatigue calculation assumes an average trip of 3,000 miles averaging 45 miles per hour. The total driving time would then be 3,000 miles / 45 mph. = 67 hours. Assume the driver stops and leaves the interstate every 4 hours and assume that one shock could be experienced during each of these stops. The return trip package behavior is assumed to be the

same as the "loaded" trip even though the cargo is no longer present. Therefore shock loading occurs  $18$  (shocks per trip)  $\times 2$  (round trip)  $\times 500$  shipments =  $18,000$  cycles.

Reference 4 specifies a peak shock loading of  $1.8$  gs in the longitudinal direction. The weight of the lid, lid bolts, and container internals is conservatively assumed to be  $5,000$  lb. (The maximum weight of the entire loaded container,  $4,715$  lb., Section 2.2) The bolt force due to shock is,

$$(5,000 \text{ lb})(1.8 \text{ gs}) / (12 \text{ bolts})(0.425 \text{ in}^2 \text{ per bolt}) = 1,765 \text{ psi.}$$

Vibration

According to ANSI 14.23<sup>(4)</sup>, the peak vibration load at the bed of a truck in the longitudinal direction is  $0.3$  gs. This results in a bolt stress of  $294$  psi, which is negligible for a high strength bolt.

D) 1 Foot Normal Condition Drop

The container is designed to transfer impact loads, due to free drop events, directly to the TN-FSV Cask body. Since the container closure lid and shell are directly supported on all sides by the interior surface the TN-FSV cask wall, the container closure bolts do not take any loads during normal or accident condition impacts. Therefore, free drops do not contribute to lid bolt fatigue.

E) Damage Factor Calculation

The following damage factors are computed based on the stresses and cyclic histories described above, a fatigue strength reduction factor,  $K_F$ , of  $4^{(7)}$ , and the fatigue curve shown in Table I-9.4 of ASME Section III Appendices.

**Summary of Fatigue Damage Factors**

Event	Stress Intensity (psi.)	S.I. $\times$ $K_F$ (psi.)	$S_a$ (psi.)	Cycles		Damage Factor $n / N$
				$n$	$N$	
Operating Preload	28,020	112,080	61,590	1,000	2,300	0.43
Pressure and Temperature	5,302	21,210	23,700	1,000	30,000	0.03
Shock	1,765	7,060	7,759	18,000	$\infty$	0.00
$\Sigma$						0.46

Here,  $n$  is the number of cycles,  $N$  is taken from Figure I-9.4 of reference 6, and  $S_a$  is defined in the following way:

If one cycle goes from 0 to  $+S.I.$ , then  $S_a = (1/2) \times S.I. \times K_F \times K_E$ .

If one cycle goes from  $-S.I.$  to  $+S.I.$ , then  $S_a = S.I. \times K_F \times K_E$ .

Where,  $K_E$  is the correction factor for modulus of elasticity. The modulus of elasticity of SA-453, Type 651, class A is  $27.3 \times 10^6$  psi. @  $250^\circ$  F. Therefore,  $K_E = 30.0 \times 10^6 / 27.3 \times 10^6 = 1.099^{(6)}$ .

Since the total damage factor is less than one, the Oak Ridge SNF Container lid bolts will not fail due to fatigue assuming the lid bolts are changed after 500 round trip shipments. Additional fatigue analysis will be required if the total number of shipments exceeds 500 round trips.

#### 2.11.4.7 Minimum Engagement Length for Bolt and Flange

The bolt material is SA-453-651, class A, with

$$S_u = 100 \text{ ksi.}, \text{ and} \\ S_y = 61.8 \text{ ksi. (@ } 250^\circ\text{F)}$$

The flange material is SA-240 Type 304 or SA-182 F304, with

$$S_u = 68.5 \text{ ksi.}, \text{ and} \\ S_y = 23.75 \text{ ksi. (@ } 250^\circ\text{F)}$$

The minimum engagement length,  $L_e$ , for the bolt and flange is (Ref. 3, Page 1149),

$$L_e = \frac{2A_t}{3.146K_{n \max} \left[ \frac{1}{2} + .57735n(E_{s \min} - K_{n \max}) \right]}$$

For a 1/2 UNC 2A bolt,

$$A_t = \text{tensile stress area} = 0.142 \text{ in.}^2, \\ n = \text{number of threads per inch} = 13, \\ K_{n \max} = \text{maximum minor diameter of internal threads} = 0.434 \text{ in.}, \text{ (Ref. 3, p. 1284).} \\ E_{s \min} = \text{minimum pitch diameter of external threads} = 0.4435 \text{ in.}, \text{ (Ref. 3, p. 1284).}$$

Substituting the values given above,

$$L_e = \frac{2(0.142)}{(3.146)0.434 \left[ \frac{1}{2} + .57735(13)(0.4435 - 0.434) \right]} = 0.365 \text{ in.}$$

A correction factor to account for different bolt and mating hole materials,  $J$ , is computed in the following way.

$$J = \frac{A_s \times S_{ue}}{A_n \times S_{ui}} \text{ (Ref. 3, p.1294)}$$

Where,  $S_{ue}$  is the tensile strength of the external thread material, and  $S_{ui}$  is the tensile strength of the internal thread material.

$$A_s = \text{shear area of external threads} = 3.1416 nL_e K_{n \max} [1/(2n) + .57735 (E_{s \min} - K_{n \max})]$$

$$A_n = \text{shear area of internal threads} = 3.1416 nL_e D_{s \min} [1/(2n) + .57735(D_{s \min} - E_{n \max})]$$

For a 1/2 UNC 2A bolt,

$$D_{s \min} = \text{minimum major diameter of external threads} = 0.4876 \text{ in. (Ref. 3, p. 1284)}$$

$$E_{n \max} = \text{maximum pitch diameter of internal threads} = 0.4565 \text{ in. (Ref. 3, p. 1284).}$$

Therefore,

$$A_s = 3.1416(13)(0.365)(0.434)[1/(2 \times 13) + .57735 (0.4435 - 0.434)] = 0.284 \text{ in.}^2$$

$$A_n = 3.1416(13)(0.365)(0.4876)[1/(2 \times 13) + .57735 (0.4876 - 0.4565)] = 0.410 \text{ in.}^2$$

So,

$$J = \frac{0.284(100.0)}{0.409(68.5)} = 1.011$$

$$Q = L_e J = (0.365)(1.011) = 0.369 \text{ in.}$$

The actual minimum engagement length = 1.50 in. > 0.369 in.

### 2.11.4.8 Vent Port Cover Bolt Analysis

The vent port cover closure geometry is given in Appendix 1.4, Drawing 3044-70-6. The 0.75 inch thick vent port cover (VPC) is bolted to the lid by 4, 1/4"-20 UNC high strength steel bolts. The bolt material is SA-193, Grade B8, which has a minimum yield strength of  $S_y = 23.7$  ksi @ 250° F (Ref. 2), and a normal condition allowable stress of  $2/3 S_y = 15.8$  ksi.

The VPC bolt diameter for stress calculations,  $D_{ba} = 0.250 - 0.9743(1/20) = 0.201$  in<sup>2</sup>. The corresponding Stress Area =  $\pi/4 (0.201)^2 = 0.0317$  in<sup>2</sup> (Ref. 1).

#### Vent Port Cover Bolt Torque and Preload

A bolt torque range of 8 to 10 in. lb. has been selected. Using the minimum torque,

$$F_a = Q/KD_b = 8/(0.1 \times 0.250) = 320 \text{ lb.}, \text{ and}$$

$$\text{Preload stress} = F_a / \text{Stress Area} = 320/0.0317 = 10,095 \text{ psi.}$$

Using the maximum torque,

$$F_a = Q/KD_b = 10/(0.1 \times 0.250) = 400 \text{ lb.}, \text{ and}$$

$$\text{Preload stress} = F_a / \text{Stress Area} = 400/0.0317 = 12,618 \text{ psi.}$$

#### Gasket Seating Load

Since an Elastomer o-ring is used, the gasket seating load is negligible.

Pressure Loads (Ref. 1, Table 4.3):

Axial force per bolt due to internal / external pressure is

$$F_a = \frac{\pi D_{lg}^2 (P_{li} - P_{lo})}{4N_b}$$

The worst case pressure load applied to the Oak Ridge Container is conservatively taken to be  $\pm 10$  psi.  $D_{lg}$  (conservatively used outer seal o.d.) = 2.976 in. Then,

$$F_a = \frac{\pi(2.976^2)(\pm 10)}{4(4)} = \pm 17.4 \text{ lb./bolt.}$$

### Temperature Loads (Ref. 2.11.4-1, Table 4.4)

From reference 2, the Vent Port Cover Bolt material, which is SA-193, Gr B8, contains 18Cr 8Ni. The Lid is made of SA-240 Type 304, or SA-182 F304, both of which are 18Cr 8Ni. Therefore, the VPC bolts and lid both have a coefficient of thermal expansion of  $8.90 \times 10^{-6}$  in./in.  $^{\circ}\text{F}^{-1}$  at 250° F (Ref. 2), and there will be no bolts loads generated by thermal expansion.

#### Vent Port Cover Bolt Analysis Conclusions:

- The specified bolt torque is adequate to maintain closure of the vent port cover since the closure force generated by the minimum bolt torque is greater than the maximum force trying to open the vent port cover (320 lb. > 17.4 lb.).
- The maximum stress in the bolt is generated by the maximum torque preload, and is less than the bolt allowable stress (12,618 psi < 15,800 psi).

#### 2.11.4.9 Conclusions

1. Bolt stresses meet the acceptance criteria of NUREG/CR-6007, "Stress Analysis of Closure Bolts for Shipping Casks".
2. A positive (compressive) load is maintained during normal and accident condition loads since bolt preload is higher than all applied loads.
3. If the Oak Ridge SNF Container lid bolts are replaced after every 500 round trip shipments, they will not fail due to fatigue during transport.
4. The bolt / flange thread engagement length is acceptable.
5. The vent port cover closure bolt design is structurally adequate.

#### 2.11.4.10 References

- 2 Stress Analysis of Closure Bolts for Shipping Cask, NUREG/CR-6007, 1992.
- 3 American Society of Mechanical Engineers, ASME Boiler and Pressure Vessel Code, Section II, Part D, 1998.
- 4 Machinery Handbook, 21<sup>st</sup> Ed, Industrial Press, 1979.
- 5 Draft American Standard, Design Basis for Resistance to Shock and Vibration of Radioactive Material Packages Greater than One Ton in Truck Transport, ANSI N14.23, 1980
- 6 Leakage Tests on Packages for Shipment for, Radioactive Materials, ANSI N14.5, 1997
- 7 American Society of Mechanical Engineers, ASME Boiler and Pressure Vessel Code Section III, Division 1, Appendix, 1998.
- 8 Design Criteria for the Structural Analysis of Shipping Cask Containment Vessels, U. S. Nuclear Regulatory Commission, Regulatory Guide 7.6, Revision 1, March 1978.
- 9 Parker O-Ring Handbook, Parker Seals, 1992.
- 10 Baumeister, T., Marks, L. S., Standard Handbook for Mechanical Engineers, 7<sup>th</sup> Edition, McGraw-Hill, 1967.

**TABLE 2.11.4-1  
DESIGN PARAMETERS FOR LID BOLT ANALYSIS**

- $D_b$  Nominal diameter of closure bolt, 0.500 in.
- $K$  Nut factor for empirical relation between the applied torque and achieved preload is 0.1 for neolube.
- $Q$  Applied torque for the preload (in.-lb.)
- $D_{lb}$  Closure lid diameter at bolt circle, 19.07 in.
- $E_c$  Young's modulus of cask wall material,  $27.3 \times 10^6$  psi. @ 250° F.
- $E_l$  Young's modulus of lid material,  $27.3 \times 10^6$  psi. @ 250° F.
- $N_b$  Total number of closure bolts, 12.
- $N_{ut}$  Poisson's ratio of closure lid, 0.305, (Ref. 2.11.4-9, p. 5-6 stainless steel).
- $D_{to}$  Closure lid diameter at outer edge, 20.19 in.
- $D_{ti}$  Closure lid diameter at inner edge, 16.58 in.
- $P_{li}$  Pressure inside the closure lid, 10 psig.
- $t_c$  Thickness of cask wall at lid interface, 1.805 in. (flange)
- $t_l$  Thickness of lid, 7.00 in.
- $l_b$  Thermal coefficient of expansion, bolt material,  $9.46 \times 10^{-6}$  in. in.<sup>-1</sup> °F<sup>-1</sup> @ 250°F.
- $l_c$  Thermal coefficient of expansion, cask  $8.90 \times 10^{-6}$  in. in.<sup>-1</sup> °F<sup>-1</sup> @ 250°F.
- $l_l$  Thermal coefficient of expansion, lid  $8.90 \times 10^{-6}$  in. in.<sup>-1</sup> °F<sup>-1</sup> @ 250°F.
- $E_b$  Young's modulus of bolt material,  $27.3 \times 10^6$  psi. @ 250°F.
- $a_i$  Maximum rigid-body impact acceleration (g) of the cask.
- $DLF$  Dynamic load factor to account for any difference between the rigid body acceleration and the acceleration of the contents and closure lid = 1.1.
- $W_c$  weight of contents = 1,600 lb.
- $W_l$  weight of lid = 500 lbs. \*\*
- $W_c+W_l$  1,600 + 500 = 2,100 lb.
- $\xi_i$  Impact angle between the cask axis and target surface
- $S_{yl}$  Yield strength of closure lid material, 23,750 psi.
- $S_{ul}$  Ultimate strength of closure lid, 68,500 psi.
- $S_{yb}$  Yield strength of bolt material (see Table 2.11.4-3, page 2.11.4-23)
- $S_{ub}$  Ultimate strength of bolt material (see Table 2.11.4-4, page 2.11.4-24)
- $P_{to}$  Pressure outside the lid, 10 psig.
- $L_b$  Bolt length between the top and bottom surfaces of closure, 1.255 in.
- $D_{lg}$  Closure lid diameter (in) at the location of the gasket load reaction, 17.967 in.
- $t_{lf}$  Thickness of the flange of the closure lid, 1.50 in.

**TABLE 2.11.4-1 (continued)**

- $F_{ar}$  Maximum residual tensile bolt force per bolt.
- $F_f$  Fixed-edge closure lid force.
- $M_t$  Torsional bolt moment per bolt.
- $M_{tr}$  Maximum residual torsional bolt moment per bolt.
- $M_f$  Fixed-edge closure lid moment.
- $M_{bb}$  Bending bolt moment per bolt caused by bent or rotated closure lid.
- $D_{lg}$  Closure lid diameter at the location of the gasket load reaction.
- $S_{ba}$  Average tensile stress caused by the tensile bolt force.
- $S_{bb}$  Maximum bending stress caused by the bending bolt moment.
- $S_{bs}$  Average shear stress caused by the shear bolt force.
- $S_{bt}$  Maximum shear stress caused by the torsional bolt moment.
- $S_{bi}$  Maximum stress intensity caused by tension + shear + bending + torsion.
- $R_t$  Ratio of average tensile stress to allowable average tensile stress.
- $R_s$  Ratio of average shear stress to allowable average shear stress.

\*\* Conservatively using higher container weight for lid bolt analysis.

**TABLE 2.11.4-2**  
**BOLT DATA (Ref. 2.11.4-1, Table 5.1)**

Bolt: 1/2" - UNC - 2A

*N*: no of threads per inch = 13

*p*: Pitch = 1/13" = 0.0769 in.

*D<sub>b</sub>*: Nominal Diameter at threads = 0.500 in.

*D<sub>ba</sub>*: Bolt diameter for stress calculations = 0.500 - 0.9743(0.0769)  
= 0.425 in.

Stress Area =  $\pi/4 (0.425)^2 = 0.142 \text{ in}^2$

**TABLE 2.11.4-3**

**ALLOWABLE STRESSES IN CLOSURE BOLTS FOR NORMAL CONDITIONS**

(MATERIAL: SA-453 Type 651 CL. A)

Temperature (°F)	Yield Stress (1) (ksi)	Normal Condition Allowables		
		$F_{tb}$ (2,4) (ksi)	$F_{yb}$ (3.4) (ksi)	$S.I.$ (5) (ksi)
100	70	46.7	28.0	63.0
200	64.2	42.8	25.7	57.8
250	61.8	41.2	24.8	56.6
300	59.4	39.6	23.8	53.5
400	56.1	37.4	22.4	50.5
500	53.1	35.4	21.2	47.8
600	50.7	33.8	20.3	45.6

Notes:

1. Yield stress values are from ASME Code, Section II, Table Y-1 (Ref. 2.11.4-2)
2. Allowable Tensile stress,  $F_{tb} = 2/3 S_y$  (Ref. 2.11.4-1, Table 6.1)
3. Allowable shear stress,  $F_{yb} = 0.4 S_y$  (Ref. 2.11.4-1, Table 6.1)
4. Tension and shear stresses must be combined using the following interaction equation:

$$\frac{\sigma_{tb}^2}{F_{tb}^2} + \frac{\tau_{yb}^2}{F_{yb}^2} \leq 1.0 \text{ (Ref. 2.11.4-1)}$$

5. Stress intensity from combined tensile, shear and residual torsion loads,  $S.I. \leq 0.9 S_y$  (Ref. 2.11.4-1, Table 6.1)

**TABLE 2.11.4-4**

**ALLOWABLE STRESSES IN CLOSURE BOLTS FOR ACCIDENT CONDITIONS**

(MATERIAL: SA-453 Type 651 CL. A)

Temperature (°F)	Yield Stress (1) (ksi)	Accident Condition Allowables		
		0.6 S <sub>y</sub> (3) (ksi)	F <sub>tb</sub> (2,4) (ksi)	F <sub>vb</sub> (3,4) (ksi)
100	70	42.0	70	42.0
200	64.2	38.5	64.2	38.5
250	61.8	37.1	61.8	37.1
300	59.4	35.6	59.4	35.6
400	56.1	33.7	56.1	33.7
500	53.1	31.9	53.1	31.9
600	50.7	30.4	50.7	30.4

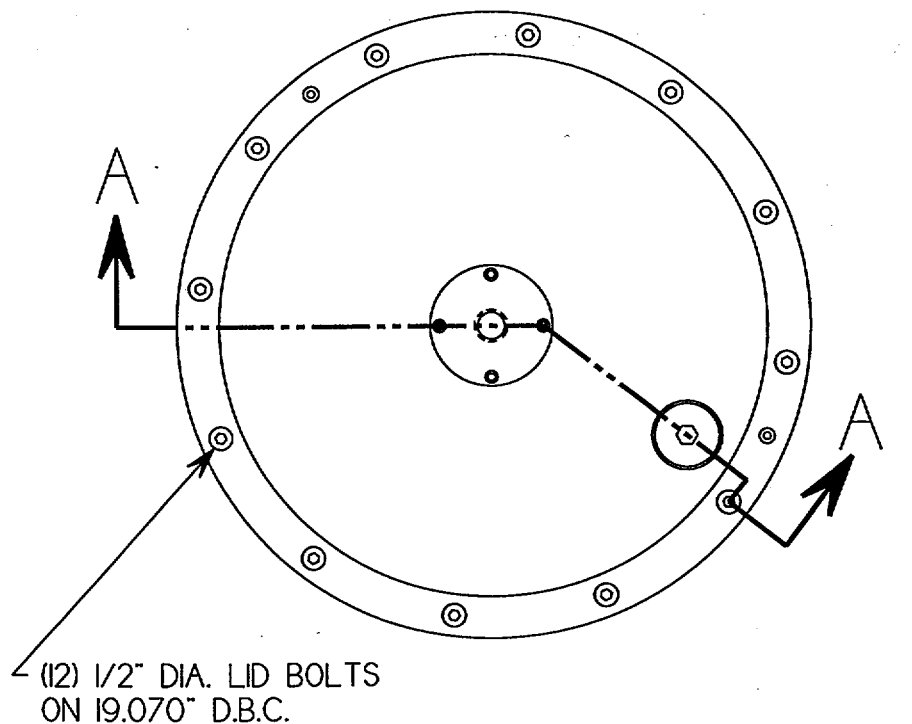
Notes:

1. Yield and tensile stress values are from ASME Code, (Ref. 2.11.4-2) Table Y-1, Note that S<sub>u</sub> is 100 ksi at all temperatures of interest.
2. Allowable Tensile stress, F<sub>tb</sub> = Lesser of (0.7 S<sub>u</sub>, S<sub>y</sub>), where 0.7 S<sub>u</sub> = 0.7 (100) = 70.0 ksi. (Ref. 2.11.4-1, Table 6.3)
3. Allowable shear stress, F<sub>vb</sub> = Lesser of (0.42 S<sub>u</sub>, 0.6 S<sub>y</sub>), where 0.42 S<sub>u</sub> = 0.42 (100.) = 42.0 ksi. (Ref. 2.11.4-1, Table 6.3)
4. Tension and shear stresses must be combined using the following interaction equation:

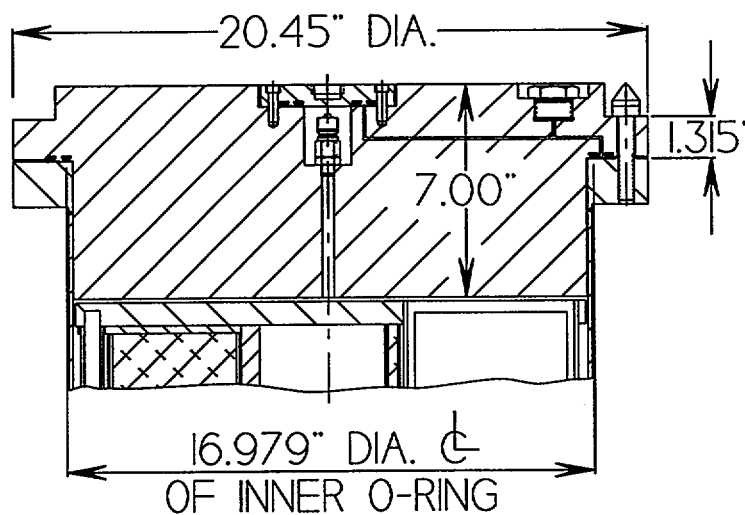
$$\frac{\sigma_{tb}^2}{F_{tb}^2} + \frac{\tau_{yb}^2}{F_{yb}^2} \leq 1.0 \text{ (Ref. 2.11.4-1)}$$

FIGURE 2.11.4-1

OAK RIDGE SNF CONTAINER LID CLOSURE ARRANGEMENT



TOP VIEW



SECTION A-A

FIGURE 2.11.4-2

OAK RIDGE SNF CONTAINER LID BOLT

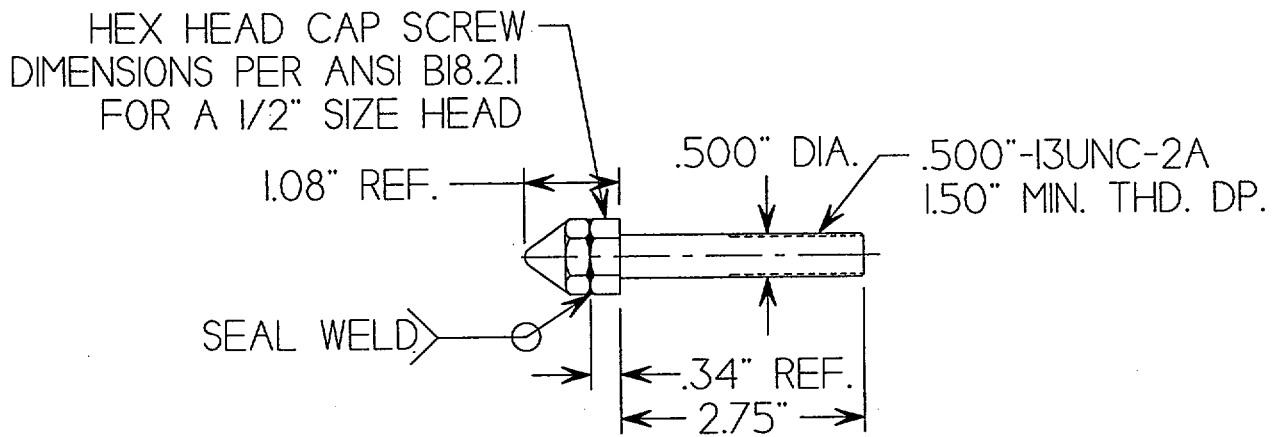
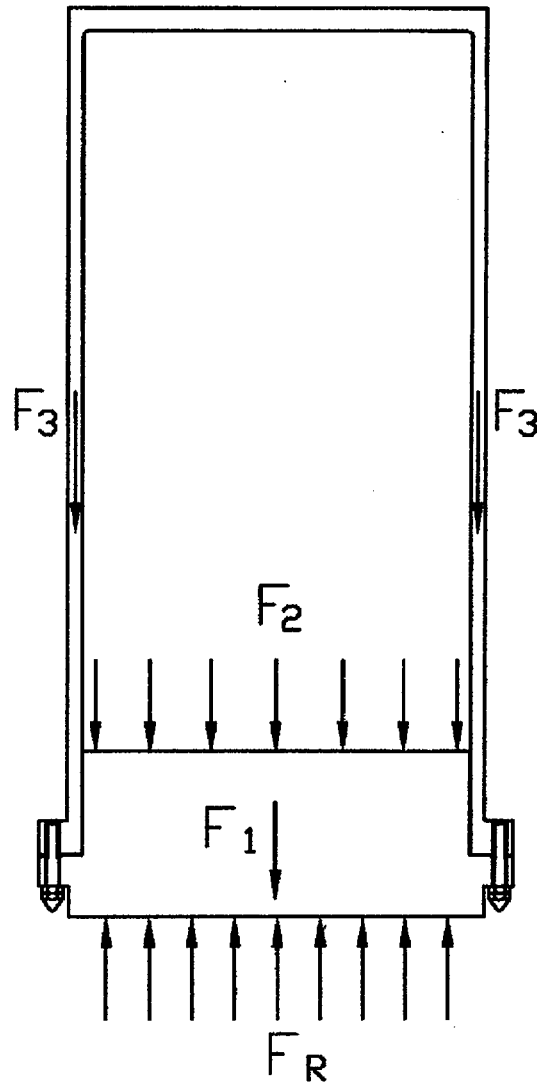


FIGURE 2.11.4-3

FREE BODY DIAGRAM OF OAK RIDGE CONTAINER  
LID CLOSURE SYSTEM SUBJECTED TO A LID END DROP



FREE BODY DIAGRAM OF OAK RIDGE CONTAINER DUE TO LID END DROP

$F_1$  = INERTIA LOAD OF LID

$F_2$  = INERTIA LOAD OF INTERNALS

$F_3$  = INERTIA LOADS OF CONTAINER FLANGE + SHELL + BOTTOM

$F_R$  = TOTAL REACTION FORCE =  $F_1 + F_2 + F_3$

**APPENDIX 2.11.5**  
**TABLE OF CONTENTS**

	<u>Page</u>
2.11.5 TN-FSV CASK AND OAK RIDGE CONTAINER SHELL FATIGUE ANALYSIS.....	2.11.5-1
2.11.5.1 Introduction .....	2.11.5-1
2.11.5.2 TN-FSV Cask Containment Vessel Fatigue Analysis.....	2.11.5-1
2.11.5.3 TN-FSV Cask Lid Bolt Fatigue Analysis.....	2.11.5-4
2.11.5.4 Oak Ridge Container Shell Fatigue Analysis .....	2.11.5-6
2.11.5.5 Conclusions .....	2.11.5-6
2.11.5.6 References.....	2.11.5-7

## APPENDIX 2.11.5

### TN-FSV CASK AND OAK RIDGE CONTAINER SHELL FATIGUE ANALYSIS

#### 2.11.5.1 Introduction

The purpose of this appendix is to describe the structural effect of fatigue on the following components during normal transport conditions:

- TN-FSV Cask Containment Vessel
- TN-FSV Cask Lid Bolt
- Oak Ridge Container Shell

The fatigue analysis of the Oak Ridge Container lid bolt is described in Appendix 2.11.4.

The purpose of the fatigue analysis is to show quantitatively that the fatigue damage to these structures during normal transport conditions is acceptable. This is done by determining the fatigue usage factor for each normal transport event. For this analysis, it is assumed that the cask lid bolts are replaced after 350 round trip shipments. The total cumulative damage or fatigue usage for all events is conservatively determined by adding the usage factors for the individual events. The sum of the individual usage factors is checked to make certain that the total usage factor is less than one. The following sequence of events is assumed for the fatigue evaluation.

1. Operating Preload (Cask Lid Bolt Analysis Only)
2. Pressure and Temperature Fluctuations
3. Road Vibration
4. Shock
5. Test Pressure
6. 1 Foot Normal Condition Drop

Symbols and terminology used for stress determination are taken from TN-FSV SAR, Section 2.10.1.3.

#### 2.11.5.2 TN-FSV Cask Containment Vessel Fatigue Analysis

The purpose of the following fatigue analysis is to show quantitatively that the cask containment vessel stresses are within acceptable limits under normal transport conditions. The stress parameter selected from each load combination is the maximum total stress intensity. The following load combinations are considered in the containment vessel fatigue analysis.

## A) Test Pressure Analysis

The proof test is  $1.5 \times \text{MNOP} = 45$  psig. The corresponding stress is 531 psi. (TN-FSV SAR, Table 2.10.1-5,  $354 \times 1.5 = 531$  psi). The loading only occurs once in the lifetime of the TN-FSV cask.

## B) Shock/Vibration

### Shock

Shock input was obtained from ANSI N14.23<sup>(1)</sup>. This standard specifies shock loads that correspond to normal transport over rough roads or minor accidents such as backing into a loading dock. Since the TN-FSV cask will be transported on interstate highways or major good roads, the shock loads will not be applied continuously to the normal transport mode for the package. The fatigue calculation assumes an average trip of 3,000 miles averaging 45 miles per hour. The total driving time would then be  $3,000 \text{ miles} / 45 \text{ mph} = 67$  hours. Assume the driver stops and leaves the interstate every 4 hours and assume that one shock could be experienced during each of these stops. The return trip package behavior is assumed to be the same as the "loaded" trip even though the cargo is no longer present. Therefore, shock loading occurs  $18$  (shocks per trip)  $\times 2$  (round trip)  $\times 350$  shipments = 12,600 cycles.

The highest surface stress intensity, under shock loading, in the cask containment boundary is 1,433 psi (TN-FSV SAR, Table 2.6-5, Location 6).

### Vibration

The input loading conditions used to evaluate the TN-FSV cask for transport vibration are also obtained from truck bed accelerations in ANSI N14.23. The peak inertia values used are 0.3g, 0.3g, and 0.6g for the longitudinal, lateral, and vertical directions, respectively. This results in a containment stress of 187 psi, which is negligible for the cask containment vessel.

## C) Pressure and Temperature Fluctuations

There are four environmental conditions identified for normal transportation. These are hot environment, cold environment, reduced external pressure, and increased external pressure. The cask containment vessel stresses in response to these environmental load combinations were reported in TN-FSV SAR, the highest total stress intensity from these four cases was calculated to occur during the reduced external pressure condition (662 psi at location 1). Conservatively assuming this cycle occurs once each trip, the total number of cycles is 700 for 350 shipments.

## D) 1 Foot Normal Condition Drop

Containment vessel stress intensities for the normal condition of transport 1 foot end drop and 1 foot side drop events are discussed in Section 2.6.7 of TN-FSV SAR. In that section, it is shown that the 1 foot side drop results in the higher total stress intensity.

The highest total stress intensity for this load combination is 9,046 psi (TN-FSV SAR, Table 2.6-9, Location 6). Although such an event is regarded as uncommon, the fatigue analysis conservatively assumes this event to occur 5 times over the transport life of the containment vessel.

E) Fatigue Evaluation – Usage Factor Calculation

The following damage factors are computed based on the stresses and cyclic histories described above, a fatigue strength reduction factor,  $K_F$ , of 4 (Ref. 2), and the fatigue curve shown in Table I-9.2.1 of ASME Section III Appendices (Ref. 3).

**Summary of Fatigue Damage Factors for the TN-FSV Cask Containment Vessel**

Event	Stress Intensity (psi.)	$S.I. \times K_F \times K_E$ (psi.)	$S_a$ (psi.)	Cycles		Damage Factor $n/N$
				n	N	
Test Pressure	531	2,336	1,168	1	$\infty$	0.00
Shock	1,433	6,305	6,305	12,600	$\infty$	0.00
Pressure and Temperature	662	2,913	2,913	700	$\infty$	0.00
1 Foot Drop	9,046	39,802	19,901	5	65,000	0.00
$\Sigma$						0

Here,  $n$  is the number of cycles,  $N$  is taken from Figure I-9.4 of reference 3, and  $S_a$  is defined in the following way:

If one cycle goes from 0 to  $+S.I.$ , then  $S_a = (1/2) \times S.I. \times K_F \times K_E$ .

If one cycle goes from  $-S.I.$  to  $+S.I.$ , then  $S_a = S.I. \times K_F \times K_E$ .

Where,  $K_E$  is the correction factor for modulus of elasticity. The modulus of elasticity of SA-240 Type 304 is  $27.3 \times 10^6$  psi. Therefore,  $K_E = 28.3 \times 10^6 / 27.3 \times 10^6 \approx 1.1$  (Ref. 3).

The above table shows that the total damage factor is less than one. Therefore the TN-FSV cask containment vessel will not fail due to fatigue.

### 2.11.5.3 TN-FSV Cask Lid Bolt Fatigue Analysis

Since the bolt preload stress applied to the TN-FSV cask lid bolts is higher than all of the other normal and accident condition loads, the stress in the bolts will never exceed the bolt preload stress. Consequently, the application and removal of preload is the only real cyclic loading that occurs in the lid bolts. The following analysis is therefore very conservative since it assumes that the usage factor is the sum of all of the individual event usage factors, and not simply the usage factor for bolt preload.

#### A) Operating Preload Analysis

Assuming that the bolts are replaced after 350 round trips, the number of preload cycles is two times the number of round trips or 700 cycles.

The maximum tensile stress due to bolt preload is 54,744 psi. (TN-FSV SAR, Table 2.10.1-24).

#### B) Test Pressure Analysis

The proof test is  $1.5 \times \text{MNOP} = 45 \text{ psig}$ . (TN-FSV SAR, Section 2.10.1.3). The corresponding stress is 2,983 psi. (TN-FSV SAR, Table 2.10.1-24). The loading only occurs once in the lifetime of the TN-FSV cask.

#### C) Shock/Vibration

##### Shock

Shock input was obtained from ANSI N14.23<sup>(1)</sup>. This standard specifies shock loads that correspond to normal transport over rough roads or minor accidents such as backing into a loading dock. Since the TN-FSV cask will be transported on interstate highways or major good roads, the shock loads will not be applied continuously to the normal transport mode for the package. The fatigue calculation assumes an average trip of 3,000 miles averaging 45 miles per hour. The total driving time would then be  $3,000 \text{ miles} / 45 \text{ mph} = 67 \text{ hours}$ . Assume the driver stops and leaves the interstate every 4 hours and assume that one shock could be experienced during each of these stops. The return trip package behavior is assumed to be the same as the "loaded" trip even though the cargo is no longer present. Therefore shock loading occurs  $18 \text{ (shocks per trip)} \times 2 \text{ (round trip)} \times 350 \text{ shipments} = 12,600 \text{ cycles}$ .

Reference 1 specifies a peak shock loading of 1.8 gs in the longitudinal direction. The weight of the lid, lid bolts, and cask internals is conservatively assumed to be 5,500 lb. The bolt force due to shock is,

$$(5,500 \text{ lb})(1.8 \text{ gs}) / (12 \text{ bolts})(0.606 \text{ in}^2 \text{ per bolt}) = 1,361 \text{ psi. (TN-FSV SAR, Section 2.10.1.3)}$$

Vibration

According to ANSI 14.23<sup>(1)</sup>, the peak vibration load at the bed of a truck in the longitudinal direction is 0.3 gs. This results in a bolt stress of 227 psi, (TN-FSV SAR, Section 2.10.1.3) which is negligible for a high strength bolt.

D) Pressure and Temperature Fluctuations

From TN-FSV SAR, Section 2.10.1.3, the stress intensity generated in the bolts due to pressure and temperature fluctuations has been conservatively computed to be 9,347 psi. The bolt stress intensity is actually less than this since the heat load of the Oak Ridge Container payload is less than the heat load analyzed in the TN-FSV SAR. Conservatively assuming this cycle occurs once each trip, the total number of cycles is 700 for 350 shipments.

E) 1 Foot Normal Condition Drop

Assume this occurs five times over the transport life. According to TN-FSV SAR, Section 2.10.1.3, the stress intensity generated in the cask lid bolts during a 1 foot drop event is 21,414 psi. This stress is a combination of the non prying and prying tensile stress, with zero preload.

F) Fatigue Evaluation – Usage Factor Calculation

The following damage factors are computed based on the stresses and cyclic histories described above, a fatigue strength reduction factor,  $K_F$ , of 4 (Ref. 2), and the fatigue curve shown in Table I-9.4 of ASME Section III Appendices (Ref. 3).

**Summary of Fatigue Damage Factors for the TN-FSV Cask Lid Bolt**

Event	Stress Intensity (psi.)	S.I. $\times K_F \times K_E$ (psi.)	$S_a$ (psi.)	Cycles		Damage Factor $n / N$
				n	N	
Operating Preload	54,744	221,166	110,583	700	840	0.83
Test Pressure	2,983	12,051	6,026	1	$\infty$	0.00
Shock	1,361	5,498	5,498	12,600	$\infty$	0.00
Pressure and Temperature	9,347	37,762	37,762	700	7,000	0.10
1 Foot Drop	21,414	85,513	43,256	5	2,000	0.00
$\Sigma$						0.93

Here,  $n$  is the number of cycles,  $N$  is taken from Figure I-9.4 of reference 3, and  $S_a$  is defined in the following way:

If one cycle goes from 0 to  $+S.I.$ , then  $S_a = (1/2) \times S.I. \times K_F \times K_E$ .

If one cycle goes from  $-S.I.$  to  $+S.I.$ , then  $S_a = S.I. \times K_F \times K_E$ .

Where,  $K_E$  is the correction factor for modulus of elasticity. The modulus of elasticity of SA-540, GR B24, class 1 is  $29.7 \times 10^6$  psi. Therefore,  $K_E = 30.0 \times 10^6 / 29.7 \times 10^6 = 1.01$  (Ref. 3).

The above table shows that the total damage factor is less than one. Therefore, the TN-FSV cask lid bolts will not fail due to fatigue.

#### 2.11.5.4 Oak Ridge Container Shell Fatigue Analysis

The only normal condition cyclic loading that results in a stress in the Oak Ridge Container containment shell high enough to necessitate a fatigue evaluation is the 1 foot side drop. The highest stress intensity in the container shell is 12,256 psi, under the 1 foot drop loading (Appendix 2.11.3).

If the maximum stress intensity is 12,256 psi., and a stress concentration factor of 4 for structural discontinuities as specified by reference 2 and correction factor for modulus of elasticity of 1.1, is applied, a simplified fatigue evaluation can be performed. The container shell alternating stress,  $S_a$ , is  $12,256 \text{ psi.} \times 4 \times 1.1$  or 53,926 psi. According to Figure I-9.2.1 of reference 3, Type 304 stainless steels can withstand an alternating stress of 53,926 psi. for  $3.5 \times 10^4$  cycles. The fatigue damage factor is  $5/35,000 \approx 0$ , therefore, the Oak Ridge Container shell will not fail due to fatigue.

#### 2.11.5.5 Conclusions

- Fatigue failure will not occur in the TN-FSV cask containment vessel
- Assuming the lid bolts are changed after 350 round trip shipments, the TN-FSV cask lid bolts will not fail due to fatigue, since the total damage factor is less than one.
- Fatigue failure will not occur in the Oak Ridge Container shell.

### 2.11.5.6 References

1. Draft American Standard, Design Basis for Resistance to Shock and Vibration of Radioactive Material Packages Greater than One Ton in Truck Transport, ANSI, N14.23 , 1980.
2. Design Criteria for the Structural Analysis of Shipping Cask Containment Vessels, U.S. Nuclear Regulatory Commission, Regulatory Guide 7.6, Revision 1, March 1978.
3. ASME Boiler and Pressure Vessel Code Section III, Division 1, Appendices, 1998.

**APPENDIX 2.11.6**  
**TABLE OF CONTENTS**

	<u>Page</u>
2.11.6 DYNAMIC AMPLIFICATION FACTOR DETERMINATION .....	2.11.6-1
2.11.6.1 Introduction .....	2.11.6-1
2.11.6.2 Dynamic Amplification Factor for End Drop .....	2.11.6-2
2.11.6.3 Dynamic Amplification Factor for Side Drop.....	2.11.6-4
2.11.6.4 Conclusions .....	2.11.6-7
2.11.6.5 References.....	2.11.6-8

**LIST OF FIGURES**

2.11.6-1 Dynamic Load Factor for Half Sine Wave .....	2.11.6-9
2.11.6-2 Support Disc Finite Element Model.....	2.11.6-10

## APPENDIX 2.11.6

### DYNAMIC AMPLIFICATION FACTOR DETERMINATION

#### 2.11.6.1 Introduction

The analysis presented in this appendix is to determine the dynamic amplification factor (DAF) for the Oak Ridge Container. The DAF accounts for the rigid body acceleration difference between the TN-FSV cask and the Oak Ridge Container.

The dynamic amplification factor is taken from the results shown in Figure 2.11.6-1, which is a reproduction of figure 2.15 of NUREG/CR-3966<sup>(2)</sup>, and is a function of the ratio of the half-sine-wave impulse duration to the natural period of the structure. The dynamic amplification factor based on a half sine wave impulse is conservative relative to that of a triangular pulse.

Two load cases will be evaluated in this calculation, one due to longitudinal loading (end drop), and one due to transverse loading (side drop).

The three main components of the Oak Ridge Container with the longest and most significant natural periods are the support discs (Appendix 1.4, Drawing 3044-70-7, Items 17A, 17B, and 17C), the fuel compartments (Appendix 1.4, Drawing 3044-70-7, Item 9 and 10 weldment), and the container shell (Appendix 1.4, Drawing 3044-70-2, Item 2, 3, 4, and 5 weldment). Each component is modeled separately. The Dynamic Amplification Factor used for the entire Oak Ridge Container is conservatively taken to be the highest of the three individual dynamic amplification factors computed.

During an end drop, the fundamental natural periods of the Oak Ridge Container fuel compartments and container shell are taken to be that of a simply supported cylindrical shell without axial constraint, under longitudinal vibration. During a side drop, the fundamental natural periods of each fuel compartment and the container shell are taken to be that of a simply supported cylindrical shell without axial constraint. Here, the length of the fuel compartment is taken to be 1/9 of the entire length of the fuel compartment since it is supported by ten evenly spaced support discs.

## Notation

The notation used in this analysis is taken from reference 1, and is as follows.

- $E$ , Modulus of Elasticity, (psi).
- $f_1, f_{11}$ , Fundamental natural frequency, (Hz.).
- $I$ , Moment of inertia of the beam, (in.<sup>4</sup>).
- $L$ , Length of beam or cylindrical shell, (in.).
- $m$ , Mass per unit length of the beam, (lb.in.<sup>-1</sup>).
- $\mu$ , Mass density, (lb.in.<sup>-3</sup>).
- $\nu$ , Poisson's ratio.
- $R$ , Outer radius of the cylindrical shell, (in.).

### 2.11.6.2 Dynamic Amplification Factor for End Drop

The fundamental natural frequency of a simply supported cylindrical shell under axial vibration simplifies to that of a uniform beam, free axially at both ends. The fundamental natural frequency of a uniform beam free at both ends, under longitudinal vibration is as follows. (Ref. 1, p. 183, Table 8-16, Case 1)

$$f_1 = \frac{\lambda_1}{2\pi L} \left( \frac{E}{\mu} \right)^{1/2}$$

Where  $\lambda_1 = \pi$ .

#### A) Fuel Compartment

For the Oak Ridge Container fuel compartment,  $E = 27.3 \times 10^6$  psi. (for stainless steel @ 250° F, Ref. 4), and  $L = 189.88$  in. Based on a stainless steel density of 0.29 lb. in.<sup>-3</sup>, and conservatively using the maximum dimension component weight, the average mass density,  $\mu$ , is calculated in the following way (container component weights are take from Section 2.2).

Weight of fuel compartment tube = 741 lb. / (5 fuel compartments) = 148 lb.

Weight of fuel assembly = 1,600 / (5 fuel compartments) = 320 lb.

Weight flux traps = 189 / (5 fuel compartments) = 38 lb.

Volume of loaded fuel compartment =  $(\pi/4)(5.563^2)(189.88) = 4,615$  in.<sup>3</sup>

Average mass density,  $\mu = \frac{148 + 320 + 38}{(386.1)(4,615)} = 0.000284$  lbm. in.<sup>-3</sup>

Therefore,

$$f_1 = \frac{\pi}{2\pi(189.88)} \left( \frac{27.3 \times 10^6}{0.000284} \right)^{1/2} = 816 \text{ Hz.}$$

The natural period of the fuel compartments is then  $1/f_1$  or  $T = 0.00123$  s.

### B) Oak Ridge Container Shell

For the Oak Ridge Container shell,  $E = 27.3 \times 10^6$  psi.<sup>(4)</sup>,  $L = 198.00$  in., and the average mass density,  $\mu$ , is calculated in the following way.

Weight of the entire Oak Ridge Container = 5,000 lb.

Volume of Oak Ridge Container =  $(\pi/4)(16.85^2)(198.00) = 44,152$  in.<sup>3</sup>

Average mass density,  $\mu = \frac{5,000}{(386.1)(44,152)} = 0.0002933$  lbm. in.<sup>-3</sup>

Therefore,

$$f_1 = \frac{\pi}{2\pi(198.00)} \left( \frac{27.3 \times 10^6}{0.0002933} \right)^{1/2} = 770 \text{ Hz.}$$

The natural period of the container shell is then  $1/f_1$  or  $T = 0.00130$  s.

### C) Support Disc

The ANSYS finite element model of support disc, described in Appendix 2.11.3, is used to perform a modal analyses in order to determine the natural period of the support discs. The support disc finite element model is shown in Figure 2.11.6-2. SHELL63 elements are used to construct the model for the end drop modal analyses. During an end drop event, the support disc is assumed to be supported at the five tie-rod locations.

The material properties of the support disc are taken as that of SA-240, Type 304 stainless steel at a temperature of 250°F. Weight densities are changed to mass densities ( $\rho_m = \rho_w / 386.1$ ). The following properties and inputs were used in the end drop modal analyses.

A conservative weight of 100 lbs. is assumed to act on the disc to account for the components attached to the disc. This load is applied by modifying the disc material density. The bottom support disc is not analyzed, because it is thicker and will consequently have a higher natural frequency, which is non-conservative.

- Modulus of Elasticity =  $27.3 \times 10^6$  psi.
- Disc model weight = 18.8 lb.
- Stainless steel density =  $0.29 \text{ lb/in}^3$
- Additional weight acting on disc = 100 lbs.
- Modified weight density =  $0.29(18.8+100)/18.8 = 1.8326 \text{ lb/in}^3$
- Mass density used in the analysis =  $1.8326/386.1 = 0.00474 \text{ lb-sec}^2/\text{in}^4$
- Master degrees-of-freedom = 500.

The finite element model is constrained at the five tie rod locations for the end drop event. At each of the five tie rod locations, the model is constrained at 9 nodes.

The fundamental natural frequency of the Oak Ridge Container support disc when subjected to an end drop acceleration was found to be  $f_1 = 346 \text{ Hz}$ . The natural period of the support discs is then  $1/f_1$  or  $T = 0.00289 \text{ s}$ .

#### D) Estimate of DAF

From the ADOC impact limiter analysis presented in TN-FSV SAR Appendix 2.10.2, for a 30 foot end drop event, the duration of impact,  $t_1$ , is in the range of 0.030 seconds to 0.040 seconds, depending on the impact limiter wood properties. Since the natural periods of the various container structures are relatively short during an end drop, it is conservative to take  $t_1$  to be 0.030 seconds, and to use the maximum period of the structure,  $T = 0.00289 \text{ s}$ . Therefore, the ratio  $t_1/T$  is  $0.030/0.00289$ , or 10.38. Based on the curve shown on the Figure 2.11.6-1, the dynamic amplification factor is only slightly larger than 1. Consequently, during an end drop, the DAF is conservatively taken to be 1.10.

#### 2.11.6.3 Dynamic Amplification Factor for Side Drop

The bending mode of a cylindrical shell is taken to be most significant vibration mode of the fuel compartment and container shell during a side drop event. The fundamental natural frequency of the bending mode of a simply supported cylindrical shell, without axial constraint, is as follows (Ref. 1, p. 304, Table 12-2, Case 4),

$$f_{11} = \frac{\lambda_{11}}{2\pi R} \left( \frac{E}{\mu(1-\nu^2)} \right)^{1/2}$$

### A) Fuel Compartment

For the fuel compartment,  $L$  is taken to be the length between support discs, 20.96 in.,  $R = 2.782$  in.,  $\nu = 0.305$  (for stainless steel, Ref. 3, p. 5-6), and  $\mu = 0.29$ . Since  $L/(jR) = 20.96/(1 \times 2.782) = 7.5 < 8.00$ , therefore simple beam theory applies<sup>(1)</sup>.

The fundamental natural frequency of the bending mode of a uniform beam pinned at both ends is as follows (Ref. 1, p. 108, Table 8-1, Frame 5).

$$f_1 = \frac{\lambda_1^2}{2\pi L^2} \left( \frac{EI}{m} \right)^{1/2}$$

Where,  $E = 27.3 \times 10^6$  psi.,  $\lambda_1 = \pi$ , and

$$I = \frac{\pi}{4} (r_o^4 - r_i^4) = \frac{\pi}{4} \left[ \left( \frac{5.563}{2} \right)^4 - \left( \frac{5.295}{2} \right)^4 \right] = 8.425 \text{ in.}^4,$$

$$m = \frac{148 + 320 + 38}{(386.1)(189.88)} = 0.006902 \text{ lbm. in.}^{-1}$$

Where  $m$  is the maximum dimension mass per unit length of a single fuel compartment, with fuel assemblies and inner spacers. Therefore,

$$f_1 = \frac{\pi^2}{2\pi(20.96^2)} \left( \frac{(27.3 \times 10^6)(8.425)}{0.006902} \right)^{1/2} = 653 \text{ Hz.}, \text{ and}$$

The natural period of the fuel compartment is then  $1/f_1$  or  $T = 0.00153$  s.

From TN-FSV SAR Appendix 2.10.2, the duration of impact during a side drop,  $t_1$ , is in the range of 0.030 seconds to 0.040 seconds, depending on the impact limiter wood properties. It is conservative to take  $t_1$  to be 0.030 seconds, since the natural period of the fuel compartment is small. Therefore the ratio  $t_1/T$  is  $0.030/0.00166$ , or 18.07. Based on the curve shown on the Figure 2.11.6-1, the dynamic factor is only slightly larger than 1. Consequently, during a side drop, the DAF is conservatively taken to be 1.10.

## B) Oak Ridge Container Shell

For the container shell,  $L = 198.00$  in.,  $R = 8.425$  in.,  $\nu = 0.305$ , and  $\mu = 0.29$ . Since  $L/(jR) = 198.00/(1 \times 8.425) = 23.5 > 8.00$ , cylindrical shell theory applies (Ref. 2.11.6-1). Therefore (Ref 2.11.6-1, p. 304, Table 12-2, Case 4),

$$\lambda_{11} = \frac{j^2 \pi^2 (1-\nu^2)^{1/2} R^2}{2^{1/2} L^2} = \frac{1^2 \pi^2 (1-0.305^2)^{1/2} 8.425^2}{2^{1/2} 198.00^2} = 0.0120, \text{ and}$$

$$f_{11} = \frac{\lambda_{11}}{2\pi R} \left( \frac{E}{\mu(1-\nu^2)} \right)^{1/2} = \frac{0.0120}{2\pi(8.425)} \left( \frac{27.3 \times 10^6}{0.29(1-0.305^2)} \right)^{1/2} = 2.31 \text{ Hz.}$$

The natural period of the container shell is then  $1/f_1$  or  $T = 0.433$  s.

Since the natural period of the container shell is relatively long, it is conservative to take  $t_1$  to be 0.040 seconds. Therefore the ratio  $t_1/T$  is  $0.040/0.433$ , or 0.092. Based on the curve shown on the Figure 2.11.6-1, the dynamic factor is much less than 1. Consequently, during a side drop, the DAF is conservatively taken to be 1.10.

Note: For the container shell natural period calculation, the weight of the container internals was not included in the calculation of the mass density,  $\mu$ , since an increased mass would increase the container's natural period and consequently decrease the DAF. Therefore, including the weight of the container's internals would be non-conservative.

## C) Support Disc

The ANSYS finite element model of support disc, described in Appendix 2.11.3, is used to perform a modal analyses in order to determine the natural period of the support discs during a side drop event. The support disc finite element model is shown in Figure 2.11.6-2. PLANE42 elements are used to construct the model for the side drop modal analyses. MASS21 elements are used to model the fuel and fuel compartment weights. During a side drop, the support disc is assumed to be supported radially over the bottom  $180^\circ$  periphery. Two orientations,  $0^\circ$  and  $36^\circ$ , are used to characterize the most extreme drop cases possible so that all possible side drop orientations are bounded.

The lateral impact load applied to the structural disc for a side drop accident include the inertial weights of the fuel canisters, the fuel compartment, and the support disc itself. The loading due to fuel canisters and fuel compartments on one support disc are applied as mass elements on nodes dispersed over the bottom  $90^\circ$  periphery of disc holes. The mass added to the periphery of the disc holes is calculated as follows.

The total load on the discs (8 intermediate and 2 end) is 3,200 lbs. Assuming end discs share  $\frac{1}{2}$  load of intermediate discs, the load on each intermediate disc =  $3,200/9 = 355.5$  lb.

Then the load per disc hole is  $355.5/5 = 71.1$  lb., and the corresponding mass added on each disc hole is  $66.7/386.1 = 0.184$  lb-sec<sup>2</sup>/in<sup>4</sup>

For the side drop event, the bottom half of the disc perimeter in the direction parallel to the drop angle vector is restrained.

The fundamental natural frequencies for both 0° and 36° side drop analyses are tabulated below:

### Summary of Support Disc Natural Frequencies

0° Drop	36° Drop
148 Hz.	127 Hz.

The lowest natural frequency of support disc is 127 Hz. and corresponds to a 36° side drop orientation. The natural period of the support discs for the side drop event is then  $1/f_1$  or  $T = 0.00787$  s.

For the support disc transverse vibration, it is conservative to take  $t_1$  to be 0.030 seconds. Therefore the ratio  $t_1/T$  is  $0.030/0.00787$ , or 3.81. Based on the curve shown on the Figure 2.11.6-1, the dynamic factor is approximately 1.10.

#### 2.11.6.4 Conclusions

Conservatively taking the maximum dynamic amplification factor computed for each component under both longitudinal and transverse vibration, the overall dynamic amplification factor for the Oak Ridge Container is taken to be 1.10.

### 2.11.6.5 References

1. Blevins, Formulas for Natural Frequency and Mode Shape, Krieger Publishing Company, 1995.
2. Methods for Impact Analysis of Shipping Containers, NUREG/CR-3966, UCID-20639, LLNL, 1987.
3. Baumeister, T., Marks, L. S., Standard Handbook for Mechanical Engineers, 7<sup>th</sup> Edition, McGraw-Hill, 1967.
4. American Society of Mechanical Engineers, ASME Boiler and Pressure Vessel Code, Section II, Part D, 1998.

**FIGURE 2.11.6-1**  
**DYNAMIC LOAD FACTOR FOR HALF SINE WAVE**

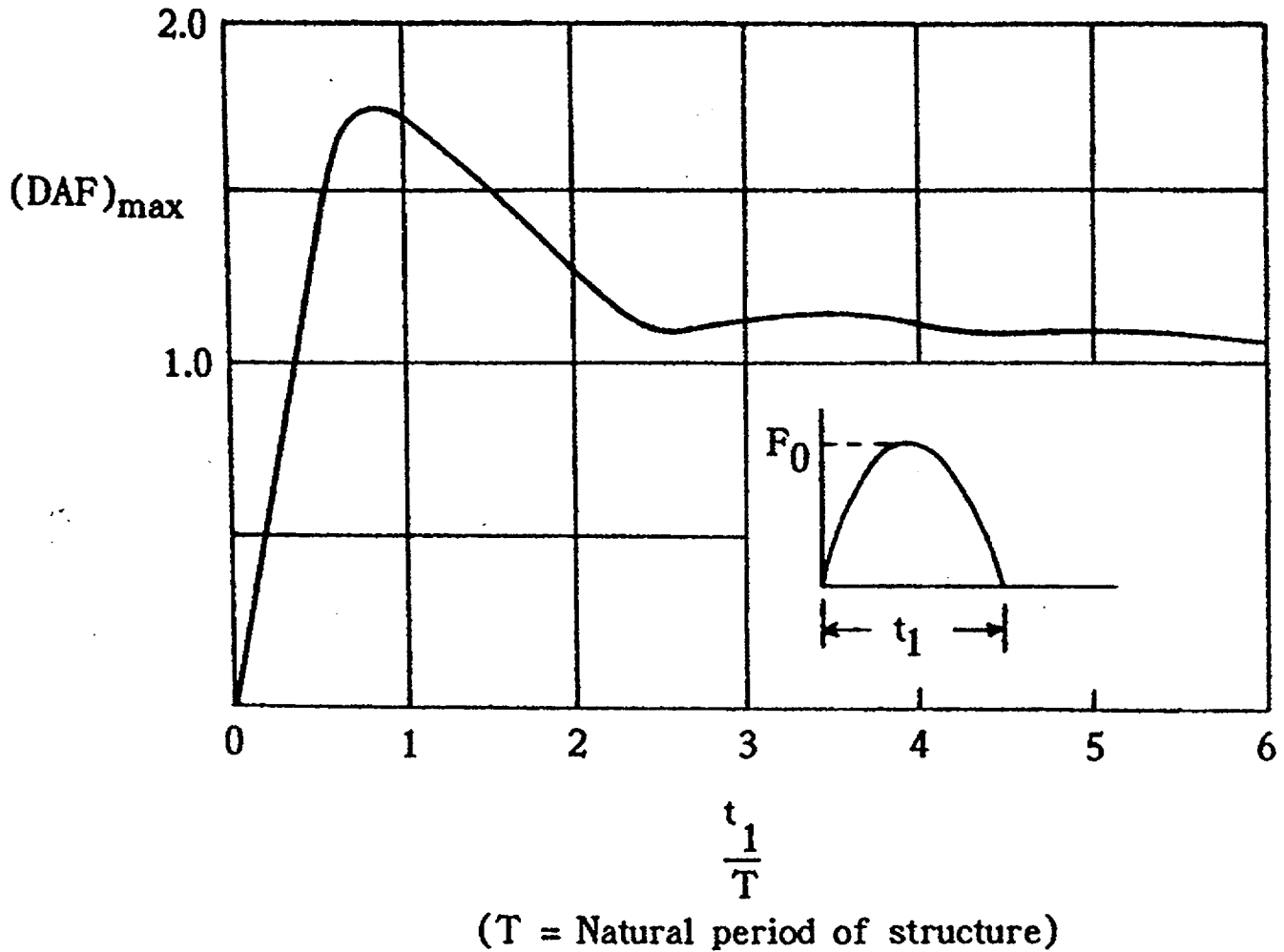
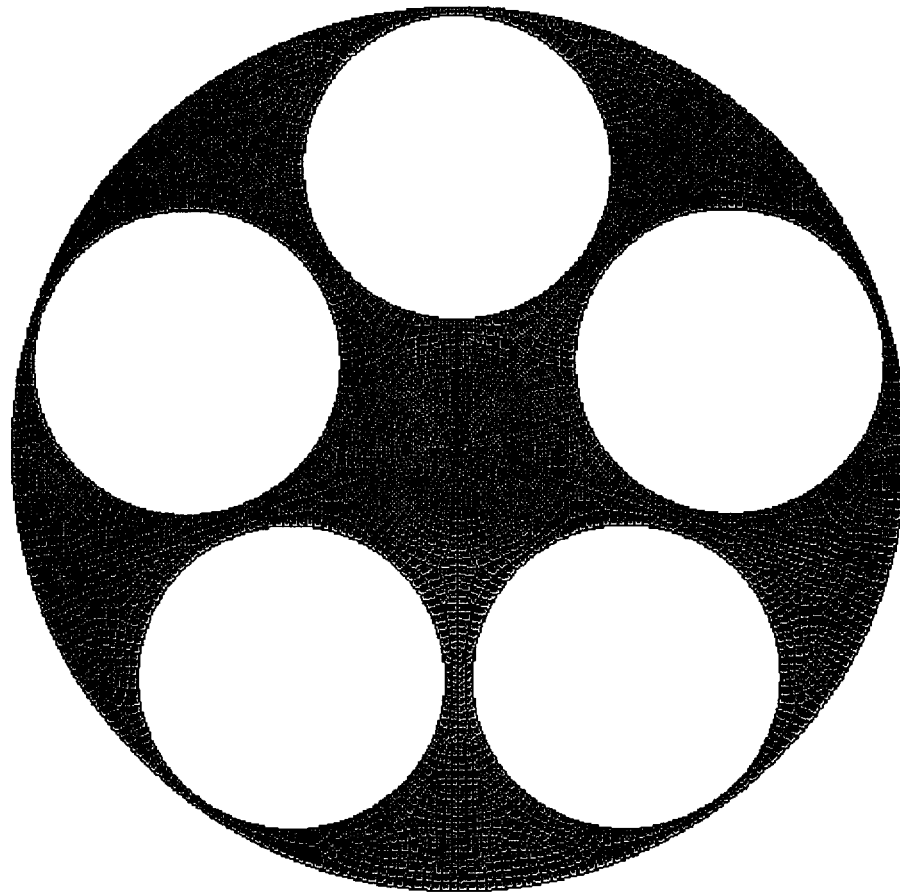


**FIGURE 2.11.6-2**  
**SUPPORT DISC FINITE ELEMENT MODEL**



## APPENDIX 2.11.7

### TABLE OF CONTENTS

	<u>Page</u>
2.11.7 OAK RIDGE CANISTER STRUCTURAL ANALYSIS.....	2.11.7-1
2.11.7.1 Introduction .....	2.11.7-1
2.11.7.2 Model Description .....	2.11.7-3
2.11.7.3 Stress Analysis .....	2.11.7-4
2.11.7.4 Stress Analysis Results.....	2.11.7-10
2.11.7.5 Canister Shell/Freeze Plug Joint.....	2.11.7-11
2.11.7.6 Conclusions .....	2.11.7-14
2.11.7.7 References.....	2.11.7-15

### LIST OF FIGURES

2.11.7-1 True Stress-Strain Curve for Type 304 at 275° F.....	2.11.7-16
2.11.7-2 Side Drop Model Loading and Support Configuration.....	2.11.7-17
2.11.7-3 Side Drop Model Plot .....	2.11.7-18
2.11.7-4 End Drop Model Plot (One Eighth Symmetry).....	2.11.7-19
2.11.7-5 Normal Condition Side Drop Membrane Stress Intensity.....	2.11.7-20
2.11.7-6 Normal Condition Side Drop Maximum Membrane Plus Bending Stress Intensity .....	2.11.7-21
2.11.7-7 Accident Condition End Drop Load-Displacement Curve for the Cap Weldment .....	2.11.7-22
2.11.7-8 Accident Condition End Drop Deformation for the Cap Weldment at 60g .....	2.11.7-23
2.11.7-9 Accident Condition Side Drop Membrane Stress Intensity....	2.11.7-24
2.11.7-10 Accident Condition Side Drop Maximum Membrane Plus Bending Stress Intensity .....	2.11.7-25
2.11.7-11 Load Path for Oak Ridge Canister Contents .....	2.11.7-26

## APPENDIX 2.11.7

### OAK RIDGE CANISTER STRUCTURAL ANALYSIS

#### 2.11.7.1 Introduction

This appendix presents the structural design criteria, mechanical properties of materials, and structural evaluations, which demonstrate that the Oak Ridge canister meets the acceptance criteria presented in Section 2.11.7.1B. No credit is taken for the confinement capabilities of the Peach Bottom canisters, since they contain intact fuel assemblies. Consequently, the Peach Bottom canisters are not analyzed structurally.

Material properties for Oak Ridge canister (Type 304 stainless steel) are taken from reference 1, Section II, Part D. Nonlinear properties are obtained as discussed below. The maximum temperature of the canister shell is 271 °F, taken from Chapter 3, Table 3-1. A uniform value of 275 °F is conservatively used for all canister components. The applied loads are taken to be the following accelerations due to normal and accident conditions for end and side drops (TN-FSV SAR Appendix 2.10.2) respectively, including a value of 1.10 for the Dynamic Amplification Factor (Appendix 2.11.6).

#### Summary of Applied Load Caused by Free Drop Event

Impact Load	Normal Conditions (1 foot drop)	Accident Conditions (30 foot drop)
Axial g load (end drop)	14 gs × 1.10 ≈ 16 gs.	54 gs × 1.10 ≈ 60 gs.
Transverse g load (side drop)	17 gs × 1.10 ≈ 20 gs.	71 gs × 1.10 ≈ 80 gs.

The weight of the canister and flux traps, which separate the canisters, is taken from Chapter 2, Table 2-5. The weight of all 20 loaded canisters is 1,600 lb, or 80 lb per canister. The weight of all 15 flux traps is 189 lb, or 12.6 lb. per flux trap. The payload is assumed to have no structural strength.

#### A) Material Properties

The Oak Ridge canister assemblies consist of a Type 304 stainless steel shell with a welded Type 304 end fitting on one end. A separate freeze plug is used on the other end. Properties are based on a conservative operating temperature of 275 °F, and are given in the following table.

**Type 304 Material Properties at 275 °F**

<b>Yield Strength (<math>S_y</math>), psi</b>	<b>Ultimate Strength (<math>S_u</math>), psi</b>	<b>Design Stress Intensity (<math>S_m</math>), psi</b>	<b>Elastic Modulus, <math>\times 10^6</math> psi</b>
23,125	67,250	20,000	27.15

Note: Material properties taken from reference 1, Section II, Part D, at a temperature of 275 °F.

For nonlinear analyses, a multi-linear stress strain curve is used, derived from data contained in NUREG/CR-0481<sup>(4)</sup>. True stress-strain curves for ASTM Type 304 stainless steel tested at various temperatures are given in Figure 7 of reference 4. A true stress-strain curve for a temperature of 275 °F was found by interpolation between the curves for data at 200 °F and 400 °F, conservatively using the lower bound of the scatter in each case. The resulting curve is shown in Figure 2.11.7-1.

**B) Acceptance Criteria**

The acceptance criteria used for the canister analyses are based on Section III, Division 1, Subsection NG (for Normal Conditions of Transport) and Section III, Division 1, Appendix F (for Hypothetical Accident Conditions) of the ASME Code<sup>(1)</sup>. Acceptance criteria are summarized in the following table.

**Stress Acceptance Criteria**

<b>Stress Category</b>	<b>Allowable Stresses</b>		
	<b>Normal Conditions (Level A)</b>	<b>Accident Conditions (Level D)</b>	
	<b>Elastic Analysis</b>	<b>Elastic/Plastic Analysis</b>	<b>Elastic Analysis</b>
Primary Membrane Stress Intensity ( $P_m$ )	$S_m$	$0.7 S_u$	Lesser of $2.4 S_m$ and $0.7 S_u$
Local Membrane Stress Intensity ( $P_L$ )	$1.5 S_m$	$0.9 S_u$	Lesser of $3.6 S_m$ and $1.0 S_u$
Primary Membrane + Bending Stress Intensity ( $P_L + P_b$ )	$1.5 S_m$	$0.9 S_u$	Lesser of $3.6 S_m$ and $1.0 S_u$
Primary Membrane + Secondary Stress Intensity Range ( $P_L + P_b + Q$ )	$3.0 S_m$	N/A	N/A
Bearing Stress ( $S_b$ )	$1.5 S_y$	N/A	N/A

The stability criterion for the canister shell is ASME Code Case N-284-1. The stability criterion for the cap weldment is based on Section III, Division 1, Appendix F, F1341.3 – Collapse Load, of the ASME Code<sup>(1)</sup>. A large deflection, plastic analysis is performed to determine the displacement-load limit line and to show that the applied impact acceleration is safely below the acceleration level which causes structural instability.

#### 2.11.7.2 Model Description

The canister has an overall length of 34.75 inches and an outer diameter of 4.75 inches. It consists of a Type 304 stainless steel shell, 31.13 inches long and 0.12 inches thick, closed at one end with a freeze plug and closed at the other end with a 0.38 inch thick welded plate. On the latter end is welded a cap weldment, consisting of a shell 3.38 inches long and 0.12 inches thick, having four cutouts 1.5 inches wide and 1.38 inches long. Finite element analyses are performed using the ANSYS<sup>®</sup> 5.5<sup>(3)</sup> finite element analysis program.

The critical sections of the canister include the central cylindrical shell, which is susceptible to buckling, and the cap weldment area, which has four cut out sections. The geometry of the freeze plug end of the canister shell is not critical with respect to buckling or stress. The freeze plug itself reinforces the reduced shell thickness region at the end of the shell. The thickness of the freeze plug is 0.216 inches, which is much greater than the nominal thickness of the canister shell in the central region (0.12 inches). Typically, buckling of cylindrical shells will occur in the middle portion of the shell, and not at the ends.

##### A) Side Drop Model

For the side drop orientation, the canister is modeled using shell elements having nonlinear capability (SHELL43), supported in the middle by a 0.75 inch thick support disk. The side drop model utilizes quarter symmetry, and therefore the shell length is 17.38 inches (half of the total length of 34.75 inches) and the support disc is 0.38 inches thick (half of the total thickness of 0.75 inches). Since the end structures play no role in the side drop, they are not given a detailed treatment in the side drop model. The ends of the model are closed with 0.12 inch thick plates to simulate the rigidity of the actual structures.

Note that this modeling approach is very conservative, since the uniform support of the fuel compartment tube (a 5 inch, schedule 10 pipe) is completely neglected, and the canister is assumed to be supported directly on a single support disk at the midpoint of the canister. The contact between the canister and support disc is modeled by fixing the canister shell nodes at the edge of the support disc for a distance of 30° from the vertical centerline, (equivalent to a total of 60° of support contact), as shown in Figure 2.11.7-2. A plot of the model is given in Figure 2.11.7-3. A multi-linear, kinematic hardening stress-strain curve is used as discussed in Section 2.11.7.1A.

The model is given a density of 0.285 lb/in<sup>3</sup> and a transverse acceleration of either 20g (normal conditions) or 80g (accident conditions). To account for the entire 80 lb of weight, nodal forces are used in a cosine distribution over the lower half of the model, as shown in Figure 2.11.7-2. Forces are uniformly distributed along the shell length. The resulting total reaction force is conservatively slightly higher than  $\frac{1}{4} \times 80 \times (g)$ , where  $g$  is the side drop acceleration and the factor of  $\frac{1}{4}$  accounts for the quarter symmetry. Model results are discussed in Section 2.11.7.3B (normal condition side drop) and Section 2.11.7.3D (accident condition side drop).

## B) End Drop Model

The end drop model is used only to evaluate the behavior of the cap weldment in the area of the four cutouts, since the shell of the canister is more readily treated using hand calculations. The model consists of a one-eighth symmetry portion of the cap using shell elements (SHELL43), as shown in Figure 2.11.7-4. The nodes at the narrow end are fixed in all degrees of freedom, consistent with the weld used at that location to attach the cap to the rest of the canister. The upper end, where the small lip is located, is free, and appropriate symmetry boundary conditions are used on the circumferential edges of the model. The model is loaded by pressures along the free edge. The pressures are coplanar with the side shell elements, and represent the load supported by the lowest canister. The governing loading case for the end drop configuration is one in which four Oak Ridge canisters and three flux traps are present in each one of the five fuel compartments. In this configuration, the load on the bottom end of the lowest canister is

$$P_e = [4(W_{can}) + 3(W_{ft})] = 357.8 \text{ lb.}$$

where the weight of the canister,  $W_{can} = 80$  lb each, and the weight of the flux trap,  $W_{ft} = 12.6$  lb each (Section 2.2). A conservatively higher load of 444 lb. is used in the analysis. A multi-linear, kinematic hardening stress-strain curve is used as discussed in Section 2.11.7.1A. Model results are discussed in Section 2.11.7.3C (Cap Weldment Buckling Analysis).

### 2.11.7.3 Stress Analysis

#### A) Normal Condition End Drop

##### Canister Shell

As shown in Section 2.11.7.2B, the weight supported by the lower end of the lowest canister is 444 lb. The normal condition end drop impact,  $g_{NCT} = 16g$ . In this configuration, the load on the lowest canister is

$$F_{NCT} = P_e (g_{NCT}) = 7,104 \text{ lb}$$

The cross sectional area of the canister shell is

$$A = \pi/4(d_o^2 - d_i^2) = 1.745 \text{ in}^2$$

where the canister shell outer diameter,  $d_o$ , = 4.75 inches, and the inner diameter,  $d_i$ , = 4.51 inches. The axial compressive membrane stress in the shell under the normal condition end drop is

$$\sigma_{NCT} = \frac{F}{A} = 4,071 \text{ psi}$$

The allowable membrane stress for normal conditions of transport is  $S_m$ , which for Type 304 stainless steel at 275 °F is 20,000 psi. The margin of safety is

$$MS = \frac{20,000}{4,071} - 1 = +3.91$$

#### Cap Weldment

The cap weldment, which also supports axial loads, has the same outer and inner diameters as the shell, including a quantity of four,  $L = 1.5$  inch wide cutouts which reduce the load carrying area. The half-angle of one cutout is

$$\frac{\theta}{2} = \sin^{-1}\left(\frac{L}{(1/2)(d_o + d_i)}\right) = 18.90^\circ$$

The total angular extent of cutouts is therefore  $8 \times \theta/2 = 151.2^\circ$ , or  $151.2/360 = 42\%$  of the total area. The area remaining is therefore

$$A_c = (1 - 0.42)A = 1.012 \text{ in}^2$$

The stress in the cap weldment is

$$\sigma_{NCT-cap} = \frac{A}{A_c} \sigma_{NCT} = 7,020 \text{ psi}$$

The margin of safety is

$$MS = \frac{20,000}{7,020} - 1 = +1.85$$

Thus, all margins of safety are positive for the normal condition end drop of 16g.

## B) Normal Condition Side Drop

### Canister Shell

The canister is analyzed utilizing the finite element model described in Section 2.11.7.2A. It was loaded with a transverse acceleration of 20g. The resulting maximum stresses occur at the upper edge of contact with the support disc (at 40° from the vertical plane), and are elastic in nature. The maximum membrane stress ( $P_m$ ) is 8,319 psi. The allowable membrane stress for normal conditions of transport is  $S_m$ , which for Type 304 stainless steel at 275 °F is 20,000 psi. The margin of safety is

$$MS = \frac{20,000}{8,319} - 1 = +1.40$$

The maximum membrane plus bending stress at the surface of the shell ( $P_m + P_b$ ) is 21,823 psi. The allowable membrane plus bending stress is  $1.5S_m$ . The margin of safety is

$$MS = \frac{(1.5)20,000}{21,823} - 1 = +0.37$$

A plot of the membrane stress intensity is given in Figure 2.11.7-5, and a plot of the maximum membrane plus bending stress is given in Figure 2.11.7-6. Thus, all margins of safety are positive for the normal condition side drop of 20g.

## C) Accident Condition End Drop

### Canister Shell Stress Analysis

Since the only difference between the normal condition and the accident condition is the magnitude of the impact severity, the accident end drop loads and stresses can be found by factoring the normal condition results by the ratio of accident impact to normal impact. The load on the lowest canister in the accident end drop is therefore

$$F_{HAC} = F_{NCT} \frac{60}{16} = 26,640 \text{ lb}$$

where the accident end drop impact is 60g and the normal end drop impact is 16g. Similarly, the axial compressive membrane stress in the shell is

$$\sigma_{HAC} = \sigma_{NCT} \frac{60}{16} = 15,266 \text{ psi}$$

The allowable membrane stress for hypothetical accident conditions is the lesser of  $2.4S_m$  or  $0.7S_u$ , which for Type 304 stainless steel is  $0.7S_u$ , equal to  $0.7(67,250) = 47,075$  psi, where  $S_u$  equals 67,250 psi at a temperature of 275 °F. The margin of safety is

$$MS = \frac{47,075}{15,266} - 1 = + 2.08$$

Canister Shell Buckling Analysis

The end drop buckling stability of the canister shell is evaluated using ASME Code Case N-284-1<sup>(2)</sup>. For hypothetical accident conditions, a factor of safety of 1.34 is applied. The axial stress in the shell is found above to be 15,266 psi. Hoop and shear stresses are zero for the end drop orientation. As shown in the following N-284-1 Summary Table, all interaction check parameters are less than unity, as required. Therefore, buckling of the canister shell does not occur due to the accident condition end drop.

**Summary of Code Case N-284 Buckling Stress Calculations**

<b>Code Case N-284 Reference Paragraphs</b>	<b>Stress Calculations</b>
Compression Stress Based on 60g Axial Acceleration	15.3 ksi
Factor of Safety (Para. 1400)	1.34
	20.50 ksi
Capacity Reduction Factor (Para. 1500)	0.2525
Elastic Amplified Stress	81.20 ksi
Plastic Reduction Factor (Para. 1600)	0.1076
Plastic Amplified Stress	754.61 ksi
Theoretical Buckling Stress (Para. 1712)	851.44 ksi
Analysis Result	754.61 ksi < 851.44 ksi

### Cap Weldment Stress Analysis

For the cap weldment in the area of the cutouts, the stress is

$$\sigma_{\text{HAC-cap}} = \sigma_{\text{NCT-cap}} \frac{60}{16} = 26,325 \text{ psi}$$

The margin of safety is

$$MS = \frac{47,075}{26,325} - 1 = +0.79$$

### Cap Weldment Buckling Analysis

The stability of the segments between the cutouts of the cap weldment is evaluated using the finite element model described in Section 2.11.7.2B. As discussed in Section 2.11.7.1B, the stability criterion for the cap weldment is based on the method described in ASME Code Section III, Division I, Appendix F, Paragraph F1341.3<sup>(1)</sup>. In this approach, the cap weldment model is run in a series of steps of increasing load, and the load-displacement response of the weldment is plotted. The axial displacement of the upper end of the weldment (at the location of the lip) is used. A collapse limit line, defined in Appendix II, Paragraph II-1430, is added to the load displacement plot. The safe load is found by the intersection of the load displacement line and the collapse limit line. For the cap weldment, this intersection occurs at a load of 62g, which is greater than the maximum accident end drop acceleration of 60g, as shown in Figure 2.11.7-7. A deformation plot of the cap weldment model for a load of 60g is shown in Figure 2.11.7-8. Therefore, buckling of the cap weldment does not occur due to the accident condition end drop.

#### D) Accident Condition Side Drop

### Canister Shell

The canister is analyzed utilizing the finite element model described in Section 2.11.7.2A. It was loaded with a transverse acceleration of 80g. The resulting maximum stresses occur at or near the symmetry plane at the edge of contact with the support disc, and are non-linear in nature. The maximum membrane stress ( $P_m$ ) is 27,500 psi. The allowable membrane stress for accident conditions is  $0.7S_u$  when elastic/plastic analysis is used, and for Type 304 stainless steel at 275 °F,  $S_u$  is equal to 67,250 psi. The margin of safety is

$$MS = \frac{(0.7)67,250}{27,500} - 1 = +0.71$$

The maximum membrane plus bending stress at the surface of the shell ( $P_m + P_b$ ) is 33,057 psi. The allowable membrane plus bending stress is  $0.9S_u$  when elastic/plastic analysis is used. The margin of safety is

$$MS = \frac{(0.9)67,250}{33,057} - 1 = +0.83$$

A plot of the membrane stress intensity is given in Figure 2.11.7-9, and a plot of the maximum membrane plus bending stress is given in Figure 2.11.7-10. Thus, all margins of safety are positive for the accident condition side drop of 80g.

**2.11.7.4 Stress Analysis Results**

The following table summarize the maximum calculated and allowable stresses generated in the Oak Ridge canister during all applicable normal and accident condition events.

<b>Summary of Calculated and Allowable Stress in Oak Ridge Canister</b>				
<b>Component</b>	<b>Applied Load</b>	<b>Stress Category</b>	<b>Maximum Stress (ksi.)</b>	<b>Allowable Stress (ksi.)</b>
Canister Shell	16 g End drop (Normal conditions)	Compression	4.07	20.00
	60 g End drop (Accident conditions)	Compression	15.27	47.08
	20 g Side drop (Normal conditions)	Membrane	8.32	20.00
		Membrane + Bending	21.82	30.00
	80 g Side drop (Accident conditions)	Membrane	27.50	47.08
		Membrane + Bending	33.06	60.53
Cap Weldment	16 g End drop (Normal conditions)	Compression	7.02	20.00
	60 g End drop (Accident conditions)	Compression	26.33	47.08

From Section 2.11.7.3C, the cap weldment will not buckle during the 60g end drop, since the allowable axial impact load is 62 gs, which is greater than the maximum accident condition impact load of 60 gs. Likewise, from Section 2.11.7.3C, the canister shell will not buckle during the 60g end drop, since the plastic amplified stress (754.61 ksi) is less than the allowable buckling stress (851.44 ksi).

### 2.11.7.5 Canister Shell/Freeze Plug Joint

The Oak Ridge canisters retain their SNF contents during normal and hypothetical accident conditions and thereby provide the confinement boundary for the fissile materials as modeled in the criticality safety analysis in Section 6. The analyses in Section 2.11.7.3 demonstrate that the central cylindrical shell and the cap weldment of the Oak Ridge canisters do not fail structurally during normal conditions of transport or during hypothetical accident conditions, and so failure of these components does not cause a release of the canister contents. In addition, the freeze plug can not become separated from the canister shell and allow a release of the contents. During transport, the loads imposed on the freeze plug joint are not sufficient to overcome the friction forces due to the 0.005 to 0.007 inch interference fit of these two stainless steel components. Also, the lengths of the Oak Ridge canisters and flux trap spacers are established such that there is not enough length in a fuel compartment for a freeze plug to disengage from a canister shell.

The arrangement of Oak Ridge canisters, flux traps, and Peach Bottom assemblies in the fuel compartments of the Oak Ridge Container prevents loads from being transferred to the freeze plug/canister shell joint in a manner that would separate this joint. In a bottom end drop, the bottom of each Oak Ridge canister is supported either by the compartment spacer at the bottom of the fuel compartment, or by the top of a flux trap spacer. During a bottom end drop under either normal or accident conditions, an axial load is developed due to the deceleration of the unrestrained contents of the Oak Ridge canister. However, the load that is developed and transferred to the freeze plug is resisted by the adjacent flux trap spacer or by the compartment spacer at the bottom of the fuel compartment, not by the interference fit forces that secure the freeze plug to the canister shell. The diagram in Figure 2.11.7-11 illustrates this load path. Analyses in Appendix 2.11.1 demonstrate the structural integrity of the flux traps under this load. Axial loads applied to the compartment spacer bear on the bottom plate of the Oak Ridge Container and are transferred to the bottom of the TN-FSV cask. Since the freeze plug joint does not carry this inertial load, there are no forces tending to cause the joint to separate.

In a lid end drop, the freeze plug in an Oak Ridge canister has inertial forces that tend to push the freeze plug into the joint, rather than to open the joint. Therefore, in this drop orientation, there are no forces that cause the joint to separate.

In a side drop, the transverse load generated does not act in a direction that would tend to separate the freeze plug from the canister shell. Therefore, in this drop orientation, there are no forces that cause the joint to separate.

In a drop on the bottom corner of the cask, the axial component of the load that is generated by the canister contents is transferred in the same manner as in the bottom end drop described above. Also, the transverse component of the load generated during a bottom corner drop does not act in a direction that would tend to separate the freeze plug from the canister shell, the same as during a side drop. Therefore, in this drop orientation, there are no forces that cause the joint to separate.

In a drop on the lid-end corner of the cask, the axial component of the load that is generated by the canister contents is transferred in the same manner as in the lid end drop described above. Also, the transverse component of the load generated during a lid-end corner drop does not act in a direction that would tend to separate the freeze plug from the canister shell, the same as during a side drop. Therefore, in this drop orientation, there are no forces that cause the joint to separate.

In a slap down event, the unrestrained contents of the canister would create loads that are a combination of the drop orientations described above. However, these loads do not create forces that cause the joint to separate.

Although there are no drop orientations that create forces that tend to separate the interference fit of freeze plug joint, there are three other safety features that contribute to preventing a release of the contents of the Oak Ridge canisters during accident conditions. These safety features are described below.

#### A) Safety Feature – Pins and Slots in the Oak Ridge Canister

The freeze plug design of the Oak Ridge canister has a secondary closure system that was included to meet hoisting safety requirements for an independent means to ensure the plug does not separate from the shell. During lifting of a canister by the handling head in a vertical orientation, the contents of the Oak Ridge canister are supported by only the freeze plug. While the interference fit of the plug in the shell can readily support this load, an independent load path is provided by two pins 180 degrees apart that fit into slots cut into the side of the canister shell. These pins are also a secondary safety feature for ensuring that the freeze plug does not separate from a canister shell during transport.

#### B) Safety Feature – Small Clearance Length Provided in a Fuel Compartment

The length of the stack of Oak Ridge canisters and flux traps, in combination with the length of the fuel compartment of the Oak Ridge Container, provides additional protection to prevent the release of fissile material from the Oak Ridge canisters. The geometry of this stack ensures that the freeze plug cannot separate from the canister shell, and so provides additional assurance that the contents remain within the Oak Ridge canister. The available clearance in the Oak Ridge Container fuel compartment when loaded with four Oak Ridge canisters and three flux traps is tabulated below, using nominal dimensions:

Oak Ridge Container fuel compartment cavity length = 188.00 in.

Oak Ridge canister length = 34.75 in.

Flux trap length = 16.00 in.

Stack of 4 Oak Ridge canisters and 3 flux traps =  $(4 \times 34.75'' + 3 \times 16.00'')$  = 187.00 in.

Clearance in fuel compartment loaded with 4 Oak Ridge Canisters and 3 flux traps  
=  $(188.00 - 187.00)$  = 1.00 in.

Oak Ridge canister freeze plug thickness = 1.12 in.

Since the freeze plug thickness of 1.12 inches is greater than the 1.00 inch clearance in the fuel compartment, the plug cannot completely separate from the canister shell even if loosened, and so provides an additional safety feature to ensure that the contents remain inside the canister.

Even in the event that all components are fabricated to the limits of their design tolerances that provide the maximum clearance in the fuel compartment, there is still insufficient clearance to allow the freeze plug to separate from the canister, as the dimensions tabulated below demonstrate:

Oak Ridge Container fuel compartment cavity length =  $(188.00 \pm .06 \text{ in.}) = 188.06 \text{ in.}$

Oak Ridge canister length =  $(34.75 \pm .01 \text{ in.}) = 34.74 \text{ in.}$

Flux trap length =  $(16.00 \pm .12 / -.00 \text{ in.}) = 16.00 \text{ in.}$

Stack of 4 Oak Ridge canisters and 3 flux traps  
=  $(4 \times 34.74'' + 3 \times 16.00'') = 186.96 \text{ in.}$

Clearance in fuel compartment loaded with 4 Oak Ridge Canisters and 3 flux traps  
=  $(188.06 - 186.96 \text{ in.}) = 1.10 \text{ in.}$

Oak Ridge canister freeze plug thickness =  $(1.12 \pm .01 \text{ in.}) = 1.11 \text{ in.}$

The clearance in the fuel compartment (1.10 in.) remains less than the freeze plug thickness (1.11 in.) and the plug cannot separate from the canister even in the event that components are fabricated to their tolerance limit that creates the maximum clearance.

Since the materials of construction are the same for the Oak Ridge Container sleeve and the Oak Ridge Canisters and flux traps, there is no relative change in these clearances due to temperature changes.

### C) Safety Feature – Use of an Inner Sleeve

The design of the Oak Ridge canister uses an inner sleeve to facilitate loading in the hot cell. By placing the spent fuel materials into the sleeve first, the amount of materials are strictly controlled in the sense that all materials must remain within the cavity of the sleeve to ensure that the sleeve fits into the cavity of the Oak Ridge canister shell. This arrangement means that when the inner sleeve is pushed into the open end of a canister, there is no chance that the contents will not fit into a canister.

The geometry of this arrangement provides an additional safety feature during transport. The sleeves are sized to closely fit the cavity of the canister, both length and diameter, so as to provide a clear indication of the space available for the contents. Since the open top of the sleeve is placed at the welded-closed end of the canister, the only path for materials from the

cavity of a sleeve to exit a loaded Oak Ridge canister, is by movement between the outside of the inner sleeve and the inside of the canister shell. However, there is only a very small diametrical clearance between these two parts. Dimensions of the Oak Ridge canister cavity and inner sleeve are as follows:

Oak Ridge canister cavity	4.50" ID × 30.0" long
Inner sleeve	4.38" OD × 29.75" long

As can be seen by the difference in diameters, particles are limited to no more than about 0.12" to move along this path. But items this small are typically preloaded into quart-sized or smaller cans before loading into the sleeve. Thus, an additional press fit lid prevents even this size material from exiting the cavity of the sleeve.

The use of an inner sleeve and the limited size of the path from the sleeve cavity to the freeze plug provide defense-in-depth to ensure that the contents are retained in the Oak Ridge canister in the inner sleeve.

#### D) Conclusions

As shown in the Sections above, the interference fit of the freeze plug does not experience forces that tend to separate the freeze plug from the shell. In addition, there are pins and slots on each canister joint that provide an independent system for keeping the plug joined to the shell. As a separate safety feature, there is not enough space in a fuel compartment for a plug to come out of a shell. Therefore, there is no possibility of separation of the freeze plug joint and there is no release of the contents of a canister.

#### 2.11.7.6 Conclusions

From the table in Section 2.11.7.4, it can be seen that all of the stresses and impact loads generated in the Oak Ridge canister are less than their corresponding allowable limits. The discussions in Section 2.11.7.5 demonstrate that the canister shell/freeze plug joint does not separate. Based on these analyses, the Oak Ridge canister contents are not released for normal or hypothetical accident conditions.

#### 2.11.7.4 References

1. American Society of Mechanical Engineers (ASME) Boiler and Pressure Vessel Code, Section II and Section III, *Rules for Construction of Nuclear Power Plant Components*, 1995 Edition, United Engineering Center, 345 East 47th Street, New York, NY.
2. American Society of Mechanical Engineers (ASME) Boiler and Pressure Vessel Code, Code Case N-284-1.
3. ANSYS, Inc., ANSYS Engineering Analysis System User's Manual for ANSYS Revision 5.5, Houston, PA.
4. Henry J. Rack, Gerald A. Knorovsky, *An Assessment of Stress-Strain Data Suitable for Finite-Element Elastic-Plastic Analysis of Shipping Containers*, NUREG/CR-0481, Sandia National Laboratories, September 1978.

**FIGURE 2.11.7-1**  
**True Stress-Strain Curve for Type 304 at 275 °F**

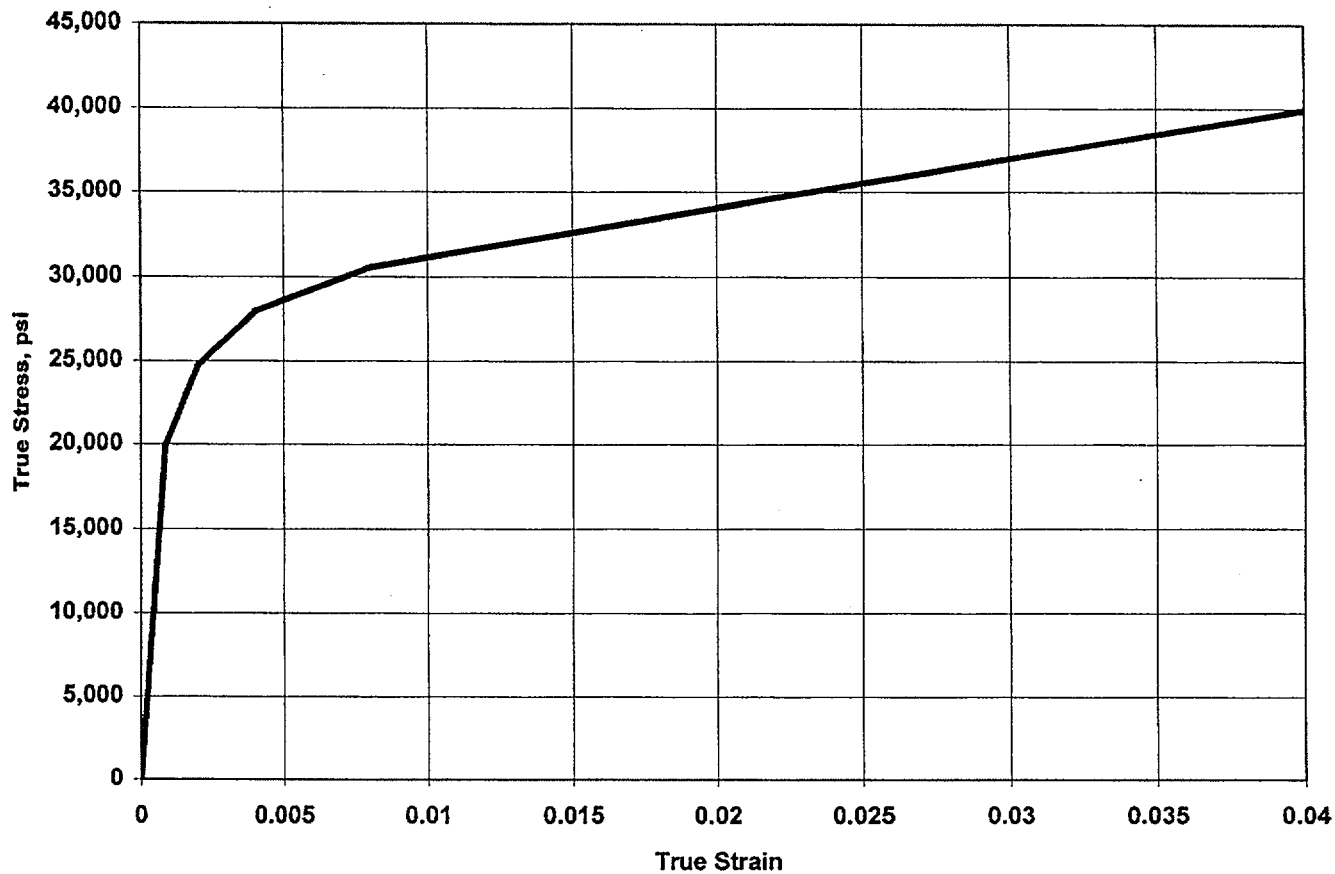


**FIGURE 2.11.7-2**  
**Side Drop Model Loading and Support Configuration**

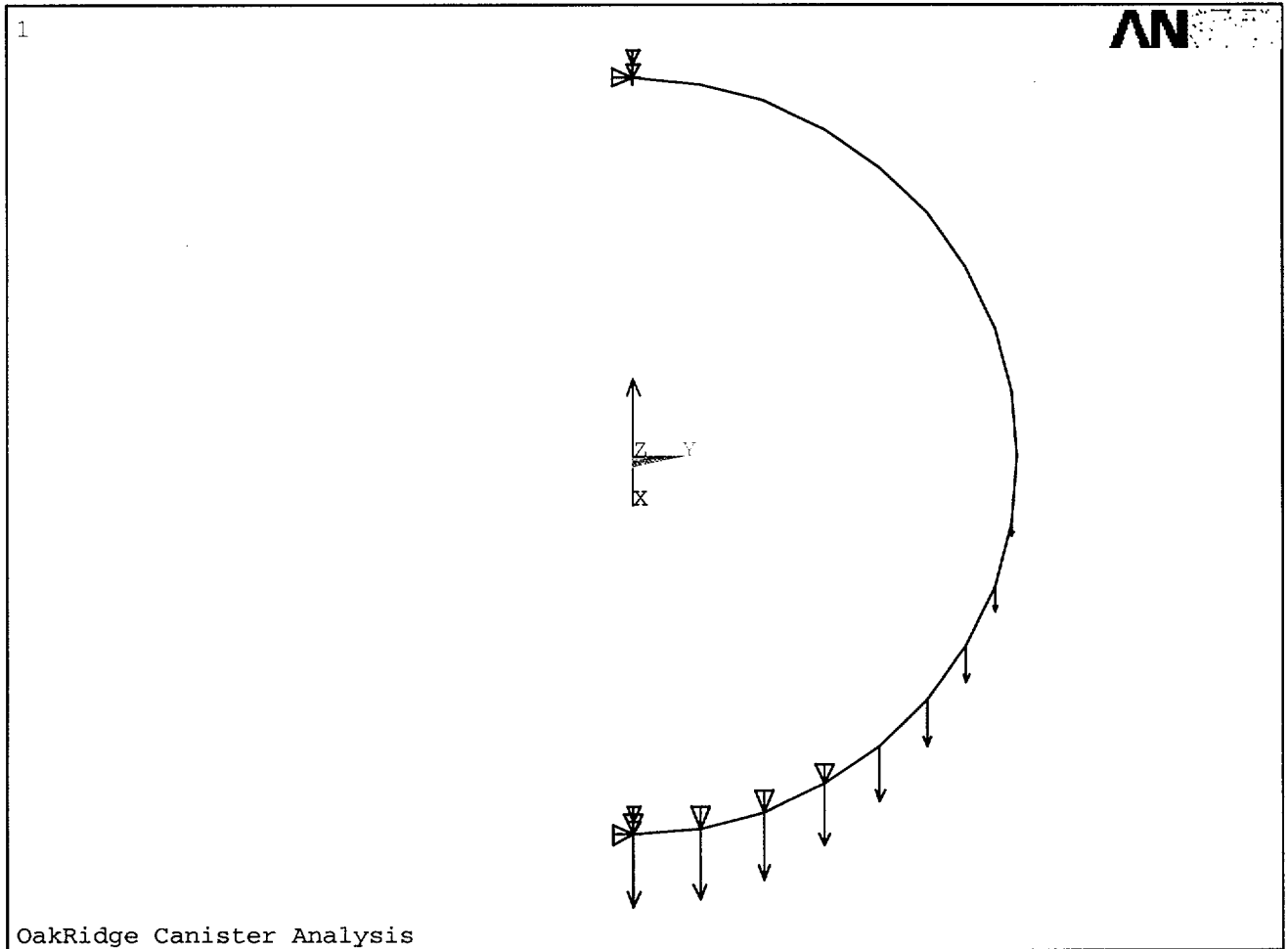


**FIGURE 2.11.7-3**  
**Side Drop Model Plot**

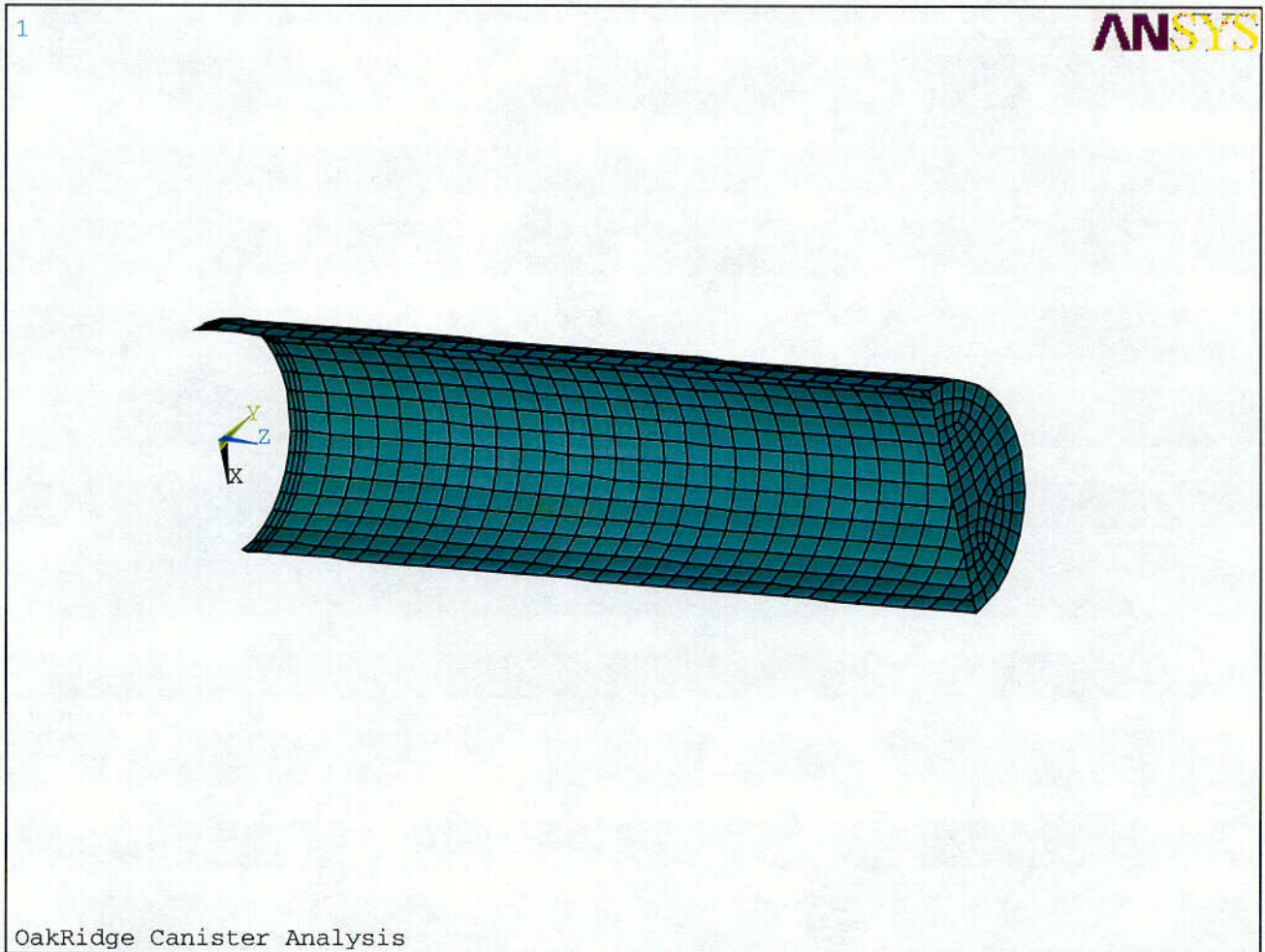


**FIGURE 2.11.7-4**  
**End Drop Model Plot (One-Eighth Symmetry)**

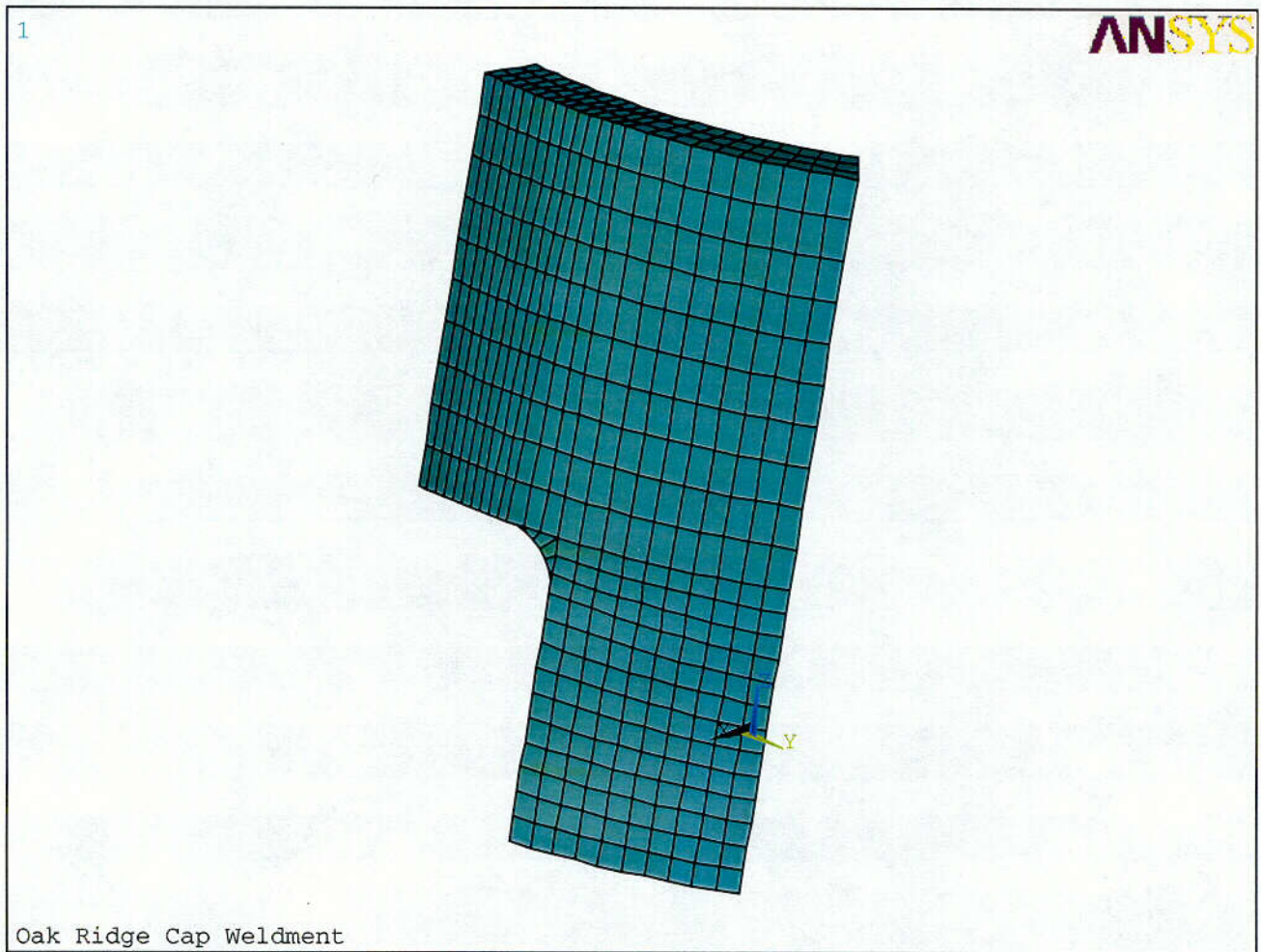


**FIGURE 2.11.7-5**  
**Normal Condition Side Drop Membrane Stress Intensity**

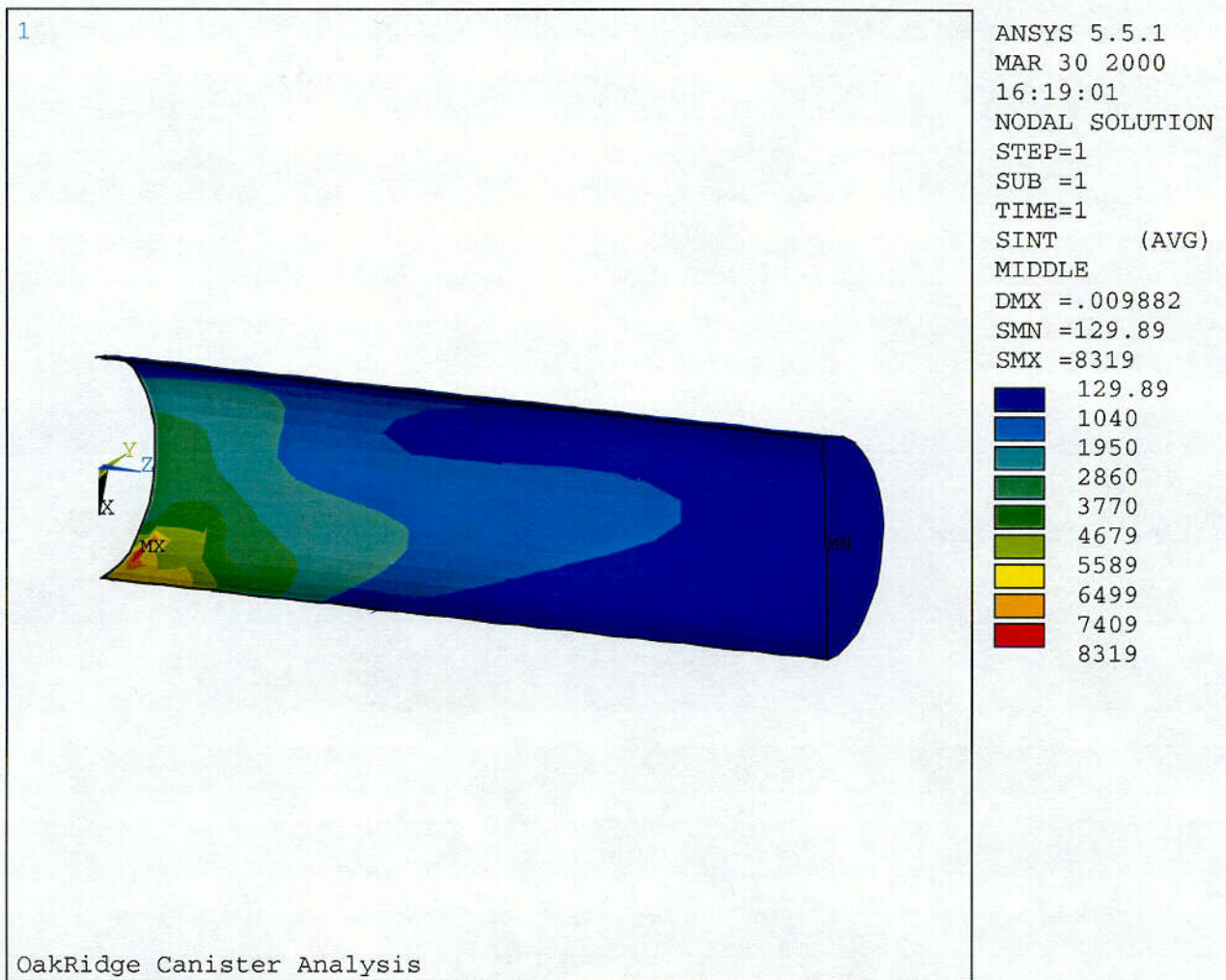


**FIGURE 2.11.7-6**  
**Normal Condition Side Drop Maximum Membrane Plus Bending Stress Intensity**

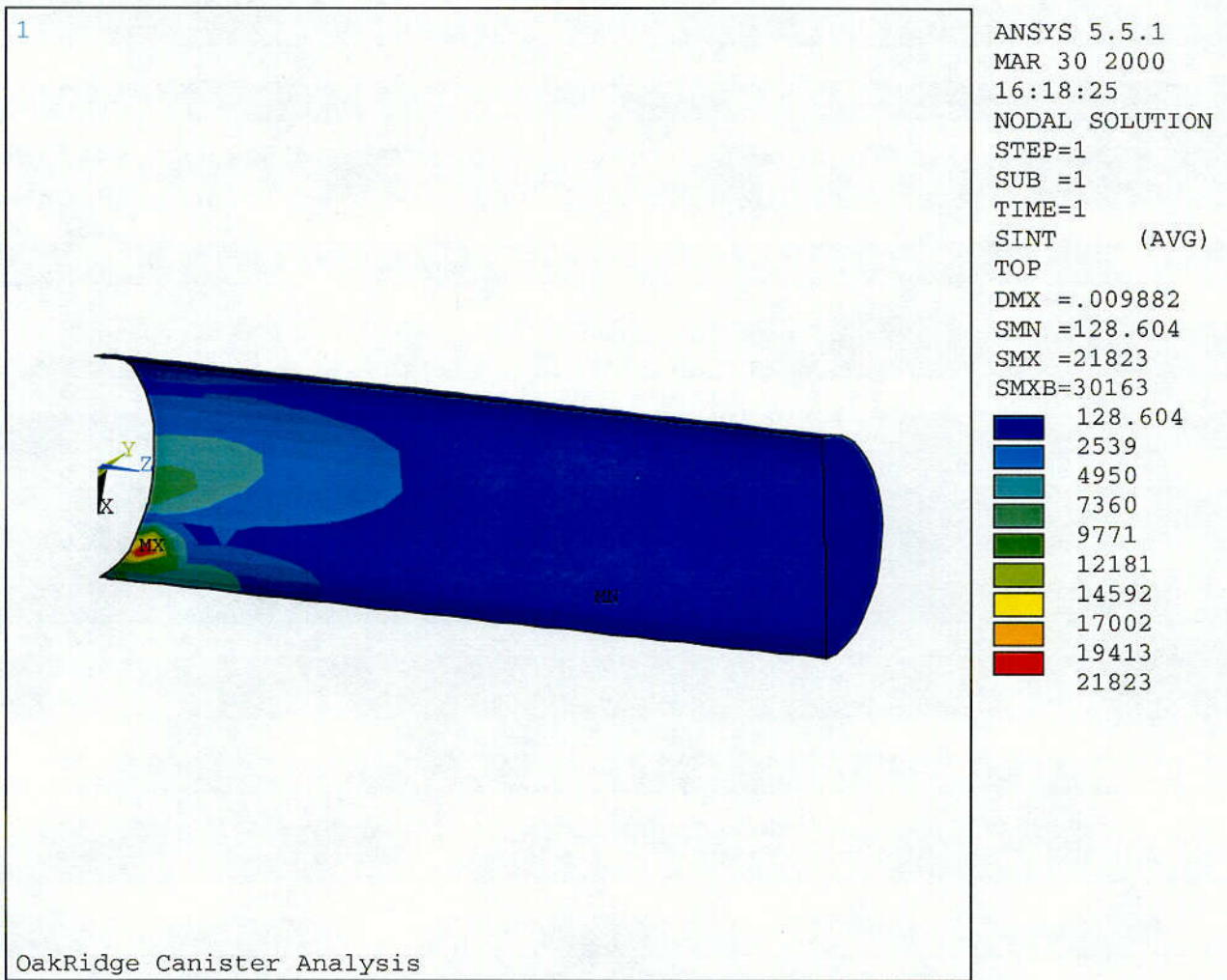


**FIGURE 2.11.7-7**  
**Accident Condition End Drop Load-Displacement Curve for the Cap Weldment**

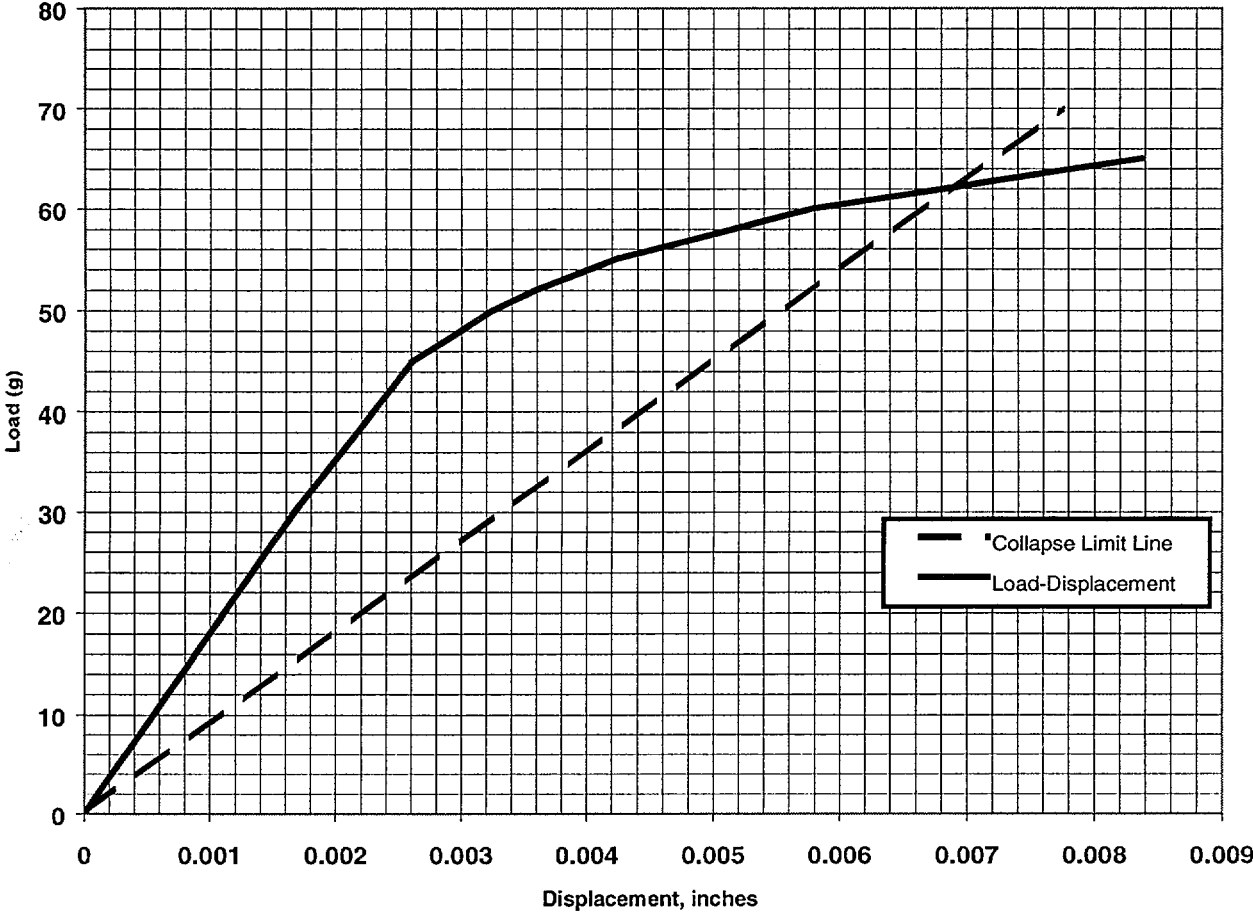


**FIGURE 2.11.7-8**  
**Accident Condition End Drop Deformation for the Cap Weldment at 60g**

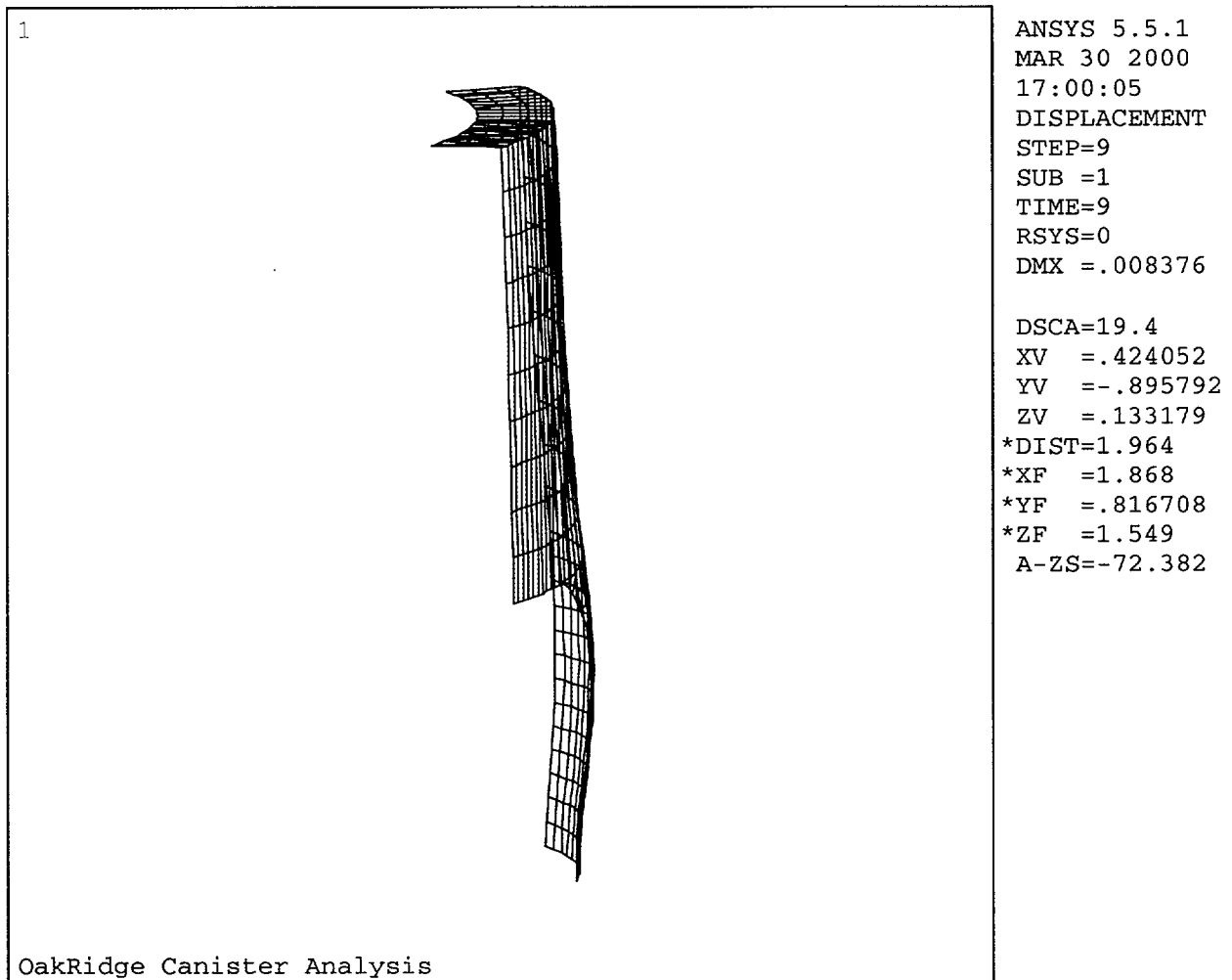


**FIGURE 2.11.7-9**  
**Accident Condition Side Drop Membrane Stress Intensity**

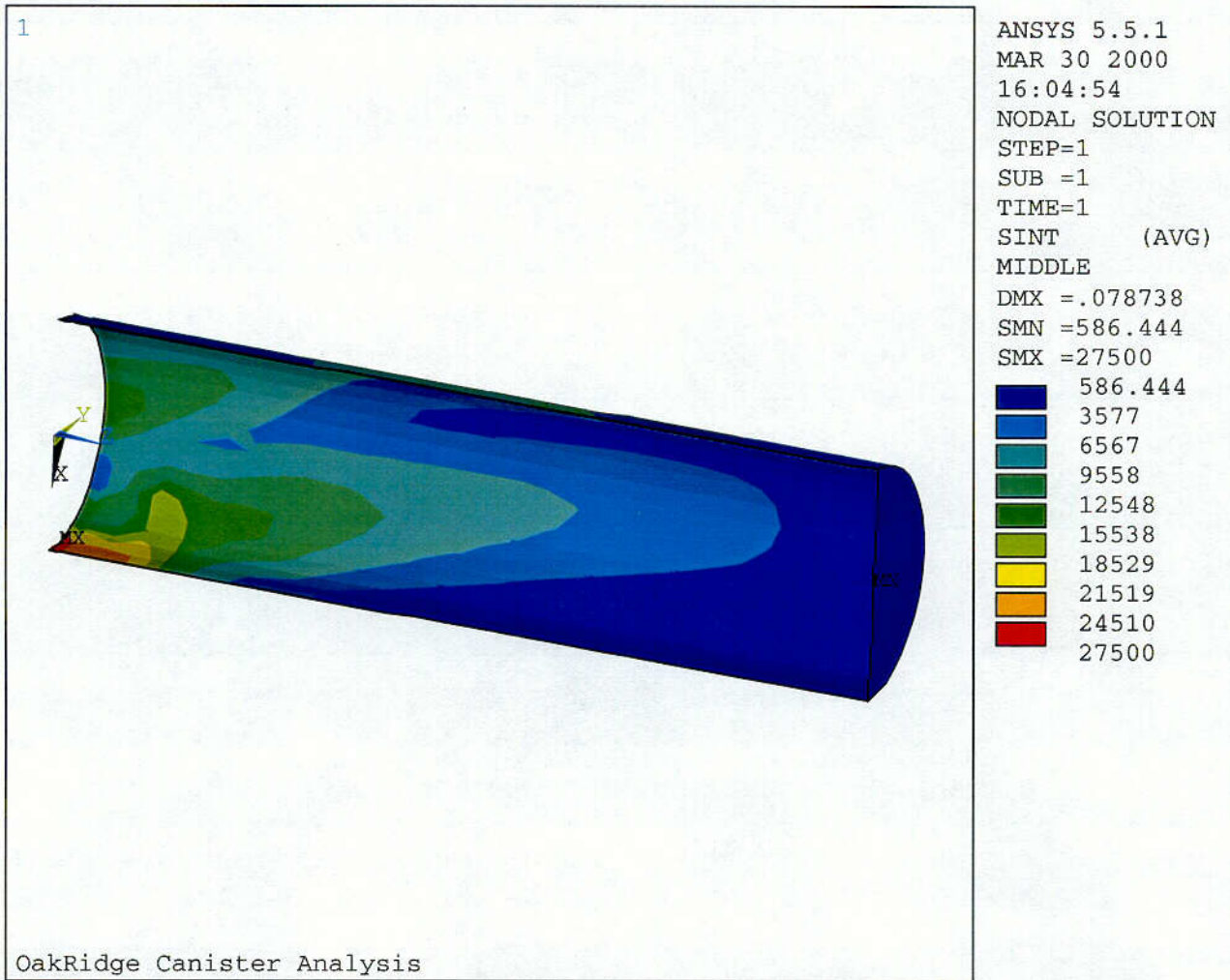


**FIGURE 2.11.7-10**  
**Accident Condition Side Drop Maximum Membrane Plus Bending Stress Intensity**

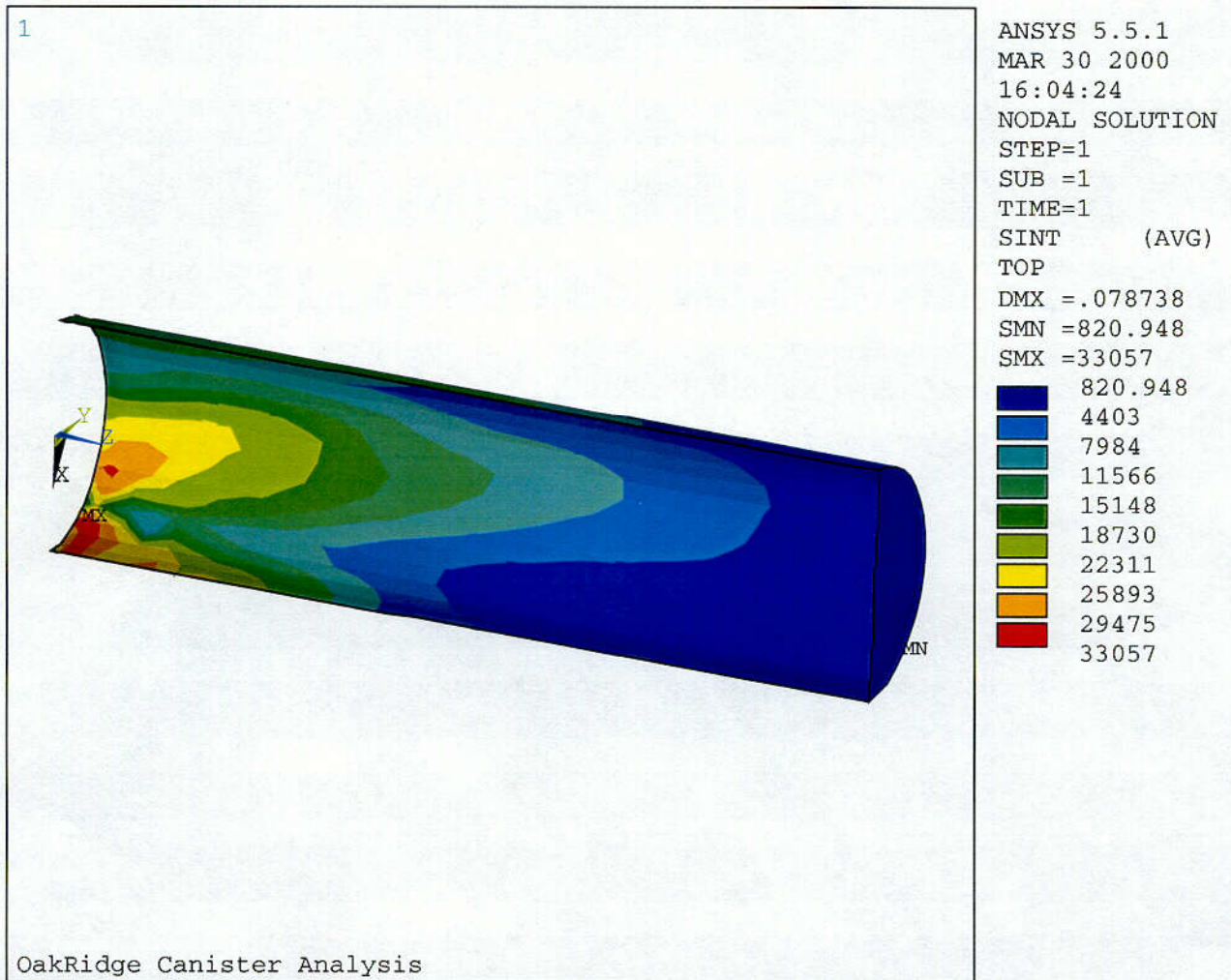


**FIGURE 2.11.7-11**  
**Load Path for Oak Ridge Canister Contents**

